Amygdala resting state functional connectivity in alcohol dependence

Csaba Orban



A thesis submitted for the degree of Doctor of Philosophy
in accordance with the requirements of the
Department of Medicine at Imperial College London

March 2017

Abstract

Alcohol dependence is a global societal problem, yet current avenues for its treatment are largely ineffective in slowing its chronic-relapsing trajectory. Animal studies of alcohol dependence have described neuroadaptations in the amygdala that may play a central role in mechanisms of relapse. In this thesis, spontaneous amygdala network function was examined in abstinent alcohol dependent patients (ADP) using functional magnetic resonance imaging within the framework of a multi-site neuroimaging platform: ICCAM. Participants underwent five scans that included baseline, as well as scans under placebo, acute antagonism of μ-opioid, Dopamine D3 (DRD3) and Neurokinin-1 (NK1) receptor systems previously implicated in mechanisms of addiction.

At baseline, amygdala – substantia nigra/ventral tegmental area (SN/VTA) resting state functional connectivity (RSFC) was elevated in abstinent ADP, despite widespread grey-matter (GM) volumetric atrophy, in both amygdala and SN/VTA, compared with age-matched healthy controls (HC). The strength of amygdala – SN/VTA RSFC in ADP was primarily associated with years of cumulative alcohol exposure, but not with amygdala or SN/VTA GM volume, length of abstinence, smoking status, or head motion.

Amygdala RSFC with other regions showed sensitivity to core clinical features of ADP at baseline. Amygdala – frontoparietal (FPN) RSFC was inversely associated with abstinence length, with ADP in the first two months of abstinence showing significantly reduced amygdala – FPN RSFC compared with HC.

Voxelwise comparison of amygdala RSFC between each drug session and placebo, did not reveal differential effects of receptor blockade on ADP and HC. Across both groups, however, the three drugs exhibited both overlapping and differential effects on distinct brain networks. Notably, amygdala RSFC in the superior temporal gyrus showed increases under NK1-antagonism, and decreases under naltrexone compared with placebo. Finally, amygdala – SN/VTA was significantly elevated in ADP relative to HC across all four sessions, suggesting that it may represent a stable neurophysiological feature of alcohol dependence.

Declaration of Originality

I declare that the work presented in this thesis is entirely my own, except where clearly indicated in the text or in this declaration. All referenced work has been cited to the best of my knowledge, and the thesis confirms to the regulations of Imperial College London.

All data presented in this work was collected as part of ICCAM, a multi-site experimental medicine study run by Imperial College London, University of Cambridge and The University of Manchester. I was one of several team members who took part in data collection and data entry at the Imperial Site.

Decisions relating to the software, parameters, and order of operations used within the resting state preprocessing pipeline were developed collaboratively with my supervisor, Dr John McGonigle. In addition, I received some help from André Santos Ribeiro with use of the ANTs software. However, the agreed pipeline was implemented using my own script according to my preferences and specifications.

The preprocessing and first-level statistical analyses of the Go/No-go and Evocative Image Tasks were done by Dr John McGonigle, but all other preprocessing and data analysis was my own work.

The calculation of the cumulative alcohol exposure measure and the determination of its cutoffs were carried out by Remy Flechais.

Copyright Declaration

The copyright of this thesis rests with the author and is made available under a Creative Commons Attribution Non-Commercial No Derivatives licence. Researchers are free to copy, distribute or transmit the thesis on the condition that they attribute it, that they do not use it for commercial purposes and that they do not alter, transform or build upon it. For any reuse or redistribution, researchers must make clear to others the licence terms of this work.

Acknowledgements

First and foremost, I would like to thank my two supervisors, Anne Lingford-Hughes and John McGonigle for their unwavering guidance and support of both my work and my personal development. I have learnt an enormous amount from them and greatly benefited from their mentorship, patience and foresight throughout the course of this PhD.

I would like to thank David Nutt for the opportunity to work in a stimulating, multi-disciplinary environment with a family-like atmosphere. In addition, a special thank you to the other ICCAM team members for providing me with the unique experience of working in a large multi-site collaboration, as well as the administrative staff at CfN for their continuous support: Margaret Collett and Sheila McKenzie. I'm also extremely thankful to all the participants who gave up their time and effort to take part in this study.

I would like to express my special gratitude to André Santos Ribeiro and John McGonigle for their tireless patience in mitigating my ignorance in programming and mathematics.

Special thanks go out to members of the foosball / table-tennis / Achtung, die Kurve! committee, for their friendship: Erik Fagerholm, Romy Lorenz, Leor Roseman, Christopher Timmermann and Inês Violante.

I am also greatly indebted to the following colleagues for countless stimulating discussions and their invaluable advice: David Erritzøe, Remy Flechais, Mendel

Kaelen, Nicola Kalk, Jim Myers, Liam Nestor, Louise Paterson, Laurence Reed, Robin Tyacke and Vicky Wing.

I am immensely grateful for the opportunity to have been part of the C_3NL family, which has greatly contributed to making my PhD experience a memorable one, thanks to: Richard Wise, James Cole, Claire Feeney, Fatemeh Geranmayeh, Rob Leech, Lucia Li, Tony Goldstone, Adam Hampshire, Gregory Scott, Sara De Simoni, David Sharp and Eyal Soreq.

I would like to thank the Medical Research Council for their financial support, and Imperial College London for offering me the opportunity to study there.

Finally, I would like to thank my parents, my brother and his wife Eszter for always being there for me.

"I think I'm more afraid of stopping than to die. […] I'd be a completely different person. I mean I'm 45. I started drinking when I was 15, so it's years of constant abuse, you know? It's like trying to take the roots out of a tree. It will never work."

-Aurelie

Drinking to Oblivion, Louis Theroux, BBC"

To all individuals suffering from alcohol dependence and to their friends and families

Contents

Abstract 2

Declaration of Originality 4

Copyright Declaration 5

Acknowledgements 6

Contents 9

List of Figures 13

List of Tables 15

List of Abbreviations 16

Chapter 1: Introduction 19

1.1 Thesis overview 19

1.2 Contributions to the field and conclusion 20

Chapter 2: Background 23

2.1 Alcohol dependence 23

2.2 Neurobiological models of substance dependence 24

2.3 The allostasis model 25

2.4 Mesolimbic dopamine system 26

2.5 Amygdala 27

2.5.1 Amygdala in alcohol dependence 28

2.6 Pharmacological modulation of amygdala RSFC 31

2.7 Principles of magnetic resonance imaging 33

2.7.1 Nuclear Magnetic Resonance 34

2.7.2 Magnetic Resonance Imaging 34

2.7.3. T1- and T2*-weighted images 35

2.7.4 Echo-Planar Imaging 36

2.7.5 The biophysical and physiological basis of BOLD 36

2.8 Resting state functional connectivity 38

2.9 Artifacts in resting state fMRI 40

2.9.1 Motion 41

2.9.2 Physiological artifacts 44

2.9.3 Nuisance regression 46
2.10 Biomarkers 48
2.11 Thesis rationale and summary of hypotheses 49
Chapter 3: Methodology 53
3.1 Study description 53
3.1.1 Introduction of ICCAM 53
3.1.2 Overview of study procedures in ICCAM 53
3.1.4 Recruitment strategy 56
3.1.4 Approvals 56
3.1.5 Inclusion and exclusion criteria 57
3.1.6 Materials 58
3.1.7 Structural acquisition 59
3.1.8 Functional acquisition 59
3.2 Preprocessing 60
3.2.1 Structural preprocessing 60
3.2.2 Functional preprocessing 60
3.2.3 Regression of noise 61
3.2.4 Rationale for preprocessing approaches used 62
3.3 Statistical modelling 64
3.3.1 Seed selection 64
3.3.2 Alternative approaches for mapping amygdala network function 64
Chapter 4: Group-level effects of alcohol dependence 66
4.1 Introduction 66
4.1.1 Neuroadaptations 66
4.1.2 Amygdala in alcohol dependence 66
4.1.3 Amygdala RSFC and GM volume in alcohol dependence 67
4.1.4 Hypotheses 68
4.2 Methodology 69
4.2.1 Participants 69
4.2.2 Preprocessing 70
4.2.3 Statistical analyses 70
4.3 Results 71
4.3.1 Amygdala RSFC and impact of cumulative alcohol exposure 71
4.3.2 Amygdala GM volume and impact of age 75
4.3.3 SN/VTA GM volume and LV volume 77
4.3.4 Effect of smoking on amygdala RSFC and GM volume 77

4.3.5 Summary model 79
4.4 Discussion 80

Chapter 5: Effects of abstinence length and anxiety 85
5.1 Introduction 85
5.1.1 Individual differences 85
5.1.2 Anxiety 87
5.1.3 Abstinence length 88
5.1.4 Hypotheses 90
5.2 Methodology 91
5.2.1 Evocative Image Task description 91
5.2.2 Go/No-Go Task description 92
5.2.3 Participants 93
5.2.4 Preprocessing 95
5.2.5 Statistical analyses 95
5.3 Results 95
5.3.1 Overall effects of state and trait anxiety 95
5.3.2 Relationship between amygdala – left posterior insula RSFC and amygdala activation within the Evocative image task 98
5.3.3 Overall effect of abstinence length 100
5.3.4 Exploring the FPN further 100
5.3.5 Subgroup analysis by abstinence length 101
5.3.6 Relationship between amygdala – FPN RSFC, Go-No/Go task-activation and inhibitory control 103
5.4 Discussion 106
5.4.1 Amygdala – posterior insula RSFC and anxiety 106
5.4.2 Amygdala – frontoparietal RSFC and abstinence 110

Chapter 6: Pharmacological modulation of amygdala RSFC 114
6.1 Introduction 114
6.1.1 Pharmacological fMRI 114
6.1.1 μ-Opioid receptor 114
6.1.2 Dopamine receptor D3 (DRD3) 115
6.1.3 Neurokinin-1 receptor (NK1) 116
6.1.4 Hypotheses 117
6.2 Methodology 119
6.2.1 Drug dosage 119
6.2.2 Pseudo-randomisation of session order 120

6.2.3 Participants 120
6.2.4 Group effects across different sessions 121
6.2.5 Stability of individual differences across sessions 122
6.2.6 Voxelwise analysis of drug effects 123
6.3 Results 124
6.3.1 Amygdala – midbrain RSFC 124
6.3.2 Subject-level stability of amygdala – SN/VTA RSFC between sessions 126
6.3.3 Effects of Naltrexone 128
6.3.4 Effects of GSK598809 (or Placebo) 132
6.3.5 Effects of Aprepitant/Vofopitant 133
6.3.6 Opposing effects Naltrexone and Aprepitant/Vofopitant 133
6.4 Discussion 136
6.4.1 Summary 136
6.4.2 Amygdala – SN/VTA RSFC 138
6.4.3 Amygdala – insula and amygdala – dorsal striatal RSFC 139
6.4.4 Amygdala – STG RSFC 141
6.4.5 Amygdala – mPFC RSFC 143
6.4.6 Neural mechanisms of Placebo 144
6.4.7 Possible effects of Vitamin C on amygdala – mPFC RSFC 147
Chapter 7: General discussion 149
7.1 Thesis summary 149
7.1.1 Summary of aims 149
7.1.2 Summary of findings 150
7.2 Implications, Limitations and Future Research 156
7.2.1 SN/VTA RSFC: a neurophysiological correlate, but not quite a biomarker 156
7.2.2 The integrative potential of network models 158
7.2.3 Strengths of exploratory analyses 159
7.2.4 Limitations of exploratory analyses 161
7.2.5 Potential follow-up studies in humans 163
7.2.6 Potential follow-up studies in animals 164
References 166
Appendix A: Figures 186

List of Figures

Figure 3.1 Timeline summary of the experimental protocol 55

Figure 4.1 Group-level comparison of whole-brain voxelwise amygdala RSFC between ADP and HC..... 73

Figure 4.2 Visualisation of the SN/VTA region of interest. 74

Figure 4.3 Distribution of amygdala – SN/VTA RSFC and family history of alcohol dependence in two groups, and association with cumulative alcohol exposure in ADP..... 75

Figure 4.4 Whole-brain voxelwise group-level comparison of GM volume between ADP and HC.. 76

Figure 4.5 The effects of age on amygdala GM volume in ADP and HC 77

Figure 4.6 Post-hoc analysis of the impact of smoking status on amygdala RSFC and GM volume. 78

Figure 4.7 Summary diagram showing linear relationships between amygdala – SN/VTA RSFC, amygdala GM volume, cumulative alcohol exposure and age. 79

Figure 5.1 Group-level comparison of trait and state anxiety between ADP and HC..... 96

Figure 5.2. The relationship between trait anxiety and amygdala - insula RSFC…..... 97

Figure 5.3. Clusters significantly activated during the Evocative Image Task..... 99

Figure 5.4 The impact abstinence length and amygdala resting state network function..... 102

Figure 5.5 Amygdala – FPN RSFC as a function of abstinence length in ADP and in HC..... 103

Figure 5.6 Parts of the FPN engaged during successful motor inhibition. 104

Figure 5.7 Association between amygdala-FPNr RSFC and FPNr activation during correct inhibition in the Go/No-Go task..... 106

Figure 6.1 SN/VTA region of interest used for small-volume correction in the midbrain.... 122

Figure 6.2 Group-level differences in amygdala RSFC across the four drug sessions..... 125

Figure 6.3 Spatial overlap of voxelwise significant group differences at Baseline and across the drug sessions. 127

Figure 6.4 Subject-level stability of amygdala – SN/VTA RSFC between sessions..... 129

Figure 6.5 Voxelwise effects of Naltrexone on amygdala RSFC. 130

Figure 6.6 Post-hoc comparison of amygdala – dorsal striatal (dSTR) RSFC between the five sessions. 131

Figure 6.7 Post-hoc comparison of amygdala – anterior insula (aINS) RSFC between the five sessions..... 132

Figure 6.8 Overlapping effects of Placebo on amygdala RSFC in the left mPFC.. 134

Figure 6.9 Whole-brain voxelwise effects of Aprepitant/Vofopitant on amygdala RSFC..... 135

Figure 6.10 Opposing effects of Naltrexone and Aprepitant/Vofopitant on amygdala – superior temporal gyrus (STG) RSFC. 136

Figure A1.1 The relationship between age and amygdala – SN/VTA RSFC in ADP and HC..... 186

Figure A1.2 Group-level comparison of whole-brain amygdala RSFC with an extended list of covariate 186

Figure A1.3 The relationship between cumulative alcohol exposure and amygdala GM volume in ADP..... 187

Figure A1.4 Clusters associated with correct inhibition trials in the Go/No-Go task in 70 participants pooled from Pilot, HC and ADP groups. 187

List of Tables

Table 4.1 Demographics and clinical characteristics of ICCAM participants analysed from the Baseline session 72

Table 5.1 Outlier characteristics of participant 3039 98

Table 5.2 Root-mean-square residuals of linear and non-linear models 99

List of Abbreviations

ACC	Anterior cingulate cortex
ADHD	Attention-deficit/hyperactivity disorder
ADP	Alcohol dependent patient
ANOVA	Analysis of variance
B_0	Static magnetic field
BIS11	Barratt impulsivity scale
BLA	Basolateral amygdala
BNST	Bed nucleus of the stria terminalis
BOLD	Blood oxygen level dependent
[11C]-(+)-PHNO	A PET radioligand for imaging DRD3 receptors in the brain
CeA	Central amygdala
CBF	Cerebral blood flow
CBV	Cerebral blood volume
$CMRO_2$	Cerebral metabolic rate of oxygen consumption
CRF	Corticotrophin releasing factor
CSF	Cerebrospinal fluid
DRD2/DRD3	Dopamine receptor D2- and D3-subtypes
DMN	Default mode network
dmPFC	Dorsomedial prefrontal cortex
dPCC	Dorsal posterior cingulate cortex
dSTR	Dorsal striatum
DVARS	Root-mean square of the temporal derivative
EPI	Echo-planar imaging
[F18]SPA-RQ	A PET radioligand for imaging NK1 receptors in the brain
FD	Framewise displacement
FLIRT	FSL's linear registration tool
FPN	Frontoparietal network
FPN-r	Revised mask of the frontoparietal network
FSL	An fMRIB software library
GABA	γ-aminobutyric acid
$GABA_A$	GABA-A receptor

$GABA_C$	GABA-C receptor
GLM	General linear model
GM	Grey matter
GNG	Go/No-Go task
GSK598809	a selective DRD3 antagonist
HC	Healthy controls
HRF	Hemodynamic response function
I-ADP	Intermediate-term abstinent alcohol dependent patient
IAPS	International Affective Picture System
ICA	Independent component analysis
ICCAM	Imperial Cambridge Manchester
ICV	Intracranial volume
IPL	Inferior parietal lobules
L822429	An NK1 receptor antagonist used in animal models
L-ADP	Long-term abstinent alcohol dependent patient
M_0	Net magnetisation vector
MNI	Montreal Neurological Institute
mPFC	Medial prefrontal cortex
NAc	Nucleus accumbens
NK1	Neurokinin-1 receptor
OFC	Orbitofrontal cortex
PAG	Peri-aqueductal grey
PBO	Placebo
PET	Positron emission tomography
PFC	Prefrontal cortex
phfMRI	Pharmacological functional MRI
preSMA	Pre-supplementary motor area
PTSD	Post-traumatic stress disorder
rACC	Rostral anterior cingulate cortex
RETROICOR	Retrospective image correction
RSFC	Resting state functional connectivity
S-ADP	Short-term abstinent alcohol dependent patient
sgACC	Subgenual anterior cingulate cortex
SPL	Superior parietal lobule

SN	Substantia nigra
SN/VTA	Substantia nigra / Ventral tegmental area
STAI-S	Spielberger State Anxiety Inventory
STAI-T	Spielberger Trait Anxiety Inventory
STG	Superior temporal gyrus
TE	Time interval from initial pulse to signal readout
TR	Time interval between consecutive pulses (repetition time)
vmPFC	Ventromedial prefrontal cortex
vPCC	Ventral posterior cingulate cortex
VTA	Ventral tegmental area
WM	White matter

Chapter 1: Introduction

1.1 Thesis overview

This chapter presents a summary of each subsequent chapter in the thesis and lists the key contributions of the thesis to the literature.

Chapter 2 provides background information and presents the rationale for this work within the context of recent developments in the field.

Chapter 3 provides an overview of ICCAM: the exclusion and inclusion criteria, the experimental procedures, data acquisition protocols, and the preprocessing methodology applied on the resting state dataset.

Chapter 4 shows voxelwise group comparison of amygdala RSFC and amygdala GM volume in alcohol dependent patients and healthy controls. The chapter also examines relative contribution of cumulative alcohol exposure and age to amygdala RSFC and GM volumes.

Chapter 5 explores the impact of individual differences in trait anxiety, and abstinence length on amygdala resting state function, while also relating them to measures of task activation.

Chapter 6 examines the effects of μ-opioid, Dopamine D3 (DRD3), and Neurokinin-1 (NK1) receptor antagonism on amygdala resting state function, with the aims of characterising differential effects on ADP and HC, and effects shared across the groups.

Chapter 7 synthesises the main findings of the thesis both in the context of their strengths, limitations and their implications for future work.

1.2 Contributions to the field and conclusion

This thesis has produced the following novel findings within the fields of neuroscience and substance dependence research:

- Abstinent alcohol dependent patients (ADP) exhibited significantly elevated amygdala – substantia-nigra / ventral tegmental area (SN/VTA) resting state functional connectivity (RSFC) compared with age-matched healthy controls (HC);
- Elevation of amygdala – RSFC in ADP was linearly associated with cumulative alcohol exposure, but not with abstinence length suggestive of long-term neuroadaptations;
- The lack of association of amygdala – SN/VTA RSFC with smoking status in ADP was suggestive of specificity to alcohol over nicotine dependence;
- Group-level differences in amygdala RSFC between ADP and HC were modulated by acute pharmacological blockade of μ-opioid, Dopamine D3 (DRD3), and Neurokinin-1 (NK1) receptor antagonism;
- In ADP, amygdala – frontoparietal (FPN) RSFC was positively correlated with abstinence length at baseline, but not under drug modulation;
- Across both groups, μ-opioid and DRD3 antagonism were both associated with reduced amygdala – anterior insula and reduced amygdala – dorsal striatal RSFC;
- Across both groups μ-opioid and NK1 antagonism were associated with opposing effects on amygdala – superior temporal gyrus RSFC, with the former showing reductions, while the latter showing increases.

The work presented in this thesis has greatly benefited from my time spent on the design and implementation of a pre-processing pipeline for optimal noise removal in resting-state datasets based on best practices according to the literature. In order to achieve this, the pipeline integrated pre-processing algorithms from multiple software libraries, in contrast to most other pipelines that stay within the constraints of a single software library.

The following four publications made use of the resting state pipeline developed over the course of my PhD work:

Carhart-Harris, R.L., Muthukumaraswamy, S.D., Roseman, L., Kaelen, M., et al. (2016) Neural correlates of the LSD experience revealed by multimodal neuroimaging. Proc. Natl. Acad. Sci. USA 113(17), 4853-4858.

Tagliazucchi, E., Roseman, L., Kaelen, M., Orban, C., Muthukumaraswamy, S.D. et al. (2016) Increased global functional connectivity correlates with LSD-Induced ego dissolution. Current Biology, 26(8), 1043-1050.

Kaelen, M., Roseman, L., Kahan, J., Santos-Ribeiro A., Orban C., Lorenz R. et al., (2016) LSD modulates music-induced imagery via changes in parahippocampal connectivity. European Neuropsychopharmacology, 26(7), 1099-1109.

Roseman, L., Sereno, M.I., Leech R., Kaelen, M., Orban, C., McGonigle, J., et al. (2016) LSD alters eyes-closed functional connectivity within the early visual cortex in a retinotopic fashion. Human Brain Mapping, 37, 3031-3040.

I have published a first-authored paper indirectly related to the topic of the Thesis:

Orban, C., McGonigle, J., Kalk N.J., Erritzoe, D., Waldman, A.D., Nutt, D.J., Lingford-Hughes, A. (2013) Resting state synchrony in anxiety-related circuits of abstinent alcohol-dependent patients. The American Journal of Drug and Alcohol Abuse 39 (6), 433-440

In conclusion, amygdala resting state network function was sensitive to several key clinical characteristics of abstinent ADP. Cumulative alcohol exposure and time since onset of abstinence were reflected in the spontaneous interactions of distinct amygdala circuits across the brain. However, the three drugs of interest examined in this study, for their putative therapeutic function, did not specifically modulate amygdala RSFC in these circuits.

Chapter 2: Background

2.1 Alcohol dependence

Alcohol dependence is a chronic-relapsing disorder affecting populations on a worldwide scale (Rehm et al., 2009). It is typically characterised by a cycle of bingeing/intoxication, withdrawal/negative affect and preoccupation/craving (Koob & Volkow, 2010). Similar to other forms of substance dependence, its onset may manifest as progressive loss of control over alcohol consumption, and an increasing prioritisation of drinking over other activities. Alcohol dependence is extremely damaging both on a personal and societal level (Nutt & Rehm, 2014). It reduces life expectancy, leads to cumulative organ damage, and may lead to social isolation and loss of employment.

To date only a few pharmacological interventions are approved for assisting-relapse prevention. Randomised double-blind placebo-controlled trials have shown, that under a daily dosing regimen, Naltrexone and Acamprosate are each capable of significantly reducing total alcohol consumption and incidence of relapse in abstinent ADP (Carmen et al., 2004; Kranzler & Van Kirk, 2001). Despite the overall significance of their effects, these treatments only work in a small subset of the patients, and only within the early stages of abstinence (first 12 weeks). There is a clear need to develop more effective pharmacological interventions for longer-term prevention of relapse.

Some experimental compounds, for example Corticotrophin-releasing factor (CRF) antagonists, have shown promise in animal models, while failing to show similar effectiveness in patients (Kwako et al., 2015). Current efforts to develop

pharmacological therapies are likely hindered by an insufficient understanding of the disease mechanisms of alcohol dependence in humans. In addition, the recent decade has witnessed a trend of large pharmaceutical companies increasingly withdrawing resources from drug development programs aimed at targeting psychiatric disorders (Hyman, 2012).

2.2 Neurobiological models of substance dependence

Various neurobiologically motivated models of substance dependence have been proposed over the years implicating system-level deficits across both cortical and subcortical regions. According to the incentive-salience model, the ventral dopaminergic system becomes sensitized to drugs and associated stimuli, resulting in craving, and accompanied by an excessive motivation or 'wanting' to take the drug, independent of its hedonic effects which diminish over repeated administrations (Robinson & Berridge, 1993). Other models have emphasised the role of frontal cortical deficits as contributing factors to impaired salience attribution, reduced response inhibition and impulsive decision making that is characteristic of substance-dependent populations (Goldstein & Volkow, 2002).

The habitual or compulsive pattern of drug taking that develops over time has been proposed to be mediated by a shift from ventral to dorso-striatal regulation of drug-taking behaviours, thereby bypassing frontal, top-down regulatory systems (Everitt & Robbins, 2005). The reward deficiency hypothesis (Blum et al., 2000) and the allostasis model (Koob & Le Moal, 2001) view substance-seeking behaviour as an attempt to normalise hypofunctioning hedonic, motivational and affective processes

that are disrupted by pre-existing brain abnormalities or as a consequence of chronic substance exposure, respectively.

These models are not necessarily mutually exclusive as they may refer to distinct processes that exert influence at different stages of the substance dependence cycle (Koob and Volkow, 2010). Constructs related to positive reinforcement such as impulsivity and incentive-salience may be important factors during the binge/intoxication stage and the acquisition of substance-use behaviour. Conversely, constructs related to negative reinforcements such as allostasis and reward deficiency may be more relevant to the withdrawal/negative affect and preoccupation/craving stages and exert a greater influence over longer-term substance dependence. One feature that is prominent in many of these models is the proposition that substance-use related neuroadaptations contribute to the persistence of the disorder.

2.3 The allostasis model

"Once an alcoholic, always an alcoholic" is a widely familiar adage. More than a simple reminder about the dangers of relapse, the statement implies a hypothesis: once a certain-level dependence to alcohol is established, the individual acquires persistent changes in its physiology, from which it does not recover with abstinence. According to Koob's allostatic model (Koob & Le Moal, 2001) alcohol dependence is the consequence of key brain regions and neuroreceptor systems subserving hedonic and motivational processes undergoing neuroadaptations in response to chronic supraphysiological levels of stimulation.

Allostasis, originally coined by Sterling & Eyer (1988), refers to the process of maintaining stability through physiological or behavioural change. It is distinct from

homeostasis: the process of returning physiological parameters to their optimal range of function through negative feedback processes. Allostasis involves the shift of physiological systems towards novel set points outside their normal range of function through feed-forward processes. This process provides an efficient and rapid mechanism for mobilizing physiological systems to respond to severe physiological and environmental changes. However, repeated activation of allostatic mechanisms comes at a cost, known as allostatic load. It becomes increasingly harder for the organism to return to its original physiological state, while also incurring cumulative damage as a result of operating outside it.

2.4 Mesolimbic dopamine system

For the past few decades, the dopaminergic mesolimbic system, which originates in the ventral tegmental area (VTA) and projects to the nucleus accumbens (ventral striatum in humans), has been an intense focus of research in studies of substance dependence (Nutt et al. 2015). Anticipation or unexpected receipt of drug rewards, including alcohol (Boileau et al., 2003; Urban et al., 2010), have been shown to trigger phasic striatal dopamine release in humans and animals alike, while blockade of dopaminergic signalling has been found to reduce the reinforcing properties of stimulants in animal models (Robledo et al., 1992). Alcohol dependent rats in withdrawal (Shen et al., 2007) or in prolonged abstinence (Diana et al., 1996) exhibit reduced VTA activity compared with controls, suggestive of long-term of neuroadaptations. Furthermore, studies of alcohol dependent patients have observed reduced ventral striatal BOLD activation during reward anticipation (Wrase et al., 2007), an effect that was inversely related to impulsivity (Beck et al., 2009).

2.5 Amygdala

The amygdala is a highly conserved collection of subcortical nuclei located bilaterally in the anterior portion of the medial temporal lobes. The name amygdala derives from its recognisable almond-like shape. In animal studies the amygdala nuclei are often grouped into subregions based on their histological features and circuitry, with the most widely studied of these being the central amygdala (CeA) and the basolateral amygdala (BLA; Ledoux, 2007). The BLA receives strong input from sensory association areas and has reciprocal connections with the hippocampus, medial prefrontal and orbitofrontal cortices unilateral efferent connections to the striatum, nucleus accumbens, CeA and Bed Nucleus of the Stria Terminalis (BNST; Ledoux, 2007; Janak & Tye, 2015). The CeA receives most of its afferent input from within the amygdala, directly from the BLA, and indirectly via so-called intercalated cells, while sending efferent connections to the BNST, hypothalamus, periaqueductal grey (PAG), and other deep brain nuclei, including the substantia nigra (SN) and VTA (Ledoux, 2007; Janak & Tye, 2015). A simplified model of the amygdala views the BLA as the main input hub of the amygdala that filters and interprets features of salient sensory stimuli, and the CeA as the output region that initiates adaptive physiological and behavioural responses to these inputs (Gilpin & Roberto, 2012).

The amygdala is thought to have evolved as a salience-detector that monitors the organism's internal and external environments for stimuli that hold relevance for its survival (Janak & Tye, 2015). It plays a role in mediating innate responses to threat stimuli, e.g. innate freezing behaviour in the presence of a predator, as well as learned responses, e.g. avoidance of stimuli that have been paired with an electric shock (Ledoux, 2014). In animal studies, the amygdala has been predominantly studied in

the context threat-conditioning paradigms (Ledoux, 2014), while human neuroimaging studies have focused on its role in processing of negatively valenced stimuli (Costafreda et al., 2008). Findings of increased amygdala responsivity to affective stimuli in panic disorder, social-anxiety disorder and post-traumatic stress disorder (PTSD), have made the amygdala one of the central regions in models of anxiety disorders (Etkin & Wager, 2007).

Although less studied outside the context of aversive processes, the amygdala has also been found to play an important role in the forming of stimulus-reward associations (Baxter & Murray, 2002). Its role in positive reinforcement mechanisms may be mediated by afferent connections from dopaminergic midbrain nuclei (See et al., 2001), and from the ventral striatum (Setlow et al., 2002). More recent findings have also suggested surprising roles for the amygdala in long-term planning of reward goals (Hernadi et al., 2015) and a fundamental role in short-term memory maintenance (Kaminski et al., 2017).

2.5.1 Amygdala in alcohol dependence

The amygdala has received significantly less attention than the VTA or ventral striatum within the context of substance-dependence. However, there is evidence to suggest that, like the regions above, it may play important roles both the acute reinforcing properties of alcohol and the chronic neuroadaptations that may reinforce alcohol dependence (Gilpin et al., 2015).

Acute ethanol treatment enhances γ-aminobutyric acid (GABA) release in a dose-dependent manner in the central amygdala (CeA) of rats as observed with *in vitro* electrophysiology (Nie et al., 2004; Roberto et al., 2003), and *in vivo* microdialysis

methods (Roberto et al., 2004). Selective $GABA_A$ receptor blockade in the CeA reduces alcohol self-administration, without affecting water intake, suggesting a role for the amygdala in reinforcement of alcohol consumption (Hyytia & Koob, 1995).

In alcohol-dependent rats, baseline levels of GABA release in the CeA are substantially elevated compared with alcohol-naïve rats (Roberto et al., 2004), an effect dependent on the upregulation of Corticotrophin Releasing Factor (CRF), a neuropeptide involved in stress-signalling (Sommer et al., 2008; Roberto et al., 2010). Selective antagonism of CRF in the CeA has been shown to eliminate symptoms of alcohol withdrawal (Rassnick et al., 1993), and to bring down excessive levels of alcohol consumption in alcohol-dependent rats to levels exhibited by non-dependent rats (Funk et al., 2007).

In stark contrast to the abundance of mechanistic studies demonstrating the importance of the amygdala in animal models of alcohol dependence, similar evidence from human patient studies is severely lacking. Most findings have come from structural data, with many patient studies reporting markedly reduced grey-matter (GM) volumes in alcohol dependent patients (ADP) relative to age-matched controls, both in early (Wrase et al., 2008) and in later stages of abstinence (Fein et al., 2006; Makris et al., 2008). One of these studies also found amygdala GM loss during early abstinence to be associated with greater levels of alcohol-craving, and higher likelihood of subsequent relapse (Wrase et al., 2008).

It remains unknown whether the findings of persistent neuroadaptations in the rat CeA following chronic alcohol exposure translate to human clinical populations. The CeA is too small of a region to reliable study with fMRI at the conventional field strength of 3 Tesla. However, since amygdala sub-nuclei are heavily interconnected,

local neuroadaptations in the CeA may influence larger-scale patterns of activity that are amenable to observation at 3 Tesla. Similarly, small-scale neuroadaptations may modulate the network-level interactions of the amygdala with other functionally related cortical and subcortical regions. These changes in the large-scale functional interactions of the amygdala may be expressed as differential patterns of resting state functional connectivity (RSFC; introduced later in Subchapter 2.8) between alcohol dependent patients (ADP) and healthy controls (HC).

If these group differences are present and are indeed the product of neuroadaptations as described by the allostatic model (Koob & Le Moal, 2001), then one would expect them to be present even in prolonged abstinence. Furthermore, the magnitude of these alterations of amygdala RSFC in ADP may reflect the allostatic load accumulated by ADP throughout their history of alcohol use. One measure that could provide a partial index of allostatic load may be a person's cumulative duration of heavy alcohol exposure. Since amygdala GM volumes are markedly reduced in ADP compared with age-matched HC, it raises the question of whether these would relate to observed changes in amygdala RSFC. Loss of grey-matter due to chronic alcohol exposure may disrupt neuronal signalling and reduce RSFC, but it may also lead to compensatory upregulation of amygdala RSFC (Upadhyay et al., 2010, Filbey et al., 2014).

While some neuroadaptations may remain persistently present even in longer-term abstinence, others may be expected to show recovery. ADP in shorter-term abstinence (e.g. under 1 year) are at significantly greater risk of relapse (Dawson et al., 2005), which suggests intrinsic differences between their brains and the brains of those in longer-term abstinence (e.g. over 1 year). Since as described above, the amygdala is

implicated in mechanisms of relapse in animal models (Gilpin & Roberto, 2015), the reduction of relapse risk over the time-course of abstinence may express itself as gradual changes in amygdala RSFC. This effect may be observable as a correlation between patterns of amygdala RSFC and abstinence length across ADP.

Anxiety levels peak during alcohol withdrawal (Roelofs et al., 1987), although ADP have been found to exhibit significantly elevated levels of anxiety even after many months of abstinence (Orban et al., 2013). Studies of healthy populations and patients with anxiety disorders have implicated the amygdala in mechanisms of anxiety. Specifically, elevated levels of anxiety have been found to be associated with concurrent elevations of amygdala – insula RSFC. However, it remains unclear whether elevated anxiety within the context of alcohol dependence has the same mechanism, since my previous work has shown increased levels of anxiety with concurrent reductions in amygdala – insula RSFC in ADP (Orban et al., 2013). Given that anxiety is a known risk factor for relapse, this question warrants further investigation (Willinger et al., 2002).

2.6 Pharmacological modulation of amygdala RSFC

The ICCAM platform study is a multi-session, multi-site, pharmacological functional Magnetic Resonance Imaging (fMRI) study designed with the aim of investigating neurophysiological correlates and the potential effectiveness of putative treatments for substance dependence (Paterson et al., 2015). Substance dependent patients with an abstinence length of at least four weeks, and healthy controls, completed scanning sessions on five separate days that included both resting state and task fMRI. Other

than the first session that was treated as Baseline, the other four involved acute drug administration of Placebo, Naltrexone, GSK598809 and Vofopitant or Aprepitant.

Naltrexone, a μ-Opioid receptor antagonist (Le et al., 2000; Liu et al., 2002), and GSK598809 (Vengeliene et al., 2006), a selective Dopamine receptor D3 (DRD3) antagonist, have both been shown to reduce alcohol-seeking and relapse-like drinking behaviours in animal models. Furthermore, Positron Emission Tomography (PET) studies have reported elevated DRD3 (Erritzoe et al., 2014) and μ-Opioid receptor availability (Heinz et al., 2005; Williams et al., 2009) in alcohol dependent populations, where the latter effect was found to be associated with higher-levels of alcohol craving (Heinz et al., 2005).

Vofopitant and Aprepitant are Neurokinin-1 receptor (NK1) antagonists, whose use in ICCAM was motivated by a landmark study showing a reduction in voluntary alcohol consumption in NK1 receptor knockout mice (George et al., 2008). The same study also showed that NK1 antagonism under a repeated dose reduced subjective and endocrine responses to an alcohol-cue challenge in recently detoxified alcohol dependent patients (George et al., 2008). The key endogenous ligand of the NK1 receptor, Substance-P, is released in the amygdala during periods of stress (Ebner et al., 2004), and antagonism of the NK1 receptor has been shown to inhibit stress-induced reinstatement of alcohol-seeking without affecting cue-induced alcohol seeking (Schank et al., 2011).

DRD3 (Murray et al., 1994; Gurevich & Joyce, 1999), μ-Opioid (Lam et al., 2008; Weerts et al., 2011) and NK1 receptors (Hietala et al., 2005) all appear to show expression in the amygdala as suggested by animal autoradiography, human post-mortem autoradiography or human PET studies. Therefore, acute administration of

these compounds may be able to exert a direct modulatory influence on amygdala activity or on its functional interactions with other regions as measured by resting state fMRI. Differences between groups in the magnitude or spatial pattern of acute pharmacological modulation, i.e. a group-by-drug interaction, may be of interest, since it may suggest underlying abnormalities in receptor numbers, occupancy or dynamics in ADP.

As discussed above, the amygdala has been shown to undergo neuroadaptations in response to chronic alcohol exposure, which may influence amygdala resting state functional connectivity. If ADP and HC turn out to show significant differences in amygdala RSFC at Baseline, then an important question to address is whether any of the three putative therapeutic compounds can normalise these abnormalities in ADP. Although the three drugs target different receptor systems, they may exert similar effects on amygdala network function, based on some overlap in their receptor distributions and behavioural effects. The ICCAM Platform study provides a unique dataset where the same group of participants have undergone a pharmacological challenge with multiple compounds. This feature of the study could be leveraged to explore the overlapping and non-overlapping modulatory effects of the three drugs on amygdala resting-state functional connectivity.

2.7 Principles of magnetic resonance imaging

The subchapters below provide a simplified description of the physical and biophysical principles of magnetic resonance imaging, based on a more detailed coverage of the topic by Huettel and colleagues (2008).

2.7.1 Nuclear Magnetic Resonance

Spin is an intrinsic property of atomic nuclei, akin to angular momentum, that is determined by atomic composition. Hydrogen nuclei are widely distributed in the human body, as they are major building blocks of water, fat and other organic molecules. Hydrogen nuclei have a non-zero spin, which means they possess a magnetic moment. Under normal conditions, they can be thought of as spinning at a constant velocity in randomly determined orientations.

When subjected to the strong magnetic field (B_0) of an MRI scanner, the orientation of the hydrogen nuclei become aligned in one of two orientations: facing away from the B_0 axis within a high-energy state or facing towards the B_0 axis within a low-energy state. In a field strength of sufficient magnitude (e.g. 3T), more hydrogen nuclei favour the low-energy state, thereby creating a net magnetization vector (M_0) towards B_0. At the same time the spin states begin to precess (i.e. "spin" in a wobbly manner) around the B_0 axis (z) at a resonant frequency determined by the scanner's field strength.

2.7.2 Magnetic Resonance Imaging

If a radiofrequency pulse of sufficient energy is emitted at the appropriate resonant frequency, two important processes occur: the hydrogen nuclei begin to precess in phase, and they tilt from their original orientation along the B_0 axis (z), towards the xy plane. Since this new orientation represents a higher energy state, the hydrogen nuclei eventually return to their prior orientation. The relaxation of the nuclei produces a magnetic moment, which induces an oscillating electric current on a receiver coil, thereby allowing measurement.

The relaxation of the hydrogen nuclei from their excited spin states occurs in two ways. The return of nuclei to alignment with the B_0 axis (z) is called T1 relaxation, while the decay of their xy component due to dephasing caused by local atomic interactions is called T2 relaxation. This loss of coherence occurs faster than would be predicted based on the dephasing effects of atomic interactions. The remaining decay time, called T2*, is accounted for by inhomogeneities in the local magnetic field, that are caused by scanner-related artifacts and variation in the biological properties of tissue, for example blood oxygenation.

2.7.3. T1- and T2*-weighted images

The versatility of MRI is derived from the experimenter's ability to manipulate T1 and T2 relaxation times through carefully calibrated pulse sequences. Two important parameters are TE, the time interval from the initial RF pulse to the signal readout, and TR, the time interval between consecutive RF pulses. A combination of short TE, and intermediate TR produces a T1-weighted image, as it allows some T1-relaxation to occur as a function of tissue-type, but only minimal T2 relaxation. T1-weighted signal is strongest in white matter (WM), significantly weaker in grey-matter (GM), and weakest in cerebro-spinal fluid (CSF), thereby providing an ideal contrast for visualizing anatomical features of the brain.

T2 and T2*-weighted images require a combination of intermediate TE, and long TR, where T1 relaxation is mostly completed, but T2 relaxation and its T2* component are still at various stages of decay. T2-weighted images show the strongest levels of signal in CSF, followed by GM and the weakest levels in WM, resulting an inverse of ordering of shades as seen for T1-weighted images. T2*-weighted images are calibrated to maximise contrast for changes in blood-oxygenation over time, but have

a poorer effective spatial resolution than T1-weighted images. In addition, they suffer dropout in regions with strong magnetic field inhomogeneities, e.g. at the orbitofrontal cortex due to its proximity to air sinuses. Therefore, experiments that acquire T2*-weighted images, also tend to acquire T1-weighted images. During data-analysis, the two images can be spatially aligned through spatial deformation methods, thereby allowing better spatial localization of the observed functional activity.

2.7.4 Echo-Planar Imaging

Echo-planar imaging (EPI) is the most widely adopted MR-based method for measuring brain activity. In this regime, an initial RF pulse is trailed by a train of gradient echo pulses that allow rapid sampling of T2* decay across a brain slice by exploiting a frequency encoding gradient. Using conventional EPI sequences, a frame of the whole brain can be acquired over 2 to 3 seconds in sequentially sampled slices of roughly 3 mm thickness. The magnitude of the derived signal is driven by (i) the initial magnetization in the xy plane (M_o), (ii) TE, and (iii) T2* decay time. M_o is determined by the net spins excited within a voxel, while TE is chosen by the experimenter to maximize BOLD sensitivity given the scanner's field strength. T2* decay time varies as a function of the underlying tissue properties within voxels (GM, WM, CSF) and crucially, brain activity, which forms the basis of the Blood-Oxygen-Level-Dependent (BOLD) signal.

2.7.5 The biophysical and physiological basis of BOLD

Neuroimaging methods such as Electroencephalography and Magnetoencephalography, can directly measure fluctuations in voltage or magnetic

fields caused by ionic currents that underpin neuronal transmission. In contrast, BOLD fMRI provides an indirect measure of brain activity by exploiting the strong local coupling between neuronal metabolism and hemodynamic regulation. There are two key mechanisms that enable the BOLD contrast to function as an index of brain activity, which were discovered independently by Ogawa and colleagues (1992), Bandettini and coworkers (1992) and Kwong and colleagues (1992).

First, increases in neuronal activity are associated with elevation of cerebral metabolic rate of oxygen consumption ($CMRO_2$). The bulk of this energy expenditure is related neuronal signaling mechanisms such as action potentials, and postsynaptic effects of glutamate, rather than maintenance of resting membrane potentials (Attwell & Laughlin, 2001). This increase in metabolism is compensated for by a disproportionate increase in cerebral blood flow (CBF) and cerebral blood volume (CBV) through vasodilation of local blood capillaries, thereby supplying a concentration of oxyhaemoglobin that outstrips the initial increase in $CMRO_2$. Second, oxyhaemoglobin and deoxyhaemoglobin have distinct magnetic properties: oxyhaemoglobin is diamagnetic, whereas deoxyhaemoglobin is paramagnetic. The paramagnetic property of deoxyhaemoglobin exerts a dephasing effect on the excited spins of the neighbouring protons, resulting in faster T2* decay times relative to oxyhaemoglobin rich regions. In summary, neuronal activity increases local oxygen consumption, which subsequently leads to an oversupply of oxyhaemoglobin, which in turn slows T2* decay in that region, thereby increasing signal levels relative to regions with lower neuronal activity.

Working on the assumption that the BOLD response is relatively uniform across the brain, task fMRI studies tend to model brain activity by convolving the BOLD signal

in each voxel with a canonical hemodynamic response function (HRF). The HRF is commonly modeled using a double-gamma function, with a fixed delay of ~6 seconds, which accounts for the interval between brain activation and the hemodynamic response (Glover, 1999).

2.8 Resting state functional connectivity

Functional connectivity was defined by Karl Friston as "the temporal correlation between neurophysiological (functional) measurements made in different brain areas" (Friston et al., 1993, Page 9). Initially, the concept was utilized in the context of characterising spatially distributed and temporally coherent patterns of activity measured during behavioural tasks with PET (Friston et al., 1993). The first experimental finding of resting state functional connectivity (RSFC) using fMRI is credited to Bharat Biswal and colleagues (Biswal et al., 1995), who found, using fMRI, that the left and right hemisphere sensorimotor regions engaged during a finger-tapping task exhibited highly-correlated spontaneous fluctuations even in the absence of a task, i.e. in the resting state (Biswal et al., 1995). In the following years, similar patterns of temporal coherence were observed in other sensory areas, as well as within functionally related regions across the association cortices. Today, resting state functional connectivity (RSFC) is a widely-used metric for elucidating functional neuroanatomy, and in studies of development, disease and therapeutic interventions.

Resting state functional connectivity is strongly predicted by direct structural connectivity, however not vice versa, as a substantial proportion of RSFC appears to be driven by polysynaptic connections. RSFC is most commonly measured using

univariate statistics such as Pearson correlation or general linear models, or multivariate methods such as independent component analysis (ICA). These approaches are agnostic regarding the directionality or even the mere presence of causal interaction between regions showing strong RSFC. One must be careful not to infer functionality in a biological sense from the word 'functional' in the acronym RSFC, as here 'functional' merely denotes the fact that the measure is derived from time-series data.

Nevertheless, RSFC may indeed have an important biological function that remains to be discovered. The high proportion of the brain's total energy expenditure accounted for by spontaneous activity speaks in favour of a possible biological function (Raichle & Mintun, 2006). According to one hypothesis, RSFC may play a role in the maintenance of synaptic weights within large-scale ensembles during periods of inactivity (Buckner & Vincent, 2007). Indeed, several studies have documented a correspondence between large-scale networks defined by resting state functional connectivity profile, and patterns of co-activation observed during specific cognitive tasks (Smith et al., 2009; Mennes et al., 2010; Cole et al., 2014). However, the degree of correspondence between rest and task-associated co-activation patterns varies across brain networks and tasks (Mennes et al., 2010; Cole et al., 2014), therefore resting state fMRI is unlikely to provide a full account of the brain's functional repertoire.

Similar to the structural connectome, the broad topography of the core canonical networks defined by resting state functional connectivity appears to be universally expressed in humans. Analogues for some of these networks, such as the default mode network (DMN), have been also been shown to exist in primates (Vincent et al. 2007)

and rodents (Lu et al., 2012). Superimposed on these broad universal features, patterns of RSFC have been shown to exhibit inter-subject variability as a function of trait-level characteristics such as age, BMI, personality (Kelly et al., 2012). RSFC in specific networks has also been found to have sufficient test-re/test stability to allow detection of longitudinal effects of ageing (Fjell & Walhovd, 2017) and neurological and psychiatric diseases (Greicius et al., 2008).

Moderate levels test-re/test reliability within many RSFC circuits has also enabled the feasibility of characterizing the effects of acute pharmacological modulation, i.e. resting state pharmacological fMRI (De Simoni et al., 2013). Since the advent of the technique, biologically plausible pharmacological effects have been reported for a wide range of compounds, for example L-dopa (Kelly et al., 2009), nicotine (Cole et al., 2010) and ketamine (De Simoni et al., 2013).

2.9 Artifacts in resting state fMRI

Since the advent of functional MRI, there has been a gradual effort to identify different sources of noise in the data and to develop effective pre-processing and modeling approaches to mitigate their effects. Some types of noise arise from biophysical constraints of functional MRI, such as signal distortion, signal dropout and thermal noise. Other types of noise originate from the subject's physiological state and behaviour, for example patterns of cardiac cycle, respiratory volume or rate, head and chest motion. These latter types of artifacts affect resting state fMRI more severely than task fMRI, and the optimal method for dealing with them has been a focal point of debate in the field.

In task fMRI analyses, data is generally analysed within the framework of a so-called cognitive-subtraction paradigm, where brain activity is modeled as a contrast of similar events or blocks, whose distinguishing feature defines the phenomenon of interest. For example, the neural correlates of facial recognition may involve comparison of brain activity during observation of familiar with unfamiliar faces. Data is typically averaged across multiple events or blocks, which in this context is an effective approach for minimizing noise. Systematic bias may creep in if certain types of noise affect the compared events or blocks differentially, for example in reaction-time experiments, more difficult trials may be associated with greater subject motion or changes in breathing patterns.

Unlike in task fMRI where the task-model is determined prior to data-collection, in resting state fMRI the model is derived from the data itself, e.g. usually the mean spontaneous signal over time across voxels within a region of interest. Spurious signal introduced from head motion or respiratory influences may corrupt the model (seed voxels), the data (non-seed voxels), or both, which can result in over or under-estimation of RSFC. These effects do not necessarily diminish when computing correlation metrics over longer durations, and a single outlier time-point can substantially alter RSFC measurements (Power et al., 2014).

2.9.1 Motion

Head motion has been known to be a major source of noise in functional MRI experiments since the mid-1990s (Hajnal et al., 1994; Biswal et al., 1995; Friston et al., 1996). It may manifest as a gradual shift in head position, a sudden change in head or body posture, or as small, periodic movements associated with respiration and cardiac pulsation.

The classical approach for correcting image misalignment is the rigid-body registration of all volumes to a single reference volume. An additional benefit of this realignment procedure is that it provides vector estimates of the frame-to-frame displacement of each volume with respect to the reference volume, along three principal dimensions (x,y,z) and three rotational axes (yaw α, pitch β and roll γ).

Framewise displacement (FD) is defined as the sum of the first derivatives of these six parameters at each frame, while absolute displacement is the sum of the six motion parameters at each frame (Power et al., 2012). Prior to both calculations the three rotational vectors can be converted to distances by calculating their arc length displacement on the surface of a 50 mm radius sphere (Power et al., 2012). FD predominantly reflects sudden movements between consecutive frames, while absolute displacement generally encodes gradual drifts in head position.

The original six motion parameters (from the rigid-body realignment), and sometimes their first derivatives, are normally regressed out of the data as an additional denoising approach to suppress motion-related spikes (Bullmore et al., 1999). Although this method is useful and widely adopted, it is unable to capture the non-uniform spatial distribution of artifacts or motion that occurs in-between the acquisition of slices. Head motion can sometimes also shift voxels into neighbouring slice positions, thereby altering the interval between RF excitation pulses. This artifact is called the spin-history effect and it can lead to large increases or decreases in signal depending on the direction of motion in relation to the slice acquisition pattern. Until recently, the consensus had been that unless a participant exhibited extreme levels of motion (e.g. > 1.0 mm mean FD), rigid-body realignment and

motion parameter regression were sufficient for removing motion-related artifacts in task and resting state fMRI data.

However, in 2012 several studies observed that even submillimetre levels of motion exerted a significant effect on RSFC estimates, suggesting that re-alignment and motion-parameter regression were by themselves inadequate (Van Dijk et al., 2012; Power et al., 2012; Satterthwaite et al., 2012). In the first of these studies (Van Dijk et al., 2012), subgroups of healthy controls matched in key demographic variables, but separated by small differences in motion on the order of tenths of mm in mean FD, exhibited significant group-differences in. This was disconcerting since these observed group differences in RSFC were comparable in magnitude to group differences reported in previous studies where they were interpreted as neural correlates of ageing, ADHD and autism.

Another important finding to arise from these studies was that motion artifacts exhibited a Euclidian distance-dependent bias, whereby subject motion lead to over-estimation of RSFC between nearby regions and under-estimation of RSFC between distant regions (Satterthwaite et al., 2012; Power et al., 2012; Power et al., 2014a). Such a systematic bias may introduce apparent reductions of RSFC in networks anchored by distant nodes such as the midline structures in the default mode network (DMN), while at the same time causing apparent increases in RSFC in limbic or fronto-striatal networks.

In order to address this problem, Power and colleagues (2012) proposed the technique of motion scrubbing, which involves removal of corrupted frames from the data. Frames were tagged for removal if they exceed a certain threshold of FD (e.g. > 0.2 mm) or percent signal change (e.g. > 0.3 %), defined as the root mean square of the

temporal derivative of the whole-brain averaged BOLD time series (DVARS). Since then, various implementations of this method have been used, including ones where both the initially preceding frame and several succeeding frames are removed in relation to the motion outlier. Additional derivations of this approach, include scrubbing by interpolation over outlier frames (Carp, 2013), and scrubbing implemented within the framework of regression (Satterthwaite et al., 2013).

Scrubbing has become a widely adopted method for removing distance-dependent motion artifacts (Power et al., 2014a). However, it does incur a trade-off, whereby aggressive censoring thresholds remove excessive variance from the data, while liberal thresholds may be ineffective in removing motion-related artifacts (Patel et al., 2014). An additional guideline that has arisen from the above work is the importance of balancing motion between experimental groups, and running post-hoc tests to make sure that motion statistics do not correlate with measures of interest, e.g. disease severity.

2.9.2 Physiological artifacts

As described above, the BOLD signal provides a spatially selective measure of brain function through the local coupling between neuronal, metabolic ($CMRO_2$), and hemodynamic physiological processes (CBV and CBF). However due to its indirect origin, the BOLD signal is vulnerable to physiological confounds that are not related to neuronal activity.

Arterial carbon dioxide (CO_2) is a strong vasodilator. Hypercapnia induced through inhalation of CO_2-enriched air has been shown to increase both CBF (Poulin et al., 1996; Ide et al., 2003) and BOLD signal (Rostrup et al., 2000). Elevation of CBF is

normally associated with a reduction of deoxyhaemoglobin concentration in the cerebral vasculature. Indeed, studies have observed global elevations of BOLD signal during cued-breath holds (Murphy et al., 2011), and reductions during epochs of cued-hyperventilation (Posse et al., 2001). Similar artifacts associated with intermittent deep breaths have also been found to be a common feature of fMRI experiments where participants are allowed to breath freely (Power et al., 2016). In addition, arterial CO_2 concentration exhibits low frequency fluctuations (0-0.5 Hz), which have been shown to introduce artifactual variance into the BOLD signal via their modulatory effects on CBF (Wise et al., 2004).

Independent of subjects' ability to keep still and to breath at a constant rate and depth, the respiratory and cardiac cycles introduce small periodic motion-artifacts. Regions near large blood vessels such as the brainstem are particularly vulnerable to pulsatile motion resulting in tissue deformation and disruption of steady-state magnetization (Dagli et al., 1999). Cerebral spinal fluid in surrounding regions also incurs pulsatile movement patterns, which can spread these artifacts to farther regions (Greitz et al., 1992). Since ventilation and pulse cycles occur at a higher frequency than the low resting state BOLD fluctuations of interest (0.01-0.1 Hz), bandpass filtering can remove some of this artifactual variance. However, a significant amount of respiratory variance remains aliased in the signal due to the slow sampling rate (TR 2-3) employed in conventional single-echo EPI sequences, which tend to prioritise whole-brain coverage and spatial resolution over temporal resolution (Birn, 2012).

Another method for removing respiratory influences from BOLD is RETROICOR (RETROspective Image CORrection), which involves slice-wise correction for respiratory and cardiac phase using multiple time-shifted regressors derived from

pulse oximeter and respiratory belt data (Glover et al., 2000). However, some studies have shown that these physiological regressors only account for a minimal amount of BOLD signal variance in grey-matter (Bianciardi et al., 2009; Jo et al., 2010). RETROICOR is maximally effective with a larger number of regressors, but this may lead to excessive loss of degrees of freedom that is a problematic in analyses of short scan (Jo et al., 2010). Furthermore, some experimenters may not have the necessary equipment or decide against the acquisition of respiratory data to minimise participant discomfort and scan preparation time.

2.9.3 Nuisance regression

As mentioned previously, the regression of rigid-body realignment parameters is a widely used method of denoising in both resting state and task fMRI studies. In resting state fMRI studies, experimenters tend also to regress additional sources of noise, so called nuisance regressors, in order to suppress spurious correlations in the data. These nuisance regressors are usually defined by averaging BOLD signal within anatomical masks of ventricles, white matter, cerebrospinal fluid and whole-brain mask that have been spatially co-registered to their corresponding functional images (Power et al., 2014b). The assumption behind nuisance signal regression is that tissue types other than grey-matter are unlikely to reflect neuronal components of BOLD (van Dijk et al., 2010). Regression of mean signal computed from a whole-brain mask, i.e. global-signal regression, therefore is controversial, since by definition it also includes signal from grey-matter regions. Here the rationale is that physiological noise is likely to comprise a large-component of correlations shared across the entire brain, the removal of which may improve detection of signal in grey-matter driven by local neurovascular coupling (Fox et al., 2009).

Without nuisance signal regression seed-based RSFC maps generally exhibit strong levels of correlations across voxels spanning almost the entire brain. As more nuisance regressors are included in the model, the RSFC maps generally become more specific to anatomically and functionally related regions, suggesting improved specificity (Jo et al., 2010). Amongst the commonly used nuisance regressors, global signal regression has the most drastic effects, while also removing the most amount of variance from the data. However, its use appears to have both desirable and undesirable features that have made it a topic of intense debate in the field (Murphy & Fox, 2016).

Global signal regression is known to introduce spurious negative correlations in the data and to exacerbate distance-related motion artifacts (Satterthwaite et al., 2012). For example, use of global signal regression may contribute to overestimation of RSFC for nearby regions, and underestimation of RSFC for distant regions, as a function overall head motion levels in the dataset. Regression of signal from non-brain tissue (Jo et al., 2010), or from principal components of white matter and ventricles have been proposed as effective alternatives for global signal regression that do not incur these same drawbacks (Behzadi et al., 2007; Muschelli et al., 2014). Furthermore, use of local white matter regression has also been found to reduce distance-related motion artifacts (Jo et al., 2010; Jo et al., 2013). This voxelwise regressor is calculated by averaging white matter signal within 25 mm radius spheres centered on each voxel.

2.10 Biomarkers

One reason for the slow rate of progress in the development of effective treatments for alcohol dependence is likely to be our relative ignorance regarding its key mechanisms. Although it is widely understood that alcohol dependence is a disorder of the brain, we have yet to develop a neuroscientific methodology for its diagnosis. On the level of an individual, even state of the art neurophysiological metrics are inadequate for determining likelihood of acquiring alcohol dependence, the evolution of its symptoms and severity, or predicting likelihood of relapse during abstinence. Animal studies typically assess the effectiveness of putative treatments by their ability to curb relapse rates under experimental manipulations that precipitate drinking behavior. Although some compounds have shown good efficacy within these animal models, more often than not, their success fails to replicate in human clinical studies.

Interspecies differences in brain physiology such as receptor distribution, or macroscopic cortical organization are likely to be a source of many failures of translation, reflecting the complexities of modeling a human disease in animals. In addition, the outcome of these studies, relapse, occurs under very different conditions. In animal models relapse is induced by carefully calibrated experimental manipulations that are observed under laboratory conditions, while in human clinical studies it occurs spontaneously in a naturalistic context, and is retrospectively reported by patients. Since large-scale clinical trials of relapse-prevention drugs are expensive and time consuming, there is a substantial incentive for the development of biomarkers that could potentially serve as surrogate-endpoints in these studies.

A biomarker may be defined as “a characteristic that is objectively measured and evaluated as an indicator of normal biologic or pathogenic processes or

pharmacological responses to a therapeutic intervention" (Biomarkers Definitions Working Group, 2001). Although diseases may express a range of physiological correlates, only those that show a sufficiently high level of specificity and sensitivity to the target disease are suitable as biomarkers. An ideal biomarker will also exhibit a number of additional desirable features (Fedota & Stein, 2015; Woo & Wager, 2015):

(i) *transparency* – the mechanism of the measure should be well understood;

(ii) *replicability* – produces similar results under constant conditions;

(iii) *robustness* – produces similar results under different conditions and is generalizable across different demographics;

(iv) *mechanistic relevance* – should be directly related to disease mechanism;

(v) *responsivity to treatment*

(vi) *non-invasiveness*;

(vii) *easy of acquisition*;

(viii) *low cost*.

2.11 Thesis rationale and summary of hypotheses

Over the last two decades, clinical neuroscience has undergone somewhat of a renaissance in its approaches to investigating diseases. There has been a gradual shift away from research aimed at modular localisation of function to network-level description of disease mechanisms. An increasing preference for systems-level models has been likely aided by significant increases in computational power over the years.

Recent times have also seen a recognition of the importance of data-sharing (e.g. ADNI; http://www.adni-info.org/), and collaborative data-collection through multi-site studies, including in the field of mental health (e.g. IMAGEN, http://www.imagen-europe.com). These efforts can greatly reduce the potential interval between hypotheses and clinically relevant insights.

Finally, the development of pharmacological functional MRI (phfMRI) has provided a powerful tool for investigating both disease mechanisms and the effects of putative treatments. The absence of ionizing radiation in phfMRI, unlike in PET, has enabled the design of imaging studies where participants undergo multiple sessions within weeks of each other, and at a fraction of the cost of PET.

My PhD aims to exploit this rich dataset provided by the ICCAM platform study to characterise amygdala resting state network function in alcohol dependence during baseline conditions, and under acute antagonism of three receptor systems (μ-opioid, Dopamine D3, Neurokinin-1) that have been closely implicated in mechanisms of addiction.

Investigating amygdala resting state functional connectivity (RSFC) through a seed-based approach will provide me with a single target of interest around which to synthesise previous findings from animal and human studies. Both of these have suggested a significant role for the amygdala in mechanisms of alcohol dependence. At the same time, applying a whole-brain approach to the seed-based analysis will leave open the possibility of discovering novel effects in regions not currently associated with amygdala function. Although resting state function is intrinsically unconstrained, the rich phenotypic data provided by ICCAM in the form of task

fMRI, neuropsychological assessment, psychological measures, and clinical variables will significantly help in interpreting my results.

The work presented in this Thesis is built around the following eleven hypotheses:

Hypothesis I: Alcohol dependent patients in abstinence would show differences in patterns of resting state functional connectivity compared with age-matched healthy controls.

Hypothesis II: Regions showing significant differences in amygdala RSFC between ADP and HC, would correlate with lifetime cumulative alcohol exposure in ADP.

Hypothesis III: The findings of lower amygdala GM volume would be replicated in the current sample of ADP, and amygdala GM volume in ADP would be inversely correlated with cumulative alcohol exposure.

Hypothesis IV: ADP with smaller amygdala GM volumes would exhibit greater differences in amygdala RSFC compared with HC.

Hypothesis V: Amygdala – insula RSFC would be positively correlated with measures of trait and state anxiety in ADP.

Hypothesis VI: There would be a positive association between amygdala – insula RSFC and amygdala responsivity within the Evocative Images Task.

Hypothesis VII: Abstinence length would be linearly associated with amygdala RSFC in ADP.

Hypothesis VIII: In regions where amygdala RSFC varies as a function of abstinence length, it would also show linear associations with magnitude of task-activation in the Evocative Images Task or the Go/No-Go task.

Hypothesis IX: One or more of the three drugs may modulate amygdala RSFC differentially in ADP than in HC, producing a group-by-drug interaction.

Hypothesis X: At least one of the three drugs would normalize alterations in amygdala RSFC in ADP to levels observed in HC.

Hypothesis XI: The three drugs may exhibit both spatially overlapping and spatially non-overlapping effects on amygdala RSFC.

These hypotheses are discussed in further detail in Chapter 4 (I-IV), Chapter 5 (V-VIII) and Chapter 6 (IX-XI).

Chapter 3: Methodology

3.1 Study description

3.1.1 Introduction of ICCAM

All imaging and clinical data in this work was collected as part of the ICCAM platform study: a multicentre, multisession study, set up with the core aims of identifying novel indicators of addiction mechanisms and to test the effectiveness of putative pharmacotherapies for relapse prevention.

As only a subset of the data from the entire ICCAM platform study is relevant to the questions addressed in this thesis, the description of ICCAM below is not exhaustive. For a comprehensive summary of ICCAM please consult Paterson et al., 2015. This chapter provides an overview of ICCAM's design, followed by a description of selection criteria used for participant recruitment, clinical assessment, the scanning protocol and the MRI acquisition parameters. Aspects of the design specifically relevant for each chapter are further described in-depth in their respective methodology sections.

3.1.2 Overview of study procedures in ICCAM

Following an initial assessment of eligibility through telephone interviews, participants attended up to five separate sessions on each site. A timeline of the experimental procedures implemented in ICCAM across various stages of the study are illustrated in Figure 3.1 below.

On the first session, (referred to as 'Baseline' throughout the thesis), the MRI imaging protocol was flanked by an extended session of clinical assessment in the morning,

and by comprehensive testing of neuropsychological function in the afternoon. The clinical assessment included general medical and physical examination, as well as an in-depth interview of current and historical psychiatric and substance-use profiles. Additionally, participants underwent urine tests for recent recreational drug use and an alcohol breath-test. The neuropsychological assessment included tasks from the Cambridge Neuropsychological Test Automated Battery (CANTAB, www.camcog.com), as well as "paper-and-pencil" tests of cognitive function and psychological traits. No experimental drugs were administered on this session.

On each of the other four sessions participants received an acute oral dose of either Naltrexone (50 mg), GSK598809 (60 mg), Vofopitant (10 mg) or Placebo (100 mg of Vitamin C), so that by completion of the study participants had under gone assessment under each drug. Vofopitant exceed its expiry date halfway through the study and was replaced by Aprepitant (80 mg), therefore this drug condition is referred to as Vofopitant/Aprepitant in the remainder of the thesis.

The four 'drug sessions' included a brief medical examination, urine drug and alcohol breath tests, and drug dosing ~2 hours before the scanning protocol. At regular intervals throughout the session both before and after drug administration, physiological indicators were monitored through measurement of blood pressure, blood oxygen saturation, resting echocardiogram measurements, while subjective state over time was assessed through visual analog scales (Bond and Lader, 1974).

The scanning protocol on Baseline sessions consisted of the following sequence of components: localiser, structural scan, resting state scan, Monetary Incentive Delay Task, Go/No-Go task and Evocative Image Task. This protocol was identical on all five sessions, except the structural scan was only acquired on the first session.

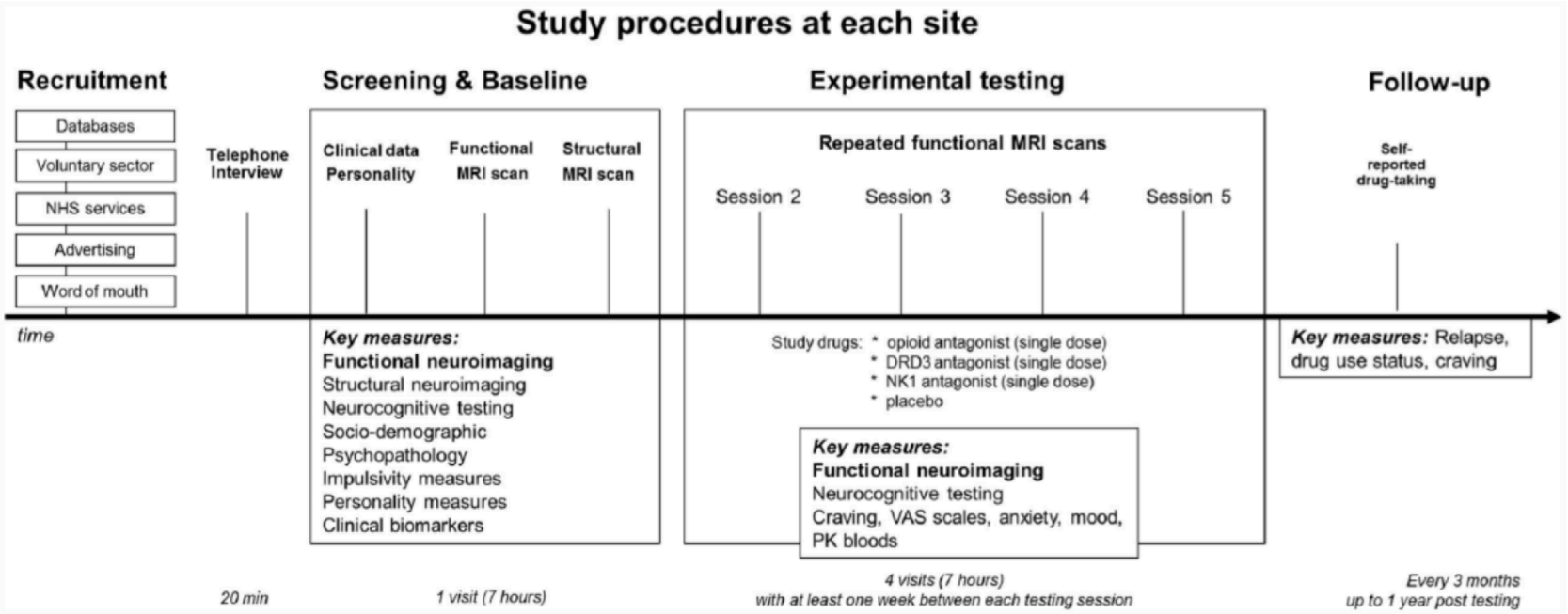


Figure 3.1 Timeline summary of the experimental protocol carried out at each of the three sites in the ICCAM platform study, reproduced with permission from Paterson et al., 2015.

3.1.4 Recruitment strategy

Participant recruitment and data-collection occurred in parallel at three collaborating institutions: Imperial College London, University of Cambridge and The University of Manchester. Study recruitment targeted both alcohol dependent patients (ADP) and polydrug-dependent patients who have reached at least one month of abstinence, as well as healthy controls (HC), who were matched for age and gender. An attempt was also made to maximise recruitment of HC with similar levels of education background and smoking status relative to the patient groups. At the Imperial site an additional cohort of healthy participants (Pilot) took part in a portion of the study protocol to fill-in unused scanner slots. The current thesis did not examine data from polydrug-dependent patients.

Further details regarding the experimental design, including pseudo-randomisation of the drug sessions, criteria for excluding participants based on data quality, the descriptions of clinical and demographic profiles of participants, a detailed description of the Go/No-Go task and Evocative Image Tasks, are to be found in the specific chapters where they are relevant to understanding the analysis.

3.1.4 Approvals

Participants provided their written informed consent in accordance with the Declaration of Helsinki. Ethical approval was obtained from West London & GTAC NRES committee (11/H0707/9) and approvals from Research Governance and PICs (Participant Identification Centres). Recruitment, clinical assessments and scanning took place at three centres in the United Kingdom: Imanova Limited, London; The

Wolfson Brain Imaging Centre, University of Cambridge; Salford Royal NHS Foundation Trust, Manchester.

3.1.5 Inclusion and exclusion criteria

Inclusion criteria required ADP to meet DSM-IV criteria for current or prior alcohol dependence, but not dependence on other drugs, except for nicotine. ADP were required to have been abstinent for at least 1 month prior to the day of scanning. Healthy controls were not permitted any history of drug or alcohol dependence, except for nicotine.

The following exclusion criteria were applied for both ADP and HC: (i) current primary axis I diagnosis; (ii) current or past history of enduring severe mental illness, including psychosis, however secondary or lifetime history of depression or anxiety was permitted due to high comorbidity; (iii) history of significant neurological diagnosis; (iv) prescription medication that could interfere with study integrity or safety (v) any MRI contra-indication (e.g. pregnancy, claustrophobia, pacemaker); (vi) positive breath alcohol or positive urine drug test on day of scan (amphetamines, barbiturates, cocaine, opiates, cannabinoids and benzodiazepines). Participants were advised to refrain from cannabis use for at least one week prior to day of scanning. On study days participants were permitted to smoke cigarettes up to ~1 h before scanning.

3.1.6 Materials

A detailed account of lifetime drug and alcohol use of each participant was obtained through a combination of clinical interviews, the Alcohol, Smoking and Substance Involvement Screening Test (ASSIST) and timeline follow-back. The presence of Axis I psychiatric diagnoses were screened using a summarized version of the Structured Clinical Interview for DSM-IV (MINI; Sheehan et al., 1998), and a study physician undertook a further psychiatric history, including family history, and performed a medical examination. All psychiatric and substance dependence histories were subsequently reviewed by two psychiatrists to ensure uniformity of diagnostic thresholds across sites, and any discrepancies arbitrated by a third psychiatrist. Structural brain scans were assessed by a neuroradiologist for any clinical issues.

Cumulative alcohol exposure measure was calculated for all ADP. This was counted in whole years due to the method of data collection using the timeline follow-back. For 1 year to be counted for a male patient it had to exceeded 50 UK units of alcohol per week, or have more than 3 binges of at least 8.75 UK units per week, and for a female patient it had to exceed 35 UK units per week or more than 3 binges of at least 7 UK units per week. Abstinence length was measured from last date of alcohol consumption. Severity of nicotine dependence was estimated using the Fagerström Test for Nicotine Dependence (Heatherton et al, 1991). Cigarette package years (pack years) were defined as number of packs of cigarettes smoked per number of lifetime years. Symptoms of anxiety were characterized using Spielberger Trait Anxiety Scale (STAI), and Spielberger State Anxiety Scale (SSAI; Spielberger et al., 1983). Premorbid IQ was estimated using Wechsler Test of Adult Reading (WTAR; Wechsler D. 2001), and handedness measured using the Edinburgh Handedness Inventory (Oldfield et al., 1971).

3.1.7 Structural acquisition

In London and Cambridge, high resolution (1mm isotropic), T1-weighted volumes were acquired with the following parameters on a Siemens scanner, TR : 2300 ms, TE : 2.98 ms, matrix = 240 x 256, TI : 900 ms, FOV : 256 mm, flip angle : 9°. In Manchester, the high resolution T1-weighted volumes were acquired with slightly different parameters, on a Philips scanner, TR : 6.8 ms, TE : 3.1 ms, TI : 900 ms, flip angle : 9°, field of view : 270 mm, matrix : 256 x 256. Slice thickness was 1.2 mm with an in-plane resolution of 1.055 x 1.055 mm. Both of these acquisitions resulted in whole-brain coverage.

3.1.8 Functional acquisition

In London and Cambridge, acquisition of functional data (EPI) was implemented according to the following parameters, TR : 2000 ms, TE : 31 ms, flip angle : 80°, field of view : 225 mm, matrix = 64 x 64. Thirty-six slices were collected, at a thickness of 3mm, with an in-place resolution of 3.516 x 3.516 mm. In order to minimise dropout near sinuses in the ventral forebrain, slices were acquired at a 30° angle to the anterior and posterior commissure line. The initial three volumes of each run were discarded. Manchester implemented identical parameters except they collected 34 slices.

3.2 Preprocessing

3.2.1 Structural preprocessing

Structural T1 images were intensity normalized (AFNI's *3dUniformize*), brain extracted (as part of Freesurfer's recon –all; followed by FSL's *bet*), and registered to FSL's default MNI152 2mm brain template using affine and diffeomorphic non-linear transformation models (ANTs' AntsRegistration with SyN; Avants et al., 2008). The native structural images were segmented in order to define white matter (FSL's *fast*), and CSF (FSL's *fast*), ventricles (as part of Freesurfer's recon –all), and a composite mask of subcortical structures (thalamus, amygdala, hippocampus, putamen, pallidum, caudate).

For subsequent voxel-based morphometry, partial volume estimates of grey matter (FSL's *fast*) were registered to MNI152 2mm space using the previously calculated transformation matrices, Jacobian modulated (ANTs' *ANTSJacobian*), and spatially smoothed at 6 mm FWHM (AFNI's *3dBlurinmask*).

3.2.2 Functional preprocessing

Functional images initially underwent despiking (AFNI's *3dDespike*), slicing timing correction (AFNI's *3dTshift*), rigid-body motion correction (AFNI's *3dvolreg*), brain extraction (FSL's *bet*) and boundary-based registration to their corresponding native T1 image (FSL's *epi_reg*). This boundary based transformation matrix and the previously calculated transforms of the T1 image were applied in a single step (ANTS' *AntsapplyTransforms*) to register the EPI images to MNI152 2mm space. EPI images were spatially smoothed at 6 mm FWHM (AFNI's *3dBlurinmask*).

After registration of EPI images, motion scrubbing was implemented for volumes with framewise displacement (FD) greater than a threshold of 0.5 mm. Scrubbing involved replacing each flagged volume with the arithmetic mean of the preceding and subsequent volumes. Following scrubbing, EPI images were bandpassed to retain frequencies between 0.01 and 0.1 Hz (AFNI's *3dbandpass*), and detrended (AFNI's *3dDetrend*). After regression of noise parameters, EPI images were grand-median scaled to a subject-specific value of 1000 to allow compatibility with FSL's feat.

The preprocessing for the functional MRI task data was identical to the resting state preprocessing, except it did not involve despiking, scrubbing, low-pass filtering and nuisance signal regression.

3.2.3 Regression of noise

Noise parameters that were regressed out of the data included the six canonical vectors derived during the motion correction step, and mean signal from the ventricles, draining veins (DV), and local white matter (WMlocal). The six motion parameters were bandpassed and detrended in an identical manner as the EPI images. Ventricles were defined by Freesurfer's automated segmentation algorithm, while DV was defined by subtracting the Ventricles from the CSF mask. WMlocal is a voxelwise regressor, calculated by assigning a value of activation to each voxel in the brain from the mean level of activation of voxels situated in white matter (FSL's *fast*) within a 25 mm radius sphere, for each volume (AFNI's *3dLocalstat;* Jo et al., 2010). Several steps were taken to minimise accidental removal of signal of interest with regression of nuisance parameters: mean time-courses were derived from an unsmoothed EPI image, all tissue masks used for nuisance regression were eroded by 2mm, and finally the previously calculated composite map of subcortical structures

was subtracted from the white matter mask of each subject. Regression of these putative nuisance time-series was undertaken in a single step during preprocessing (AFNI's *3dBandpass*).

3.2.4 Rationale for preprocessing approaches used

As readily apparent from the preceding subchapter, the preprocessing pipeline for the resting state data made use of algorithms from several software suites. The intention here was not to systematically compare distinct preprocessing approaches and their parameter spaces. Instead, the aim was to make maximal use of recent findings and observations in the field of preprocessing methodology. This subsection presents a number of salient examples of how insights from the literature were implemented in the current analysis.

Rigid-body registration between the native T1 and native functional image was carried out in FSL using Boundary-Based Registration (BBR), an algorithm that was originally developed for Freesurfer (Greve & Fischl, 2009). BBR presents a significant improvement over FSL's FLIRT approach, which is vulnerable to systematically misaligning structural and functional images due to the presence of signal dropout in the latter (Greve & Fischl, 2009).

Non-linear registration accuracy is particularly important when studying patient populations with strong underlying structural abnormalities such as ADP. The ANTs' SyN algorithm was chosen to non-linearly register the T1 images of participants to the MNI152 2mm template (Avants et al., 2008), due to its highly favourable performance across different brain regions and subject groups compared with other, more popular algorithms such as FSL's FNIRT (Klein et al., 2009).

The threshold for scrubbing outlier time points was set at 0.5 mm, instead of the commonly used threshold of 0.2 mm in studies of healthy controls (Power et al., 2014a). This was to be able to retain at least 5 minutes of data (150 time points) in ADP following scrubbing, which is the minimum amount of data recommended for safely interpreting RSFC (Van Dijk et al., 2012). Taking on the advice of Carp (2013), the scrubbing interpolation step was implemented prior to temporal bandpass filtering of the data to avoid spreading of movement artifacts to neighbouring time points.

Global signal was not used as a nuisance regressor to avoid introduction of spurious negative RSFC, or unintended removal of signal of interest (Murphy et al., 2009). Instead, a draining vessel-based mask distributed within sulcal CSF was used to attempt to remove excessive variance of probable physiological origin (Jo et al., 2010), without sampling signal from GM voxels. In order to avoid blurring in signal of interest from neighbouring GM voxels all tissue masks were unsmoothed and eroded prior to extraction of nuisance regressors (Jo et al., 2010). A localWM (voxelwise) regressor was used instead of the more conventionally derived global WM regressor. This has been shown to be effective at reducing distance-dependent motion artifacts (Jo et al., 2013), and spatially localised spikes caused by defects of coil arrays (Jo et al., 2010).

Since the six motion parameters and nuisance time-courses were derived prior to bandpass-filtering of the data, these were separately band-pass filtered to prevent reintroduction of undesirable frequencies into the data during multiple regression, as suggested by Hallquist and colleagues (2013).

3.3 Statistical modelling

3.3.1 Seed selection

A bilateral amygdala seed (Figure 3.2) was defined by placing two 5mm radius spheres in grey-matter, centred within activation clusters reported in a previously published Activation Likelihood Estimation analysis of amygdala responsivity (Costafreda et al. 2008). Amygdala time series were extracted from the fully preprocessed resting state EPI of each participant and modelled within the framework of a GLM (FEAT, FSL), after correcting for local temporal autocorrelations (FILM, FSL). The resulting statistical maps provided a voxelwise estimate of amygdala resting state functional connectivity (RSFC) for each subject.

3.3.2 Alternative approaches for mapping amygdala network function

In this study, the amygdala seed was defined as bilateral 5 mm radius spheres placed on foci consistent with a large-scale meta-analysis of amygdala task-activation. Other studies have also defined the amygdala based on manual tracing (Entis et al., 2012), task-based functional localisation (Sutherland et al., 2013), automated segmentation of T1 images (Chupin et al., 2009), probability map from the Harvard-oxford atlas (Kim et al., 2011), AAL atlas (Hahn et al., 2011), or the Juelich histological atlas (Roy et al., 2009). The range of methodologies reveals the fact that there is no consensus on the optimal way of defining the amygdala. A systematic comparison of these various approaches may help the field converge on a single approach, which would facilitate interpretability of meta-analyses, and relating results across different studies. Although with in-vivo imaging methods ground truth is difficult to find,

benchmarks such as functional homogeneity, biological plausibility of RSFC maps and susceptibility to artifacts may prove useful.

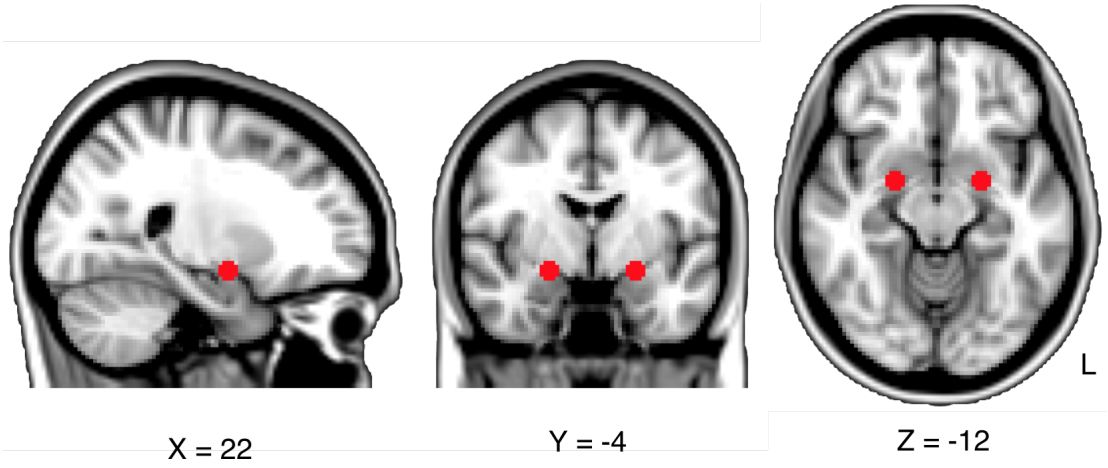


Figure 3.2 Amygdala seed used throughout this thesis for resting state functional connectivity analyses. Co-ordinates were placed according to a large Activation Likelihood Estimation study of emotional processing (Costafreda et al., 2008).

Another related question is whether seed-based RSFC analyses of the amygdala should define the amygdala as a whole, or further subdivide it into subregions. Currently, the Juelich atlas (Amunts et al., 2005) is the most widely adopted atlas for defining amygdala subregions in fMRI studies. However as discussed in Chapter 2, the accuracy of this atlas is questionable due being based on a small sample of participants (n = 10) and its reliance on outdated, affine spatial registration. High field (7T) MRI studies offer another avenue for constructing subregional parcellations for in vivo-studies, although current efforts have also been hindered by small samples sizes (Solano-Castiella et al., 2012). Additionally, high tesla gradient echo-sequences suffer from susceptibility artifacts caused by nearby sinuses, the sinus sphenoidalis is located next the amygdala), while turbo spin echo sequences are known to incur contrast and intensity distortion caused by RF field inhomogeneity (Van de Moortele et al., 2005).

Chapter 4: Group-level effects of alcohol dependence

4.1 Introduction

4.1.1 Neuroadaptations

Chronic, excessive alcohol consumption is associated with widespread neuroadaptations, whose effects become unmasked during withdrawal as intense autonomic and emotional disturbances, which in turn negatively reinforce alcohol consumption (Koob, 2008). Relapse is common within the initial months of abstinence (Charney et al., 2010), while in those who achieve longer-term abstinence, symptoms of anxiety and dysphoria often persist (Heilig et al., 2010). An influential model proposes that cumulative alcohol exposure elicits an allostatic load, a persistent shift in the baseline function of motivational and stress circuits, thereby predisposing individuals to relapse to their original state of alcohol consumption (Koob and LeMoal, 2008).

4.1.2 Amygdala in alcohol dependence

Animal models have highlighted the amygdala as a critical site for allostatic changes which drive escalation of alcohol intake and stress-induced reinstatement (Koob, 2009). The amygdala is an evolutionarily well-conserved complex of subcortical nuclei involved in fear conditioning, acquisition of stimulus-reward associations and bodily responses to stressors (Janak and Tye, 2015). Chronic alcohol exposure has been shown to augment GABA release in the central nucleus of the amygdala (Roberto et al., 2004) via upregulation of ‘pro-stress’ neuropeptides (Roberto et al.,

2010). The resulting increase in local inhibition in the central amygdala has been hypothesized to drive the net disinhibition of downstream effectors, e.g. hypothalamic, dopaminergic or noradrenergic brainstem nuclei, thereby providing a possible feed-forward mechanism for maintaining positive and negative reinforcement of alcohol consumption (Koob, 2009, Gilpin and Roberto, 2012, 2015).

4.1.3 Amygdala RSFC and GM volume in alcohol dependence

Although animal studies have made great strides in elucidating local neuroadaptations within circumscribed brain regions, a more comprehensive neurobiological model of alcohol dependence requires a systems-level mapping of interactions between multiple brain regions in man. Resting state functional connectivity (RSFC) has been increasingly applied to characterise network-level dysfunction in substance dependent populations. Studies that have looked at amygdala RSFC in alcohol (Orban et al., 2013), cocaine (Gu et al., 2010) and opioid dependent patients (Upadhyay et al., 2010) have reported reductions in amygdala RSFC.

However, to date no study has specifically explored chronic alterations in amygdala functional connectivity at rest with reference to cumulative alcohol exposure in abstinent alcohol dependent patients. Additionally, there is evidence that alterations in RSFC in substance-dependent populations may be related to volumetric atrophy, possibly through loss of function or compensatory neuroadaptive mechanisms (Upadhyay et al., 2010, Filbey et al., 2014). Amygdala grey-matter (GM) atrophy is widely documented in alcohol dependent populations (Fein et al., 2006, Makris et al., 2008, Beck et al., 2012), and has been linked to increased likelihood of craving and relapse at 6 months follow-up (Wrase et al., 2008), yet its relationship to amygdala RSFC has not been specifically investigated.

4.1.4 Hypotheses

As described above, animal models of alcohol dependence have shown neuroadaptations in the amygdala that persist in prolonged abstinence. These neuroadaptations may not only manifest as changes in local patterns of activity, but may also influence large-scale circuit-level interactions of the amygdala (Gilpin and Roberto, 2015). Based on this premise, I hypothesised that:

Hypothesis I: Alcohol dependent patients in abstinence would show differences in patterns of resting state functional connectivity compared with age-matched healthy controls.

This analysis was whole-brain, i.e. not constrained to specific regions of interest, since chronic alcohol exposure has been shown to affect a large number of both cortical and subcortical regions, and changes in amygdala network interactions may include both regions with direct and indirect connections.

The allostatic model of Koob suggests that chronic alcohol exposure may shift brain systems outside their normal state of functioning in a cumulative fashion over time. Based on the notion that neurodaptations may be cumulative, I hypothesised that:

Hypothesis II: Regions showing significant differences in amygdala RSFC between ADP and HC, would correlate with lifetime cumulative alcohol exposure in ADP.

In other words, those with a longer history of dependence, would show greater deviation in amygdala RSFC from healthy controls.

A large number of studies have shown reductions in amygdala volume in abstinent ADP compared with age-matched healthy controls. Therefore, I also hypothesised that:

Hypothesis III: The findings of lower amygdala GM volume would be replicated in the current sample of ADP, and amygdala GM volume in ADP would be inversely correlated with cumulative alcohol exposure.

Finally, I also hypothesised that:

Hypothesis IV: ADP with smaller amygdala GM volumes would exhibit greater differences in amygdala RSFC compared with HC.

4.2 Methodology

4.2.1 Participants

On their first, baseline visit, 68 HC and 28 ADP underwent a 5-minute resting state scan with eyes closed. In the analyses presented here, 7 of these participants (3 HC, 4 ADP) were excluded due to containing less than 5 minutes of resting state data after scrubbing of volumes with excessive head motion (>0.5 mm framewise displacement). Four additional ADP were excluded: 1 due to corrupted acquisition, 3 due to abstinence of less than one month at the time of baseline scan. From the remaining pool of 65 HC, 39 were selected to maximise matching to the ADP group on age, gender, smoking status and head motion in scanner (mean framewise displacement). The demographic and clinical characteristics of the final groups are described in Table 4.1.

4.2.2 Preprocessing

The preprocessing methodology for the functional resting state, and structural brain images is described in depth in Chapter 3.

4.2.3 Statistical analyses

Comparison of amygdala RSFC in ADP versus HC was implemented in a mixed-effects model (*FLAME1*, FSL*)*, controlling for site of scanning. Results were presented as Z statistic images, thresholded using clusters determined by $Z > 2.3$ and a corrected cluster significance threshold of $p < 0.05$. Comparison of grey-matter volumes (GM) in ADP versus HC was carried using a permutation-based two-sample, non-parametric *t*-test (FSL's *randomise;* Nichols & Holmes, 2002)*,* controlling for site and intracranial volume (ICV). Group differences in GM volume were calculated based on 5000 permutations with threshold-free cluster enhancement (Smith & Nichols, 2009) and family-wise error correction at $p < 0.05$.

Further analyses of amygdala RSFC or GM volumes in regions of interest were undertaken using subject-level parameter estimates, after controlling for effects of site and ICV (only for GM volume) across the entire cohort (n = 59). Linear relationships between clinical variables and brain measures were examined using Pearson correlations (Python, *Scipy*) and multiple regression (Python, *Statsmodels)* where applicable.

4.3 Results

Demographic and clinical characteristics of the 20 ADP and 39 HC participants are presented in Table 4.1. No significant group differences were observed for age, gender, body weight, handedness, IQ score, head motion, resting heart rate, systolic and diasystolic blood pressure. ADP reported significantly fewer years in full time education (t = -2.4, p = 0.02) and scored significantly higher on measures of trait (t = 3.9, p = 2.3 x 10^{-4}) and state anxiety (t = 3.5 p = 9.5 x 10^{-4}), compared with HC. A greater proportion of ADP had family history of alcohol dependence (χ = 5.2, p = 0.02). There were trend level effects of ADP containing more smokers than HC (χ = 3.5, p < 0.06), and for ADP smokers showing greater lifetime cigarette package years than HC smokers (t = 1.9, p = 0.06).

4.3.1 Amygdala RSFC and impact of cumulative alcohol exposure

Comparison of voxelwise amygdala RSFC between ADP and HC revealed significantly elevated RSFC in patients in a single cluster located in the midbrain (peak Z: 4.1, $p_{corrected}$ < 0.05, 3936 mm^3, MNI: 8,-20,-14), encompassing substantia nigra (SN) and ventral tegmental area (VTA) bilaterally (Figure 4.1). No additional clusters showed significant increases or reductions in amygdala RSFC in ADP compared with HC.

To refine the anatomical specificity of this midbrain cluster, it was constrained to an anatomical mask of the substantia-nigra/ventral tegmental area (SN/VTA). This mask was originally published in the form of separate probability maps of the substantia nigra and ventral tegmental area (Murty et al., 2014).

Table 4.1 – Demographics and clinical characteristics of ICCAM participants included in the analysis of the Baseline dataset

	ADP (n = 20)		HC (n = 39)			
Measures	**Mean ± SD**	**Range**	**Mean ± SD**	**Range**	**t stat**	**p value**
Age	46.0 ± 8.1	30 - 60	44.3 ± 7.4	31 - 56	0.8	0.43
Sex	15 male, 5 female		32 male, 7 female		$\chi = 0.1$	0.8
Body weight (kg)	77.6 ± 17.9	49.6 - 117.0	77.6 ± 13.4	51.4 - 103.6	-0.01	0.99
Handedness score	50.0 ± 75.3	-100 - (+100)	51.9 ± 62.9	-100 - (+100)	-0.1	0.92
Head motion (FD in mm)	0.20 ± 0.08	0.081 - 0.32	0.17 ± 0.06	0.089 - 0.31	1.5	0.15
WTAR IQ score	105.0 ± 7.7	91 - 118	108.0 ± 9.1	78 - 120	-1.2	0.22
Full time education (years)	12.0 ± 2.4	9 - 19	13.6 ± 2.5	10 - 18	-2.4	0.02
Family history of alc. dependence	7 positive, 13 negative		3 positive, 36 negative		$\chi = 5.2$	0.02
Cumulative alcohol exposure (years)	21.7 ± 8.4	10 - 41	–		–	
Abstinence (months)	11.2 ± 10.8	1 - 38	–		–	
Smoking status	16 smoker, 4 non-smoker		20 smoker, 19 non-smoker		$\chi = 3.5$	0.06
Cig. pack years among smokers*	30.0 ± 17.9	6.7 - 77.9	19.9 ± 11.1	0.1 - 41.6	1.9	0.06
Spielberger Trait Anxiety score	39.6 ± 12.5	21 - 72	29.4 ± 7.5	20 - 48	3.9	<0.001
Spielberger State Anxiety score	33.4 ± 11.2	21 - 61	25.7 ± 6	20 - 48	3.5	<0.001
Resting heart rate (bpm)**	70.1 ± 8.8	56 - 86	67.1 ± 10.4	42 - 97	1.1	0.3
Systolic blood pressure	127.4 ± 13.5	99 - 150	125 ± 14.5	93 - 164	0.6	0.6
Diasystolic blood pressure	78.1 ± 9.0	62 - 95	78.6 ± 9.9	55 - 107	-0.2	0.9

ADP - alcohol dependent patients; HC - healthy controls, FD – Framewise displacement, WTAR - Wechsler Test of Adult Reading;

* missing data: 1 ADP, 2 HC, ** 1 HC

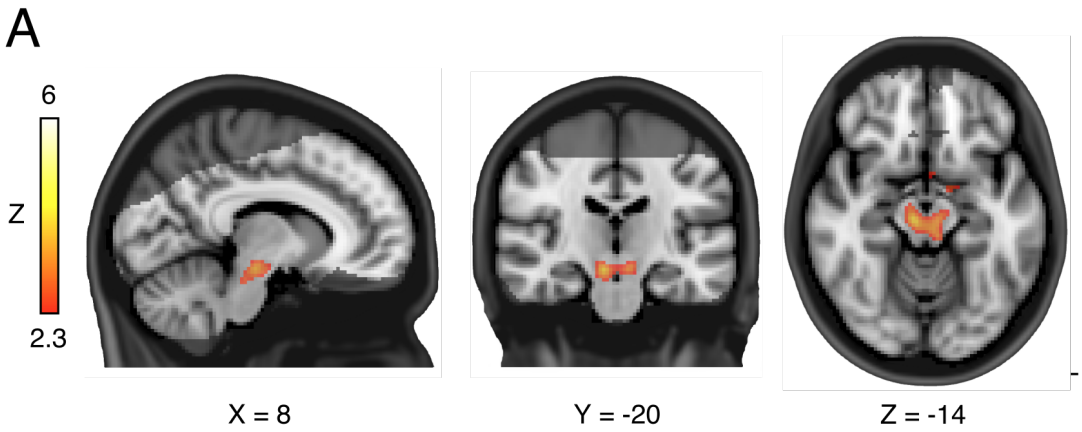


Figure 4.1 Group-level comparison of whole-brain voxelwise amygdala RSFC between ADP and HC. ADP exhibited significantly greater amygdala RSFC in the midbrain relative to HC. Significant voxels were determined by a threshold of Z > 2.3 and a corrected cluster significance threshold of $p < 0.05$. Slice coordinates are presented in MNI space. Shaded out regions depict voxels without coverage.

The two probability maps were each thresholded at 50% tissue-type probability, summed together, binarised, and multiplied with the midbrain cluster to produce the SN/VTA region of interest used in the analysis below (Figure 4.2).

Mean RSFC between amygdala and SN/VTA was significantly elevated in ADP compared with HC ($t = 3.3$, $p = 0.002$; Figure 4.3A), and effect that remained significant after excluding those with family history of alcohol dependence ($t = 2.5$, $p = 0.02$). In ADP, amygdala – SN/VTA RSFC was positively correlated with both cumulative alcohol exposure (r = 0.68, $p = 0.001$; Figure 4.3B) and age (r = 0.49, $p = 0.03$; Appendix, Figure A1.1), when examined separately.

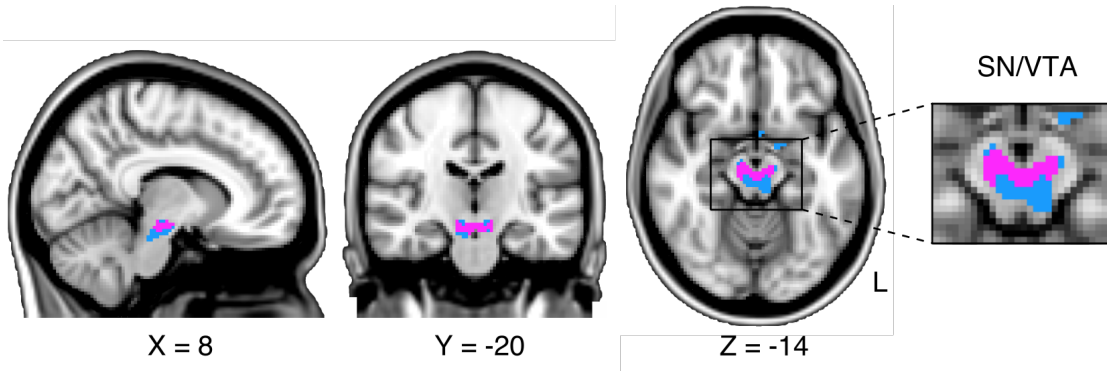


Figure 4.2 Visualisation of the SN/VTA region of interest. The SN/VTA region of interest (violet) was derived by multiplying voxels showing significant group differences in amygdala RSFC in Figure 4.1 (blue), with joint anatomical probabilistic maps of the substantia nigra and ventral tegmental area thresholded at 50% tissue-type probability (Murty et al., 2014). Slice coordinates are presented in MNI space.

However, with both variables entered into the same multiple regression for ADP, only cumulative alcohol exposure was significantly associated with amygdala – SN/VTA RSFC ($t = 2.7, p = 0.02$), while age was not significant ($t = -0.36, p = 0.7$). Amygdala–SN/VTA RSFC was not significantly correlated with abstinence length, head motion, state anxiety, trait anxiety, amygdala GM, SN/VTA GM, resting heart rate, systolic and diasystolic blood pressure in ADP.

It is worth noting that the effect size of the correlation between cumulative alcohol exposure and amygdala – SN/VTA may be overestimated in the above analysis. The SN/VTA region of interest was chosen based on voxels that demonstrated a significant group effect of increased RSFC in ADP compared with HC, within the same sample that was used to compute the correlation. Since the region of interest was not defined entirely independently of the exploratory group effects observed in

the same dataset, the strength of the above correlational findings could have been inflated through statistical circularity (Kriegeskorte et al., 2009).

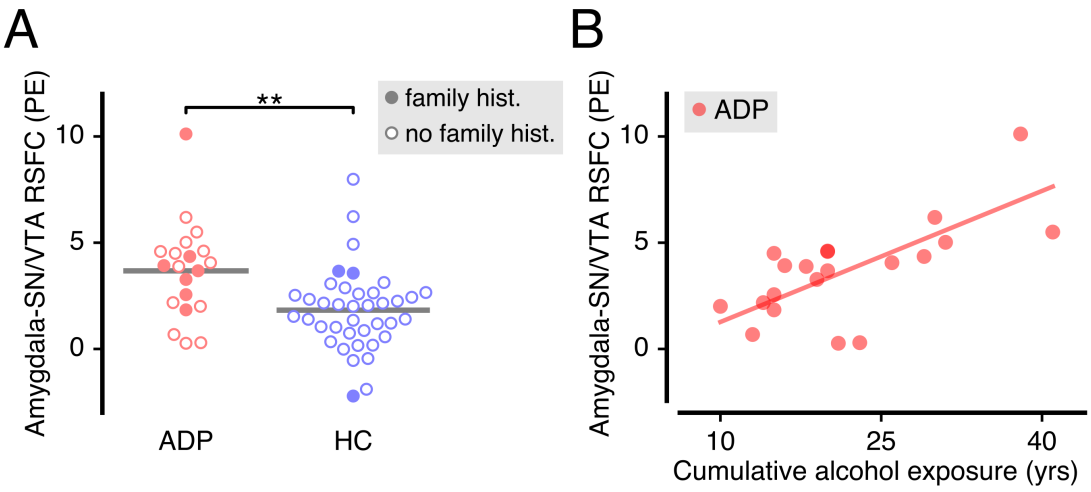


Figure 4.3 Distribution of amygdala – SN/VTA RSFC and family history of alcohol dependence in two groups, and association with cumulative alcohol exposure in ADP. (A) Amygdala – SN/VTA RSFC is significantly increased in ADP relative to HC (t = 3.3, p = 0.002). Bars denote group means. Legend denotes first-degree family history of alcohol dependence. (B) Amygdala – SN/VTA RSFC is positively correlated with cumulative alcohol exposure (r = 0.68, p = 0.001). PE: parameter estimate.

In order to rule out effects of GM atrophy on RSFC, the voxelwise amygdala RSFC group comparison between ADP and HC was repeated while accounting for scanning site, amygdala GM volume, ICV and voxelwise GM volume in a single model. This, more conservative, model produced almost identical results (Appendix, Figure A1.2) to the original findings (Figure 4.1).

4.3.2 Amygdala GM volume and impact of age

Voxelwise comparison of GM volume revealed smaller volumes in subcortical, midbrain and cerebellar regions, including in the amygdala, in ADP relative to HC (Figure 4.4). The amygdala region of interest in the GM volume analysis below was

identical to the amygdala seed region used in the RSFC analysis to allow their comparison. Amygdala GM volume, like amygdala – SN/VTA RSFC, was not significantly correlated with abstinence length.

Age (Figure 4.5A; r = -0.63, $p = 0.003$) and cumulative alcohol exposure (r = -0.47, $p = 0.03$; Appendix, Figure A1.3), were both inversely correlated with amygdala GM in ADP. In order to separate their relative contributions, the two measures were entered into a multiple regression. In direct contrast to the findings related to amygdala – SN/VTA RSFC, amygdala GM volume remained significantly associated with age ($t = -2.3$, p = 0.04), but not with cumulative alcohol exposure ($t = 0.2$, p = 0.9) in the multiple regression. The observed age-related decline of amygdala GM volume was specific to ADP, as HC did not show the same pattern (Figure 4.5B). An ANOVA revealed a significant group by age interaction ($F_{1,55} = 5.8$, $p = 0.02$).

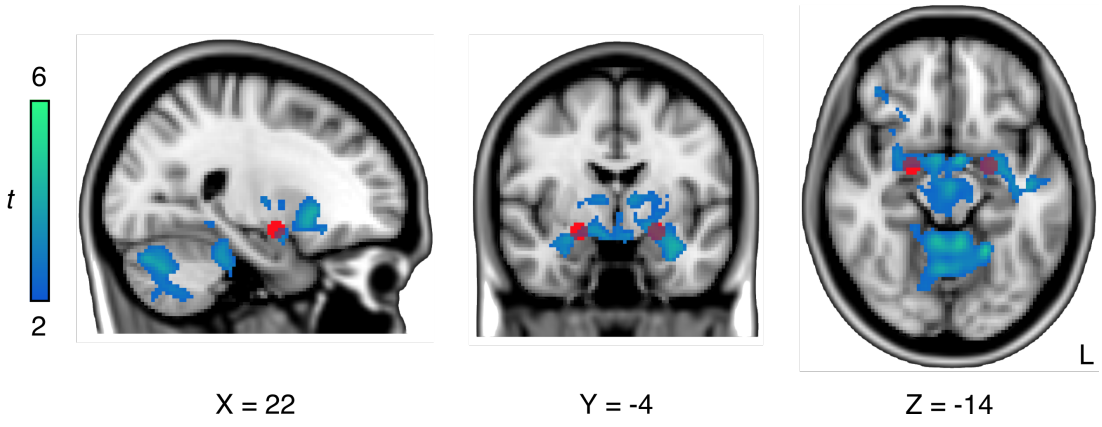


Figure 4.4 Whole-brain voxelwise group-level comparison of GM volume between ADP and HC. ADP exhibited significantly lower GM volume than HC in subcortical regions, including in the amygdala (red sphere). Significant voxels were determined using permutation-based non-parametric testing, applying 5000 permutations, threshold free cluster enhancement and family-wise error correction at $p < 0.05$. The red sphere depicts the amygdala seed region used in the RSFC analysis (5mm radius sphere at MNI: +-22,-4,-12).

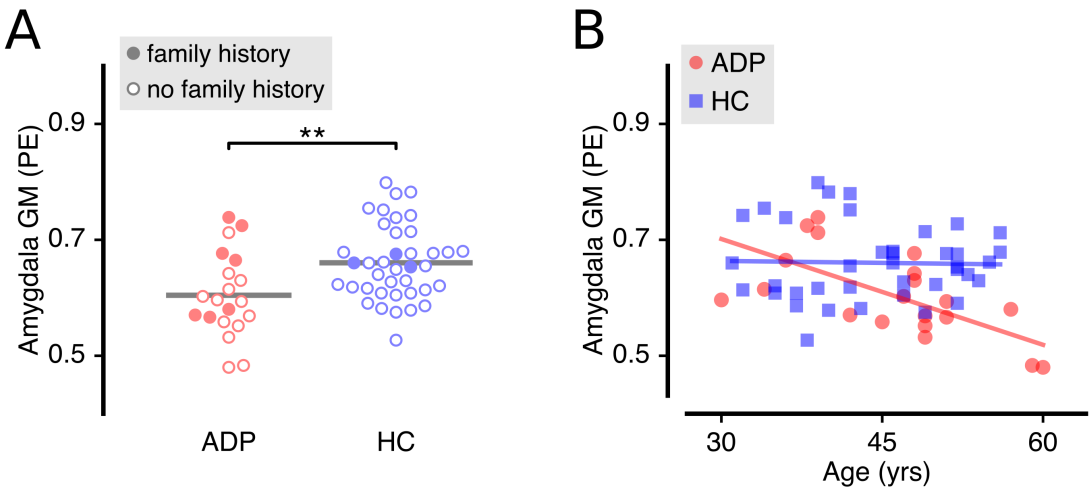


Figure 4.5 The effects of age on amygdala GM volume in ADP and HC (A) ADP showed significantly reduced amygdala GM volume relative to HC (t = -3.0, p = 0.004). Difference between groups remained significant when excluding those with family history of alcohol dependence (t = -3.6, p = 0.0007). Bars denote group means. Legend denotes first-degree family history of alcohol dependence. (B) Amygdala GM volume was inversely correlated with age in ADP (r = -0.63, p = 0.003), but not in HC (r = 0.0, 0.87), exhibiting a significant group-by-age interaction ($F_{1,55}$ = 5.8, p = 0.02). PE: parameter estimate.

4.3.3 SN/VTA GM volume and LV volume

SN/VTA GM volume was significantly lower (t = -2.6, p = 0.01), while LV volume was significantly greater in ADP relative to HC (t = 2.5, p = 0.02). Additionally, SN/VTA GM volume and LV volume showed trend-level positive (r = 0.44, p = 0.05) and negative associations with abstinence length (r = -0.44, p = 0.05), respectively. Neither LV nor SN/VTA GM was significantly correlated with age or cumulative alcohol exposure.

4.3.4 Effect of smoking on amygdala RSFC and GM volume

Only 4 of the ADP were non-smokers, therefore ADP smokers and non-smokers were grouped together for these analyses. This also meant that it was not possible to test for

a potential interaction between the effects of alcohol dependence and smoking on amygdala – SN/VTA RSFC or amygdala GM volume.

ADP exhibited significantly greater amygdala – SN/VTA RSFC relative to both smoker and non-smoker HC subgroups (Figure 4.6A). Amongst ADP smokers, pack years were significantly correlated with amygdala - SN/VTA RSFC ($r = 0.62$, $p = 0.02$), although this association was no longer significant ($t = 1.2$, $p = 0.25$), after accounting for age and cumulative alcohol exposure in a multiple regression.

Amygdala GM volume was significantly lower in ADP relative to both HC smokers and HC non-smokers (Figure 4.6B). ADP smokers showed a trend-level association between pack years and GM volume ($r = -0.48$, $p = 0.07$), although when age and cumulative alcohol exposure were also accounted for in a multiple regression the effect of pack years on amygdala GM volume was no longer significant ($t = -0.39$, $p = 0.7$).

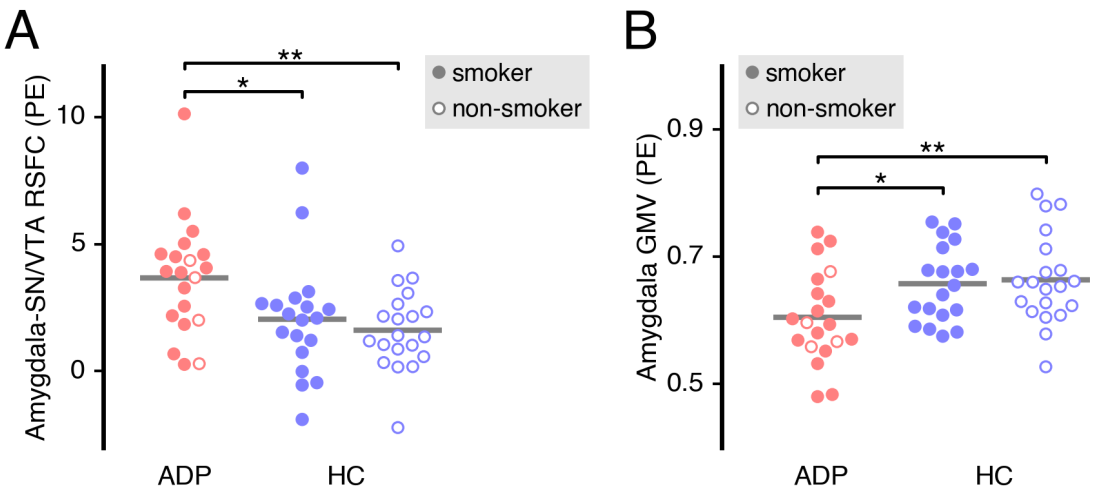


Figure 4.6 Post-hoc analysis of the impact of smoking status on amygdala RSFC and GM volume. (A) Amygdala – SN/VTA RSFC was significantly greater in ADP relative to both HC smokers and non-smokers. (B) Amygdala GM volume was significantly lower in ADP relative to HC smokers and non-smokers. ADP smokers and non-smokers were treated as a single group for these comparisons due to the low number of ADP non-smokers ($n = 4$).

4.3.5 Summary model

The relationships between amygdala – SN/VTA RSFC, amygdala GM volume, age and cumulative alcohol exposure are summarised in Figure 4.7. Cumulative alcohol exposure and age were strongly positively correlated ($r = 0.78$, $p = 4.4 \times 10^{-5}$), i.e. older ADP were more likely to have accumulated lifetime years with heavy levels of alcohol consumption. However, cumulative alcohol exposure appeared to show a stronger correlation with amygdala – SN/VTA, while age exhibited a stronger correlation with amygdala GM volume, than vice versa. Notably, amygdala GM volume and amygdala – SN/VTA were not significantly correlated with each other ($r = -0.15$, $p = 0.5$).

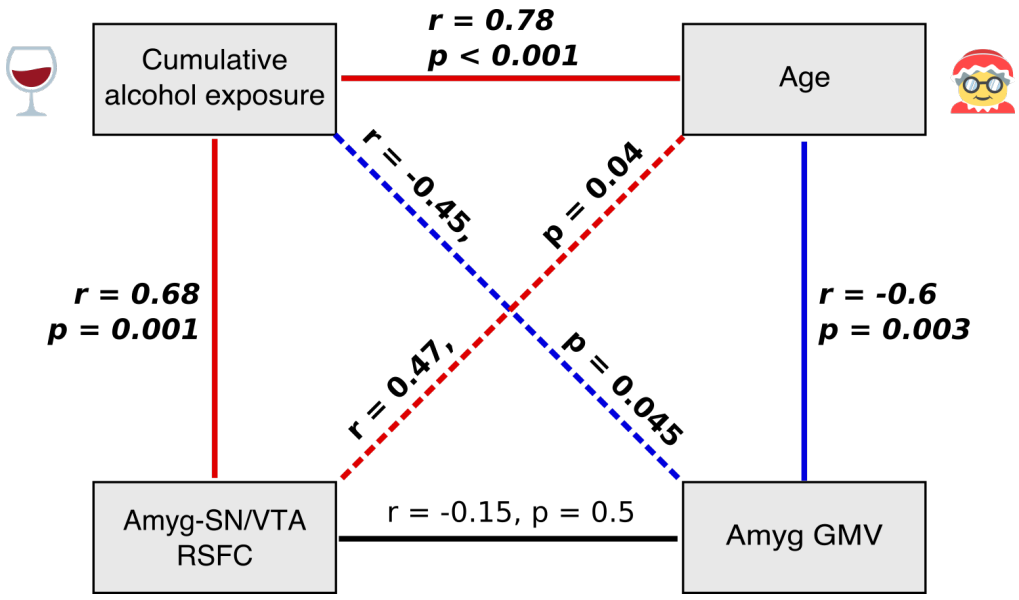


Figure 4.7 Summary diagram showing linear relationships between amygdala – SN/VTA RSFC, amygdala GM volume, cumulative alcohol exposure and age. Red and blue lines indicate significant positive and negative correlations, respectively, while black line indicates lack of significance. All statistics refer to separate Pearson's correlations. Dotted lines indicate weak but significant correlations.

4.4 Discussion

Abstinent ADP showed significant elevations of amygdala – SN/VTA RSFC and widespread reductions in GM in subcortical regions, including the SN/VTA and amygdala, compared with age-matched HC. Multiple regression analysis revealed that amygdala – SN/VTA RSFC elevations were associated with cumulative alcohol exposure, while amygdala GM volume reductions were associated with age in ADP. Amygdala GM volume did not exhibit the same decline with age in HC, suggesting accelerated age-related atrophy in ADP. Neither amygdala – SN/VTA RSFC nor amygdala GM showed an association with abstinence length, indicating persistent effects. These findings demonstrate long-term changes to structural and functional properties of the amygdala in ADP and suggest distinct underlying processes.

The presence of group differences between ADP and HC in amygdala – SN/VTA RSFC and its association with cumulative alcohol exposure supported Hypotheses I and II, respectively. Hypothesis III received partial support since amygdala GM volumes were indeed reduced in ADP, however these reductions were better explained by age than cumulative alcohol exposure per se. Finally, Hypothesis IV, which predicted that greater amygdala GM volume reductions across ADP would be associated with proportionately greater alterations in amygdala RSFC relative to HC was not supported.

Results of higher amygdala – SN/VTA RSFC in abstinent ADP are consistent with animal studies showing synaptic neuroadaptations in the amygdala (Roberto et al., 2004, Gilpin and Roberto, 2012) and VTA (Diana et al., 1996, Shen et al., 2007) following chronic alcohol exposure. They raise the intriguing possibility that synaptic-level changes in response to chronic alcohol exposure may contribute to a

persistent increase in large-scale interactions between these regions. The amygdala and VTA are increasingly viewed as hubs that integrate circuits processing both aversive and appetitive motivational signals (Lüthi and Lüsher, 2014). While the biological significance of RSFC remains elusive, one model proposes a role for RSFC in maintaining synapses between functional networks (Fair et al., 2007). Based on this model, chronic co-activation of the amygdala and SN/VTA during the cycles of anticipation, intoxication and withdrawal that characterise alcohol dependence (Koob and Volkow, 2010), may account for persistent elevations of RSFC, as observed in this study.

Anatomical tracing studies show direct projections from the central amygdala to the SN/VTA (Fudge & Haber, 2000; Lee et al., 2010, Beier et al., 2015), as well as indirect inputs via the BNST (Georges & Aston-Jones, 2000; Jennings et al., 2013), both rich in CRF receptors (Rodaros et al., 2007). Neuroadaptations in the extended amygdala may influence dopaminergic firing in the SN/VTA through direct glutamatergic afferents (Hahen et al., 2009), local SN/VTA-GABA interneurons (van Zessen et al., 2012, Tan et al., 2012) or indirectly through altering SN/VTA autoreceptor function (Kim et al., 2009). The SN/VTA (Loughlin & Fallon, 1983) and the PAG/dorsal raphe (Poulin et al.,2014) both send dopaminergic projections to the extended amygdala, with the latter expressing specific molecular-genetic markers absent in cortical and striatal dopaminergic projections. Dopamine release in the central amygdala has been found to modulate conditioned place preference/aversion in animal models of substance dependence (Rezayof et al., 2002; Zarrindast et al., 2003).

The observed association between cumulative alcohol exposure and amygdala – SN/VTA RSFC may represent a pathological shift in brain function, i.e. the long-term negative consequence of alcohol exposure. Alternatively, higher amygdala – SN/VTA RSFC could also reflect a mechanism for achieving and maintaining abstinence. Of note, Beck and colleagues (2012) have shown increased SN/VTA-amygdala connectivity during cue-reactivity in early abstinent ADP patients who 3 months later maintained abstinence versus those who relapsed. They proposed that the hyperconnectivity of this circuit could have contributed to maintaining abstinence through representation of aversive aspects of alcohol-cues. While ADP showed increased levels of trait and state anxiety relative to HC, an association between these anxiety measures and amygdala – SN/VTA RSFC was not observed in ADP. However, the functional significance of amygdala – SN/VTA connectivity may be context dependent, showing distinct effects at rest and during exposure to alcohol cues as in the study by Beck and colleagues (2012).

To my knowledge this is the first study to show a linear relationship between cumulative alcohol exposure and amygdala – SN/VTA RSFC in abstinent ADP. Previous studies have reported correlations between duration of substance use and RSFC in other circuits, albeit only in recently abstinent ADP (Camchong et al., 2013), currently using cocaine (Gu et al., 2010) and prescription opioid dependent populations (Upadhyay et al., 2010). In this study abstinence length was not associated with recovery of amygdala – SN/VTA RSFC, despite the ADP group comprising patients with up to 38 months of abstinence. The extent to which alterations of this circuit characterise other forms of substance dependence remains to be established, although in this study nicotine dependence was not sufficient to increase RSFC. In addition, it is possible that increased amygdala-SN/TA RSFC

could predate alcohol dependence, however its association with cumulative alcohol exposure and its lack of association with family history of alcohol dependence in this study is suggestive of neuroadaptive effects.

Consistent with previous literature, ADP showed widespread smaller GM volume in subcortical regions including the amygdala and SN/VTA, and larger lateral ventricles (LV) relative to HC (Makris et al., 2008). Alterations of amygdala GM, like amygdala – SN/VTA RSFC, were more severe for ADP with longer cumulative alcohol exposure. However, in contrast to previous findings in prescription opioid dependent populations (Upadhyay et al., 2010), amygdala GM volume was not correlated with amygdala – SN/VTA RSFC in ADP. After accounting for both age and cumulative alcohol exposure in a multiple regression, amygdala GM volume was only associated with age (not cumulative alcohol exposure), while amygdala – SN/VTA RSFC was only associated with cumulative alcohol exposure (and not age). Accelerated age-related GM atrophy has been previously described in recently abstinent ADP (Pfefferbaum et al., 1992) and in currently using cocaine dependent populations (Ersche et al., 2013), although this study is the first to find it in the amygdala in longer-term abstinent ADP.

While SN/VTA GM and LV volumes varied with abstinence length in ADP which is consistent with and indicative of recovery, amygdala GM volume did not. Previous studies have reported amygdala GM atrophy in both shorter (mean: 17 days, Wrase et al., 2008) and longer-term abstinent ADP populations (7.1 yrs, Fein et al., 2006; 5.9 yrs, Makris et al., 2008). These with the current study suggest lack of recovery of amygdala volume with abstinence and together with previous findings of decreased amygdala GM in offspring or unaffected first-degree relatives of ADP (Dager et al.,

2004; Hill et al., 2001, Benegal et al., 2006) has been cited as evidence that reduced amygdala GM may be a predisposing trait to alcohol dependence, and to relapse susceptibility (Wrase et al., 2008). Although the findings here do not rule out this possibility, they do indicate that ageing may interact with chronic alcohol use to further reduce amygdala GM volume. It is possible that progressive age-related atrophy may additionally contribute to relapse risk in ADP.

In summary, these findings suggest that alcohol dependence is associated with persistent alterations in amygdala morphology and resting-state network function compared with age-matched controls, and that these two effects may differentially interact with age and cumulative alcohol exposure. Longitudinal studies will be necessary to characterise the time course of these processes and to delineate their roles in mechanisms of abstinence and relapse.

Chapter 5: Effects of abstinence length and anxiety

5.1 Introduction

5.1.1 Individual differences

Alcohol dependent patients comprise a heterogeneous population with diverse clinical, demographic, psychological and physiological profiles. This heterogeneity speaks against the possibility of discovering a single marker or therapeutic approach relevant to all cases of alcohol dependence. The cross-section of the alcohol dependent population in the current study presented with varying durations of abstinence, cumulative alcohol exposure, histories of detoxification, nicotine dependence, anxiety and impulsivity.

The previous chapter examined the potential influence of many such moderating variables on amygdala – SN/VTA RSFC in ADP, but found only cumulative alcohol exposure to exert a significant effect on RSFC in this circuit[1]. However, some of these variables may still exert a moderating influence on other amygdala circuits, without necessarily showing group-level differences between ADP and HC. Both symptoms of anxiety and length of abstinence are indicators of relapse risk and are frequently reported in clinical studies (Elholm et al., 2011), yet our understanding of their respective effects on amygdala RSFC is limited. This chapter fills in an important gap

[1] Age was also significantly associated with amygdala – SN/VTA RSFC in ADP, however multiple regression analysis showed that the effect of age was driven by shared variance with cumulative alcohol exposure.

in the literature by examining the potential effects of anxiety and abstinence length on amygdala RSFC within ADP.

It may be difficult to assess the significance of variation across ADP in amygdala RSFC associated with abstinence or anxiety by itself, without ADP showing overall group differences with respect healthy controls. However, the interpretation of such associations may be informed by correlation of amygdala RSFC with task-activation data across ADP. As previously described in the background chapter, large-scale network interactions as indexed by RSFC relate intimately to activation patterns during cognitive tasks. Individual variation in amygdala RSFC patterns may help explain individual variation in brain activation patterns during cognitive tasks. The ICCAM Platform study provides a unique dataset, where in addition to resting state, participants also underwent several cognitive tasks in the scanner, with potential relevance to substance-dependence.

Variants of the Evocative Images Task, which index responsivity to aversive visual stimuli, robustly engage the amygdala, and have been used to demonstrate elevations of amygdala responsivity in patients with anxiety disorder (Shah et al., 2009) or alcohol dependence (Gilman & Hommer, 2008). The Go/No-Go task measures neural correlates of motor inhibition (Rubia et al., 2001), a cognitive process whose deficiency has been proposed to be a contributing factor to relapse (Goldstein & Volkow, 2011). Abstinent alcohol dependent patients have been shown to exhibit altered patterns of responses during motor inhibition in the frontal cortex and in subcortical regions, including in the amygdala (Li et al., 2009).

5.1.2 Anxiety

Anxiety is a core symptom of alcohol withdrawal, which dissipates over the time course of abstinence (Roelofs et al., 1987), although it may continue to be elevated compared with age-matched HC even in longer-term abstinence (Orban et al., 2013). Higher levels of trait anxiety (Willinger et al., 2002), and stress-induced anxiety (Sinha et al., 2011) have been associated with greater risk of subsequent relapse, while in animal models stressors are an established approach for reinstating alcohol consumption (Le et al., 2000).

Recent studies of anxiety in healthy populations and in those with anxiety disorders have converged on the notion that amygdala – insula interactions may play a general role in mechanisms of anxiety. Both amygdala and insula are hyper-responsive to emotional stimuli in anxiety-prone healthy individuals (Stein et al., 2007), in patients with social anxiety (Shah et al., 2009), PTSD or specific phobia (Etkin & Wager, 2007). They have also been shown to be responsive to pharmacological modulation by anxiolytic medications (Paulus et al., 2005; Aupperle et al., 2011).

In young healthy adults, RSFC and structural connectivity (axial diffusivity) between left amygdala and left anterior insula have been found to be strongly correlated with individual differences in state and trait anxiety respectively (Baur et al., 2013). Consistent with this model, two studies have also shown amygdala – insula RSFC elevations in PTSD patients (Rabinak et al., 2011; Sripada et al., 2012), although here increases were observed in the posterior rather than the anterior aspect of the insula.

Based on these findings, I previously hypothesised that abstinent ADP would show increased amygdala – anterior insula RSFC relative to HC, due to the greater levels of anxiety of ADP (Orban et al., 2013). In contrast to this prediction, ADP showed

marked reductions of amygdala RSFC in the anterior insula relative to the control participants, and levels of state anxiety were not associated with amygdala – insula RSFC across ADP (Orban et al., 2013).

Since ADP exhibited elevated state and trait anxiety also in the current study compared with HC, this provided an additional opportunity to examine the effect of anxiety on amygdala – insula RSFC in ADP using the ICCAM baseline dataset. Given the previous body of evidence on the impact of anxiety on amygdala – insula interactions, and the counterintuitive reductions in amygdala – insula RSFC observed in my earlier work in abstinent ADP (Orban et al., 2013), this subchapter focuses on amygdala – insula RSFC using a voxelwise approach with small-volume correction to an insula region of interest.

5.1.3 Abstinence length

Without medication, physiological symptoms of alcohol withdrawal in those with alcohol dependence (e.g. tremor, autonomic disturbances) typically peak at ~72 hours (Kosten et al, 2003), and diminish over the course of 7-14 days after last use. This withdrawal period is also characterised by cognitive deficits manifesting in the form of impaired perceptual-motor (Mann et al., 1999), short-term memory (Seifert et al., 2003), as well as affective symptoms in the form of anxiety, dysphoria or depression (Liappas et al., 2002). Relative to the physiological symptoms of withdrawal, affective symptoms generally follow a more gradual rate of recovery spanning 4-6 weeks after cessation of drinking, but may persist longer (Liappas et al., 2002).

The literature is conflicted regarding the rate of recovery of cognitive deficits, with some longitudinal studies reporting rapid normalisation in the first weeks, in some

cases even days (Seifert et al., 2003), while others finding evidence of recovery on the scale of months (Loeber et al., 2010). A recent meta-analysis examined effect sizes of deficits in cognitive function in studies as a function of abstinence length (Stavro et al., 2012). In that meta-analysis, effect sizes were found to be moderate across a wide range of cognitive domains in both early (less than 1 month) and intermediate abstinence (1-12 months), while effect sizes were diminished in longer-term abstinence (greater than 12 months), indicative of a slow rate of recovery.

Functional neuroimaging of resting state provides a potential avenue for characterising mechanisms that underpin recovery of cognitive and affective function. However, to my knowledge no study has examined how resting state network function evolves over the course of abstinence. Camchong et al. (2013) scanned ADP in early abstinence, and found that RSFC in ventral striatal and sgACC networks was associated with subsequent relapse 6 months later. The same two RSFC measures were not, however, associated with abstinence length in their study. It is worth noting that their sample was comprised of ADP in their first two to three months of abstinence, which would preclude detection of linearly associated individual differences in RSFC suggestive of longer-term recovery. In contrast, ADP in the current study had a wide range of abstinence lengths (1 to 36 months), thereby providing the opportunity to investigate effects of abstinence length on RSFC across a longer timescale of potential recovery.

5.1.4 Hypotheses

As outlined above, there is a significant body of evidence supporting the importance of amygdala – insula circuits in anxiety states and disorders. This literature predicts a positive association between amygdala – insula RSFC and measures of anxiety. In contrast, my previous work has found significantly reduced amygdala – RSFC in abstinent alcohol dependent patients, who showed elevated levels of trait and state anxiety (Orban et al., 2013). This subchapter revisited this topic by testing the hypothesis that:

Hypothesis V: Amygdala – insula RSFC is positively correlated with measures of trait and state anxiety in ADP.

In order to maximise statistical power, the analysis was small-volume corrected within a bilateral insula region of interest. Neuroadaptations or pre-existing traits that underlie symptoms of anxiety in alcohol dependence may be reflected in both spontaneous amygdala interactions as indexed by RSFC, as well as in amygdala responsivity to affective stimuli. Therefore I hypothesised that:

Hypothesis VI: There would be a positive association between amygdala – insula RSFC and amygdala responsivity within the Evocative Images Task.

I then moved on to test the following hypothesis:

Hypothesis VII: Abstinence length would be linearly associated with amygdala RSFC in ADP.

Linear effects may be expected to occur because amygdala RSFC could exhibit gradual recovery of function following longer periods of abstinence. This analysis

was run across the whole-brain in a voxelwise manner, since there is no prior knowledge on impact of abstinence on amygdala RSFC.

In addition, the chapter also explored whether regions where amygdala RSFC is associated with abstinence length, also show differential patterns of task-activation. Here, the hypothesis was that:

Hypothesis VIII: Amygdala RSFC in regions associated with abstinence length, would show linear associations with magnitude of task-activation in the Evocative Images Task or the Go/No-Go task.

5.2 Methodology

5.2.1 Evocative Image Task description

The Evocative Image Task was designed to measure brain activation in response to aversive visual stimuli. For each of the five sessions, 24 aversive and 24 neutral images were selected from the International Affective Picture System (IAPS; http://csea.phhp.ufl.edu/media/). The aversive stimuli selected depicted scenes of threat, violence, corpses, disease, traffic accidents, dangerous animals, environmental disasters, wounds, and emotional facial expression, while neutral stimuli depicted non-threatening scenes of human interaction, faces, animals, or geometric objects. Pictures depicting drugs or alcohol were not chosen from the IAPS database for this study to avoid effects of conditioned cue-reactivity in the ADP group.

Aversive and neutral images were presented in alternating mini-blocks consisting of six stimuli presented for five seconds with an inter-trial-interval of 400 ms. Mini-

blocks were separated by a rest period of 15 seconds. Each of the two runs began with the presentation of a fixation cross for 12 seconds.

Each mini-block contained only aversive or neutral images. Stimuli were assigned so that mean valence and arousal ratings (http://csea.phhp.ufl.edu/media/) were balanced across neutral and aversive mini-blocks, respectively. Participants were advised to passively watch the stimuli without looking away and to click a button on seeing each image, as a way of providing feedback on their continuous participation.

The 48 stimuli (24 aversive, 24 neutral) were presented across two runs, with the same set of images shown on the second run. In order to minimize habituation effects on the second run, the order of the mini-blocks and the order of images within each mini-block were shuffled.

The main contrast of interest for this task was aversive > neutral images. It was modeled separately for the two runs for each participant, and subsequently averaged using a fixed-effects model as implemented in FSL.

5.2.2 Go/No-Go Task description

The Go/No-Go task was adopted as a means of measuring patterns of brain activation associated with motor inhibition in a conceptually simple design (Rubia et al., 2001). Participants were presented with series of alternating ‘X’ and ‘Y’ characters, with each character shown for 900 ms, followed by an inter-trial-interval of 100 ms. Participants were told to press a button as fast as possible, whenever the current character differed from the previously shown character (Go trial). On trials where the character shown was identical to the character shown on the previous trial participants were required to inhibit their response (No-go trial).

The task was administered across two runs, with each run containing a total of 250 trials, 30 of which were no-go trials, and 220 were Go trials. No-go trials appeared at an average frequency of ~8 seconds, and a range of 4 to 14 seconds. On the beginning of each run a fixation cross was shown for 12 seconds. Reaction times and accuracy rates were recorded for further analysis.

The main contrast of interest was successful No-go trials versus the implicit baseline of all Go trials. Following the approach outlined above for the Evocative Image Task, each run was modeled separately and the two runs were subsequently averaged in a fixed effects model for each participant.

5.2.3 Participants

The primary focus of this chapter was the baseline resting state data from the 20 ADP previously described in Chapter 4.2.1. In addition, the chapter also made use of task data collected from these same participants on the same baseline session, and data collected from an independent group of healthy participants, described below.

ICCAM Pilot is an independent sample of 17 healthy participants that underwent the same fMRI scanning protocol (Resting state, Monetary Incentive Delay, Go-No/Go, and Evocative image tasks) administered to ADP and HC. This data was collected at Imperial, using the same scanner and acquisition parameters as for the ADP and HC cohorts. The participants were volunteers recruited through word of mouth locally at the university, some of whom were researchers involved in the ICCAM study. The reason for acquiring this data was to fill-in unused scanner slots, and in the process, build-up an independent dataset that can be used to test parameters and hypotheses,

independent of the main arm of ICCAM, thereby potentially avoiding problems of statistical circularity.

The Pilot cohort was substantially younger (27.8 ± 4.2) than the HC cohort (44.3 ± 7.4; t = 8.5, p = 1.4 x 10^{-11}), although the two groups exhibited similar male to female ratios (Pilot 12 : 17, HC 32 : 7; $\chi = 0.4$, p = 0.5). Although the clinical history of the Pilot cohort was not comprehensively assessed as other ICCAM participants, none declared current or past substance dependence, other than to nicotine. None of the participants had to be excluded within this cohort due to excessive movement during their resting state scan (FD: 0.11 ± 0.05, range 0.05 - 0.26)

Evocative and Go/No-Go task data from baseline sessions were analysed to relate measures of task activation relevant to amygdala RSFC across participants. For this reason, task data was only analysed from 76 participants who were included in the original ADP (n = 20), HC (n = 39) or Pilot cohorts (n = 17). There were additional task-specific criteria for inclusion in the analysis to ensure sufficient data quality, described below.

For the Evocative image task analysis participants were excluded if their mean head motion (FD) during the scan was greater than 0.5 mm in at least one run (n = 3). Three participants were excluded due to this criterion, leaving a total of 73 participants across the three groups with usable Evocative image task data.

For the Go-No/Go task analysis, participants were excluded if their mean head motion (FD) was greater than 0.5 mm in at least one run (n = 2), or if they presented with excessive dropout in the parietal lobules (n = 1). Omissions on Go trials were used as an indicator of inattention or poor task compliance, therefore participants with more

than 15% omission were also excluded (n = 3). Six participants were removed based on these criteria, leaving 70 participants with usable Go/No-Go task data.

5.2.4 Preprocessing

The preprocessing methodology for the resting state and two task datasets have been described in Chapter 3.

5.2.5 Statistical analyses

The three main explanatory variables of interest in this chapter: abstinence length, trait anxiety and state anxiety were entered into separate general linear models with voxelwise amygdala RSFC as the response variable, and site of scanning as a covariate of no interest. The models were implemented using FSL (*FLAME1)*, and results were thresholded at $Z > 2.3$ with a corrected cluster significance threshold of $p < 0.05$. Voxelwise analyses for trait and state anxiety were small-volume corrected within a binarised, unthresholded bilateral mask of the insula from the Harvard-Oxford atlas as available in FSL. All other statistical analyses were implemented in Python's *scipy, numpy,* and *StatsModels* modules.

5.3 Results

5.3.1 Overall effects of state and trait anxiety

ADP presented with significantly higher scores on self-report measures of trait ($t = 3.9$, $p = 0.0002$, Figure 5.1A), and state anxiety ($t = 3.5$, $p = 0.0009$, Figure 5.1B) relative to HC. ADP also showed greater within-group variation of both trait anxiety and state anxiety relative to HC. The relatively wide distribution of scores provided

the opportunity to explore how self-reported anxiety levels were related to amygdala RSFC. State and trait were correlated with each other both in ADP (r = 0.65, p =0.002) and HC (r = 0.58, p =0.0001).

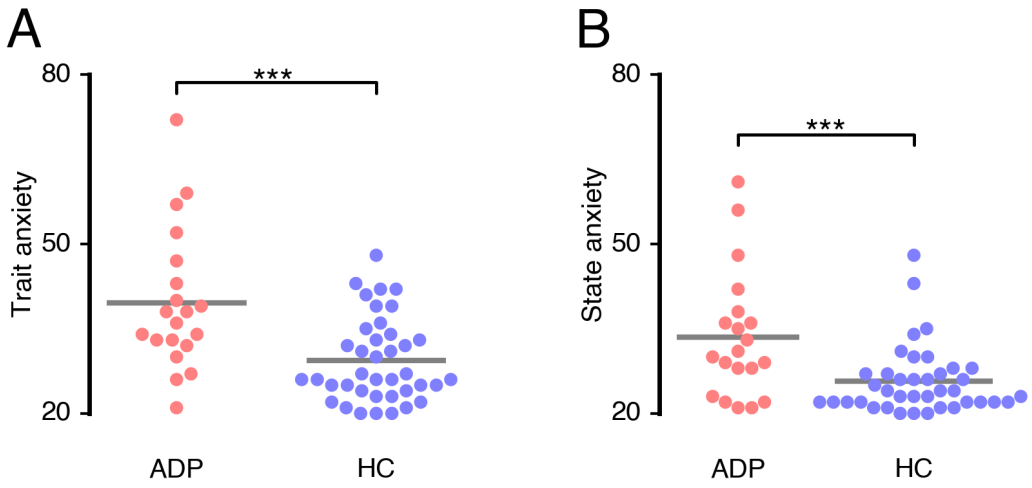


Figure 5.1 Group-level comparison of trait and state anxiety between ADP and HC. Horizontal lines denote mean. Anxiety scores were assessed using Spielberger's State-Trait Inventory, where higher scores are associated with greater levels of subclinical anxiety. *** p < 0.001

Separate voxelwise analyses were conducted to examine the effects of state and trait anxiety on amygdala RSFC in bilateral masks of the insula in ADP. State anxiety was found not to be associated with amygdala RSFC in the voxelwise analysis within bilateral insula. Trait anxiety was found to be positively associated with amygdala RSFC in the left posterior insula (Figure 5.2A). Scatter plot visualisation of this relationship showed a strong positive linear association between the two variables (r = 0.73, p = 0.0003), and the presence of a potential outlier (Figure 5.2B). Excluding this participant from the post-hoc correlational analysis reduced the significance of this relationship (r = 0.51, p = 0.03), although it was still significant. However, recalculation of the original voxelwise analysis without this participant no longer yielded a significant effect in any voxels. It is worth noting that this participant not

only exhibited an extreme level of amygdala – insula RSFC, but also outranked its peers for trait and state anxiety, and was ranked second amongst ADP in cumulative alcohol exposure and head motion (Table 5.1).

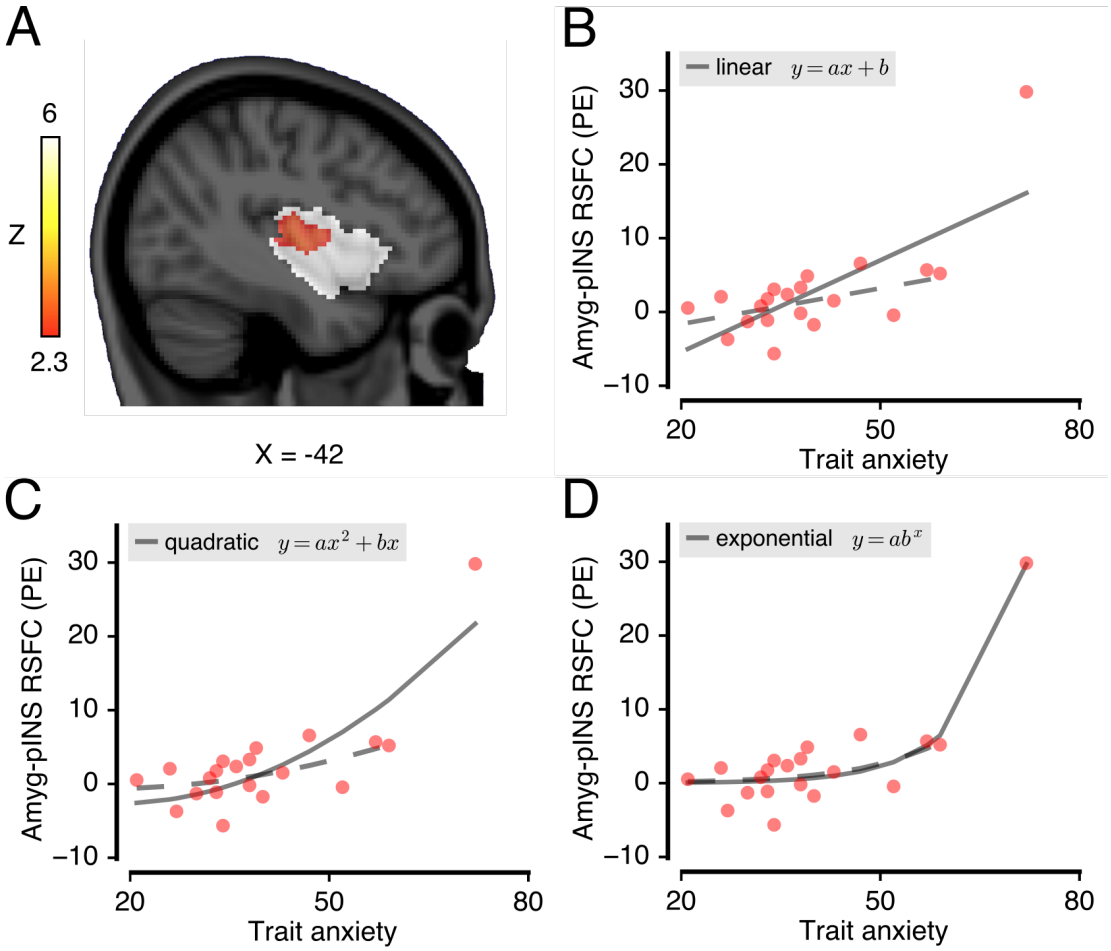


Figure 5.2. The relationship between trait anxiety and amygdala - insula RSFC. (A) Voxelwise regression shows a cluster in the left posterior insula where RSFC with amygdala was positively associated trait anxiety in alcohol dependent patients (ADP). Significant voxels were determined by a threshold of $Z > 2.3$ and a corrected cluster significance threshold of $p < 0.05$. Cluster correction was restricted to masks of the insula from Harvard - Oxford atlas. **(B)** Scatter plot visualisation of significant linear relationship between trait anxiety and mean amygdala - left posterior insula RSFC (Pearson's $r = 0.73$, $p = 0.0003$). The significance of this relationship fell after excluding a potential outlying participant (Pearson's $r = 0.51$, $p = 0.03$). Lines of best fit were calculated using linear, (C) quadratic and (D) exponential polynomials. Dashed lines depict curve fit without potential outlying participant. Please note that the quadratic and exponential curve fits should be regarded as post-hoc.

In order to explore the possibility of a non-linear relationship between amygdala – left posterior insula and trait anxiety, quadratic (Figure 5.2C), and exponential models (Figure 5.2D) were also fit to the parameter estimates derived from the original analysis of 20 ADP. Visual comparison of these models, suggested that the exponential model provided an optimal fit to all data points, including the participant that was flagged as a potential outlier in the linear model.

Table 5.1 Outlier characteristics of participant 3039

	ADP group	Participant 3039		
Measure	Mean ± SD	Value	Rank	SD from Mean
Amygdala – insula RSFC	2.7 ± 7.1	29.8	1.	3.8
Trait anxiety (STAI-T)	39.6 ± 12.5	72	1.	2.6
State anxiety (STAI-S)	33.5 ± 11.2	61	1.	2.5
Alcohol exposure (mo)	21.7 ± 8.4	38	2.	1.9
Head motion (FD, mm)	0.19 ± 0.07	0.32	2.	1.6

'Amygdala – insula RSFC' refers to amygdala – left posterior insula RSFC parameter estimates, 'mo' refers months, and 'FD' to framewise displacement.

Table 5.2 (on the next page) summarises the fit for the linear, quadratic and exponential models through root-mean-square residuals (RMSR), both with and without inclusion of the potential outlier participant. Note that the robustness of the exponential model fit to the exclusion of the potential outlier participant.

5.3.2 Relationship between amygdala – left posterior insula RSFC and amygdala activation within the Evocative image task

Amygdala exhibited significantly greater activation when participants viewed aversive images versus when they viewed neutral images presented in a blocked design (Figure 5.3). Individual parameter estimates averaged within the amygdala

from this contrast (aversive > neutral) were correlated with parameter estimates of amygdala – left posterior insula RSFC.

Table 5.2 Root-mean-square residuals of linear and non-linear models, with and without potential outlier participant

		Root-mean-square residuals	
Model	Form	ADP (n =20)	ADP w/o 3039 (n = 19)
Linear	$y = ax + b$	3.57	2.28
Quadratic	$y = ax^2 + bx$	3.23	2.20
Exponential	$y = ab^x$	2.14	2.16

The explanatory variable is trait anxiety as measured by STAI-T, while the response variable is amygdala –left posterior insula RSFC parameter estimate. The third term in the quadratic model was omitted in order to have an equal number of parameters in all three models.

This analysis was implemented in ADP and in a larger group of 73 participants pooled from ADP, HC and Pilot cohorts. However, the two variables were not significantly correlated in either case.

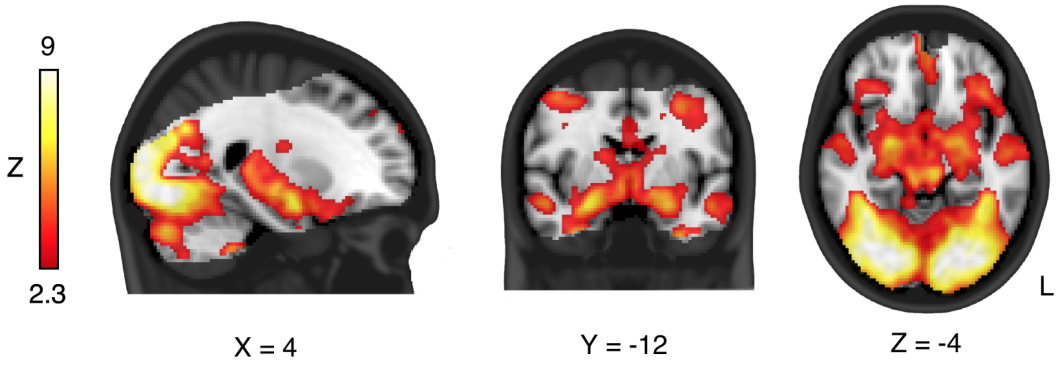


Figure 5.3. Clusters significantly activated during passive viewing of aversive versus neutral images presented in a blocked design. Statistical map was calculated from 73 participants pooled from Pilot, HC and ADP groups. Significant voxels were determined by a threshold of $Z > 2.3$ and a corrected cluster significance threshold of $p < 0.05$. Slice coordinates are presented in MNI space.

5.3.3 Overall effect of abstinence length

Whole-brain analysis in ADP revealed that amygdala RSFC was positively associated with abstinence length in a frontoparietal network (FPN) comprised of three regions: the pre-supplementary motor area (preSMA), the dorsal posterior cingulate cortex (dPCC) and the superior parietal lobules, as shown in Figure 5.4A.

In order to explore the anatomical specificity of this effect to the amygdala, post-hoc RSFC analysis was undertaken using the entire FPN as seed and abstinence length as the explanatory variable. Indeed, abstinence-associated effects on FPN-seeded RSFC were found to be predominantly localised to the amygdala bilaterally. There were a few additional clusters that were significant, although all in nearby regions such as hippocampus, subcallosal cortex and ventral pallidum (Figure 5.4B).

with only a limited number of clusters in neighbouring regions to the amygdala, such as hippocampus, subcallosal cortex and ventral pallidum (Figure 5.4B). As only a few regions outside the amygdala were statistically significant, this would suggest the initial above effect to primarily reflect amygdala – FPN network interactions.

5.3.4 Exploring the FPN further

Subsequently, analyses were undertaken to assess whether the FPN regions delineated that emerged from the analysis above were suggestive of a single functional network or whether it was more appropriate to treat them as an ensemble of functionally distinct regions. As a means of establishing the construct of FPN as a functional network, superior parietal lobule seed-based RSFC analysis was run within the Pilot group (see Chapter 5.2.2 for details regarding this cohort). The superior parietal lobule seed was defined as a 5-mm sphere around the voxel (MNI co-ordinates: 48, -

38, 46) that showed the strongest effect of abstinence length on amygdala RSFC in ADP. This analysis confirmed that the preSMA and dPCC exhibited strong RSFC with the superior parietal lobules at rest in an independent healthy cohort (Figure 5.4C).

Additionally, it revealed that the ventral PCC (vPCC) and medial PFC (mPFC) exhibited significant inverse RSFC with the superior parietal lobule seed region. Most notably however, the amygdala did not exhibit significant RSFC to this superior parietal lobule seed. Therefore, while the three frontoparietal regions, that emerged from the analysis of abstinence length above, may be thought of as a single functional network, the amygdala is not intrinsically part of this network under resting state conditions in healthy participants.

5.3.5 Subgroup analysis by abstinence length

Amygdala RSFC was averaged across significant voxels shown in Figure 5.4A, and plotted versus abstinence length in order to visualise the strong underlying relationship between them (Figure 5.5A). Visual inspection of the scatter plot did not reveal any outliers. Overall HC and ADP were not significantly different in terms mean amygdala – FPN RSFC. The group mean Z-stat representing amygdala – FPN RSFC in ADP was 0.0, suggesting that overall in ADP amygdala did not exhibit strong RSFC with the FPN. However, as can be seen in Figure 5.5A, ADP exhibited considerable variability, with some patients showing negative, while others showing positive amygdala – FPN RSFC.

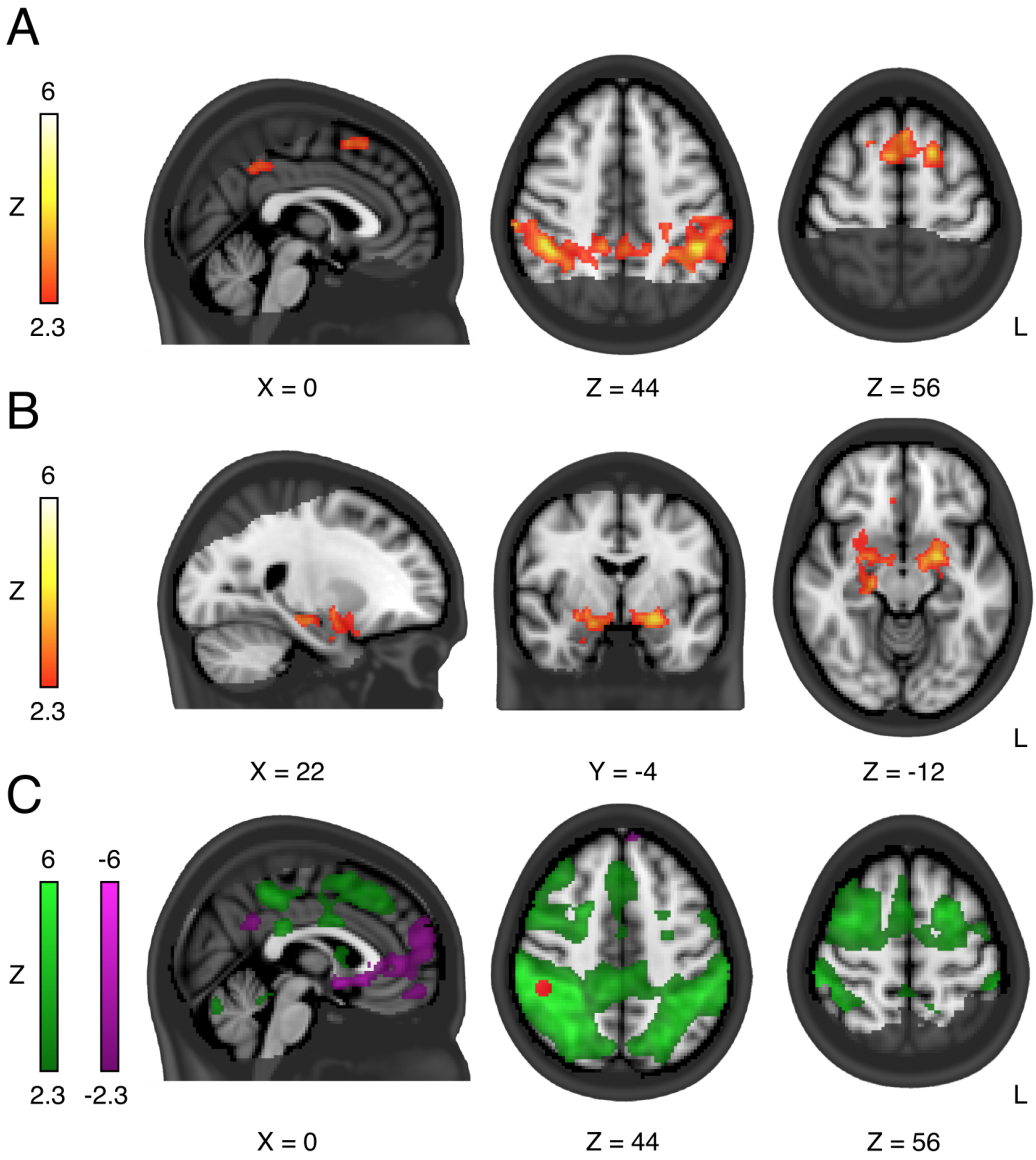


Figure 5.4 The impact abstinence length and amygdala resting state network function. (A) Effect of abstinence length on whole-brain voxelwise amygdala RSFC in ADP (n = 20), showing significantly greater RSFC in frontoparietal regions such as superior parietal lobule, dorsal posterior cingulate cortex (dPCC) and pre-supplementary motor cortex (preSMA). (B) Effect of abstinence length on frontoparietal seed-based RSFC in ADP. Frontoparietal seed was defined post-hoc based on all significant voxels from Panel A, to assess the anatomical specificity of effect, shown in Panel A, to the amygdala (C). Superior parietal lobule seed-based whole-brain RSFC in an independent group of healthy participants (n = 17, ICCAM Pilot), showing significant positive RSFC (green) with dPCC and preSMA (green) and significantly negative RSFC (violet) in ventral PCC and medial prefrontal cortex. Seed (red) was a 5-mm radius sphere centred on the voxel with highest Z-stat (MNI: 48,-38, 46) in Panel A.

To further explore these results ADP were subdivided into shorter-term (S-ADP; 1-2 months; n = 6), intermediate-term (I-ADP; 2 months to 1 year'; n = 8) and longer-term abstinent subgroups (L-ADP; at least 1 year; n = 6). As shown in Figure 5.5B, relative to HC, S-ADP exhibited significantly lower amygdala – FPN RSFC (t = -3.3, p = 0.002), while L-ADP showed significantly greater positive amygdala – FPN RSFC (t = 2.4, p = 0.02). Despite the fact that the S-ADP subgroup represented patients across a substantially narrower window of abstinence length, it revealed a greater variability of amygdala – FPN RSFC (SD: 1.6) relative to I-ADP (SD: 0.6), L-ADP (SD: 0.7) and HC (SD: 1.2).

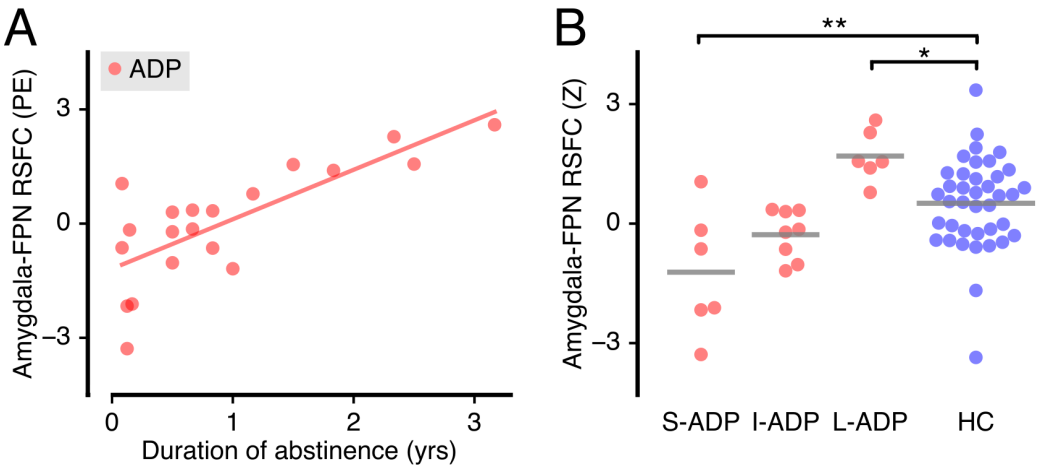


Figure 5.5 Amygdala – FPN RSFC as a function of abstinence length in ADP and in HC. (A) Correlation plot showing relationship between abstinence length and amygdala – Frontoparietal Network (FPN) RSFC in ADP (n = 20). (B) Comparison of amygdala – FPN RSFC in subgroups of ADP defined by abstinence length relative to HC. S-ADP (n = 6): 1 to 2 months' abstinence; I-ADP (n = 8): 2 months to 1 year abstinence, L-ADP (n = 6): at least one year of abstinence. Horizontal line denotes mean. * $p < 0.05$, ** $p < 0.01$

5.3.6 Relationship between amygdala – FPN RSFC, Go-No/Go task-activation and inhibitory control

Neural activation was modelled voxelwise during successful inhibition in the Go/No-Go task in the sample of 70 participants who had both usable resting state and Go/No-

Go task data pooled from the baseline session of the Pilot, HC and ADP cohorts (Section 5.2.2). The previously identified FPN was overlaid with a statistical map of regions significantly engaged during correct inhibition in the Go/No-Go task (Appendix, Figure A1.4) in order to isolate parts of the FPN that were associated with inhibitory control (Figure 5.4). This revised mask of the FPN (FPN-r) retained most of the SPL and preSMA clusters, while excluding the dPCC.

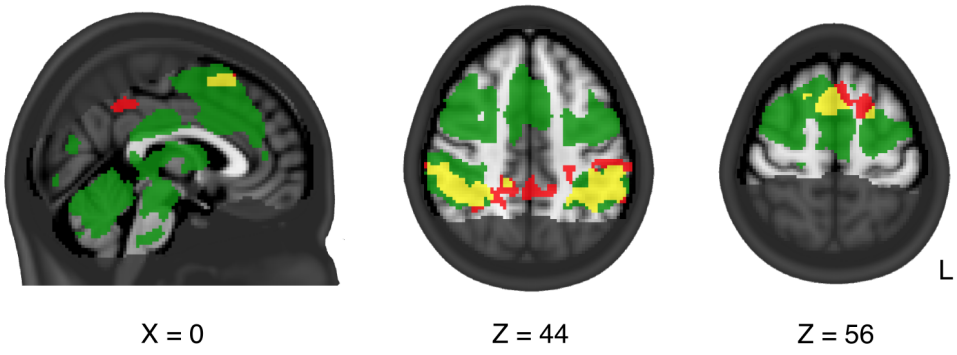


Figure 5.6 Parts of the FPN engaged during successful motor inhibition. Conjunction of voxels (yellow) engaged during successful inhibition in the Go/No-Go task (green) and voxels showing significantly greater amygdala RSFC with longer duration of abstinence in ADP (red). Both statistical maps were thresholded at $Z > 2.3$ with a corrected cluster significance threshold of $p < 0.05$, and binarised.

Within this pooled sample of 70 participants, there was a trend-level positive correlation between amygdala – FPNr RSFC and activation in the FPNr during successful inhibition in the GNG task ($r = 0.22$, $p = 0.067$; Figure 5.7A). In other words, participants with greater amygdala – FPNr RSFC showed a trend for greater activation of the FPNr during successful inhibition in the Go/No-Go task. A breakdown of this relationship per group, revealed a strong significant correlation in the Pilot Cohort ($r = 0.61$, $p = 0.008$; Figure 5.7B), while the same relationship in HC (Figure 5.7C) and ADP (Figure 5.7D) groups was not significant.

Amygdala – FPNr RSFC was not correlated with any of the reaction time (go trials RT) or accuracy measures (% correct NoGo trials, % correct Go trials) in the Go/No-Go task across the 70 participants, in the Pilot, HC or ADP groups alone.

In ADP and HC examined separately, or in the two groups combined, amygdala – FPN RSFC was not significantly correlated with measures of working memory (forward digit span), executive function (backward digit span), trait anxiety (STAI-T), state anxiety (STAI-S) or impulsivity (BIS-11). These measures were not collected for the Pilot cohort.

In 73 participants, pooled from Pilot, HC and ADP groups, who had both usable resting state and Evocative Image Task data (Section 5.2.2), the relationship between amygdala – FPN RSFC and amygdala activation was examined. The two measures were not significantly correlated within the pooled group, nor across the Pilot, HC and ADP groups alone.

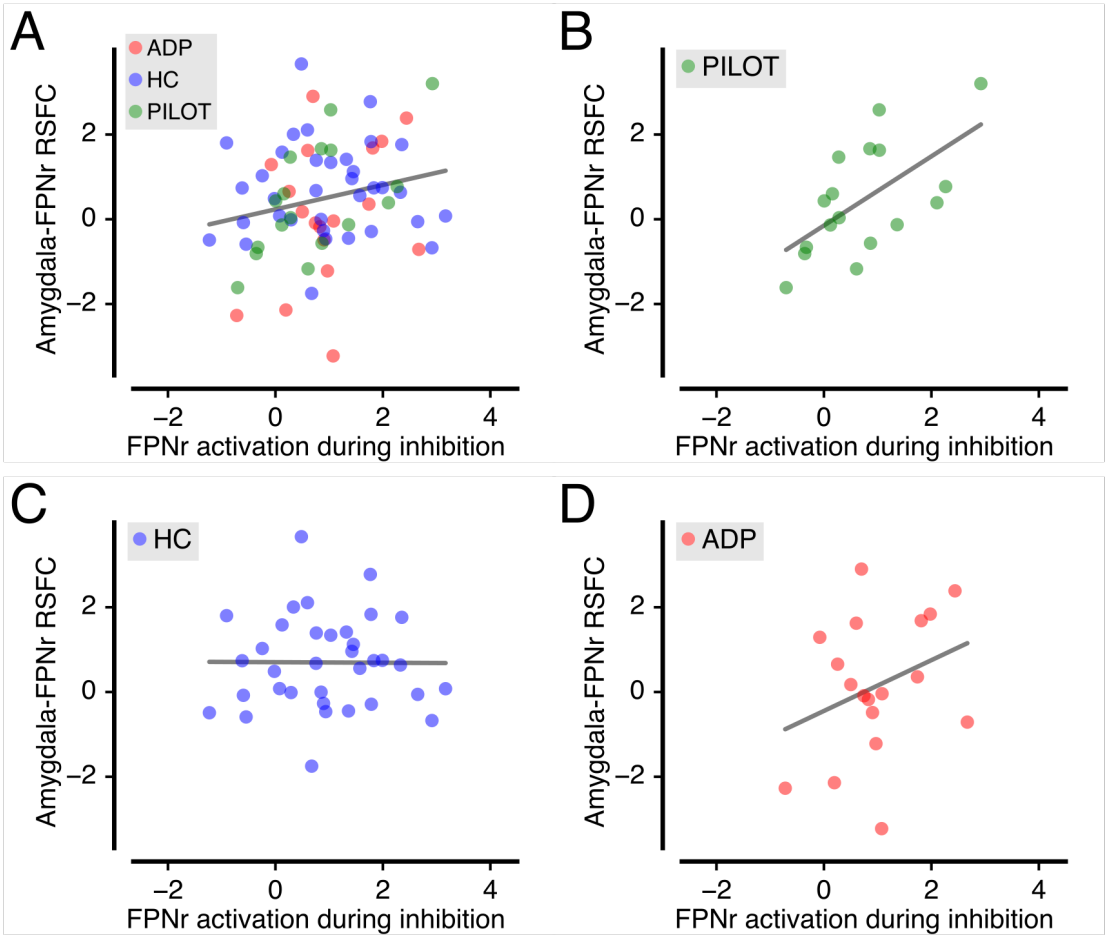


Figure 5.7 Association between amygdala-FPNr RSFC and FPNr activation during correct inhibition in the Go/No-Go task. (A) Scatter plots are shown together in the combined group of 70 participants (r = 0.22, $p = 0.067$), **(B)** and in the Pilot (r = 0.61, $p = 0.008$), **(C)** HC (n.s.) and **(D)** ADP groups separately (n.s.). FPNr refers to the frontoparietal network of interest defined in Figure 5.5.

5.4 Discussion

5.4.1 Amygdala – posterior insula RSFC and anxiety

This chapter examined the hypothesis that amygdala – insula RSFC would be positively correlated with self-reported state or trait anxiety in ADP (Hypothesis V). This hypothesis was based on consistent evidence of elevated amygdala – insula RSFC in patients with anxiety disorders (Rabinak et al., 2011, Sripada et al., 2012), in

healthy patients following exposure to stressful stimuli (van Marle et al., 2010) and in young, healthy participants with high scores of self-reported state anxiety (Baur et al., 2013). The result of a voxelwise analysis, small-volume corrected to a bilateral insula mask of interest, was congruent with this hypothesis, showing a strong positive association between trait anxiety and amygdala RSFC in voxels located in the left posterior insula. However, a closer inspection of parameter estimates suggested a potential outlier participant. Recalculation of the voxelwise statistics without this participant no longer yielded a significant effect, although when the participant was removed from the correlational analysis using the original parameter estimates, this remained marginally significant.

Amongst ADP this participant had the highest level of trait anxiety (2.6 SD from mean), state anxiety (2.5 SD from mean) and by far the strongest amygdala – left posterior insula RSFC (3.8 SD from mean). The disproportionately elevated RSFC in this particular participant may be indicative of an artifact, since the same participant also exhibited relatively high levels of head motion (mean FD: 0.32 mm , 2nd highest amongst ADP, 1.6 SD from mean). As described in Chapter 3, head motion may result in overestimation of RSFC between nearby regions (Power et al., 2012), so this is a possibility that cannot be ruled out. However, there were no categorical reasons to exclude this participant from the analysis, especially since the participant strongly exhibited the phenotype of interest: high, sub-clinical levels of anxiety and a history of alcohol dependence.

Alternatively, higher levels of trait anxiety may indeed be associated with a disproportionate increase in amygdala – insula RSFC in ADP that is not captured by the linear models conventionally applied within the context of seed-based RSFC

analyses. Post-hoc visualisation of quadratic and exponential curve fits suggested a close agreement of the outlying data with the exponential model. Nevertheless, it should be noted that this model fit was strictly post-hoc and therefore should be further explored in an independent dataset.

This chapter also tested a related hypothesis of whether individual differences in amygdala – insula RSFC were related to amygdala task-activation within the context of an Evocative Image Task (Hypothesis VI). One may expect to see an association between the two measures since the same functional properties of the amygdala may impact regional activation and its large-scale network interactions. Furthermore, participants underwent the EIT within the same scanning session as the resting-state task, hence the two scan segments would share both trait and state-related effects. Although the EIT produced robust engagement of the amygdala, there was no association between amygdala – insula RSFC and amygdala activation during the EIT or between state or trait anxiety and amygdala activation. The lack of association between the amygdala RSFC and amygdala activation in the EIT is consistent with findings by Mennes and colleagues (2013), who observed a poor correspondence for subcortical regions between their resting state function and task-activation patterns.

The statistical power to detect effects related to anxiety may have been limited by insufficient prevalence of anxious ADP within the current sample. Although the group effect of greater trait and state anxiety in ADP relative to HC was robust, only four ADP (20%) scored above 50 for STAI-T, and two ADP (10%) scored above 50 for the STAI-S, on a scale where scores ranged from 20 (not anxious) to 80 (highly anxious). At the same time, one must be careful not to mistake this for a reflection of prevalence rates of anxiety in the general population of abstinent ADP. In ICCAM

those with comorbid diagnosis of anxiety disorders were excluded from participation, yet future studies may want to recruit such participants in order to effectively characterise the role of amygdala – insula circuits in anxiety states in abstinent ADP.

A meta-analysis of studies between 1990 and 2000 that reported estimates of reliability for the Spielberger State-Trait Anxiety Inventory's found reasonable test/re-test reliability (STAI-S 0.70±0.20; STAI-T, 0.88±0.05) and internal consistency (STAI-S 0.91±0.05; STAI-T 0.89±0.05) for both trait and state anxiety subscales (Barnes et al., 2002). Nevertheless, the self-report approach for quantifying anxiety in this study possesses some intrinsic limitations that may have reduced the accuracy of detecting a state/trait – brain relationship in this study.

For instance, participants may vary in their ability to introspectively assess and recall the intensity of their subjective states. Alexithymia is a stable personality trait associated with a reduced capacity to identify and describe emotional states (Taylor & Bagby, 2004). Prevalence is estimated at around ~10% in the general population (Salminem et al., 1999; Franz et al., 2008), while, estimates amongst substance dependent populations, including ADP are substantially greater at around 50-70% (Loas et al., 1997; Thornberg et al., 2009). A potentially greater incidence of this trait in the ADP group may interfere with the ability of participants to accurately assess and report their anxiety, thereby introducing systematic bias into the STAI-T and STAI-S scores.

Second, the factor of social desirability may lead a subset of participants with high anxiety to underreport the intensity of their anxiety. Baur and colleagues (2013), dealt with this potential problem by removing those who scored high on subscales of the Eysenck Personality Inventory associated with susceptibility to social desirability

(Eysenck & Eysenck, 1964). The filtering of participants in this manner may have improved their ability to detect a strong relationship between amygdala – insula RSFC and state anxiety within their study. Susceptibility to social desirability was not assessed in the current study therefore it was not possible to implement this approach.

Given that there is currently no universally accepted method for quantifying anxiety without reliance on subject's own estimates, it is of paramount value for clinical neuroscience studies to continue to expand our understanding of anxiety's physiological and neural correlates. This chapter sought to do the latter by attempting to translate a neurophysiological correlate of anxiety from studies of patients with anxiety disorders and healthy participants to a sample of abstinent ADP.

5.4.2 Amygdala – frontoparietal RSFC and abstinence

Consistent with Hypothesis VII, the results revealed that amygdala RSFC in several regions varies linearly as a function of abstinence length in ADP. Specifically, longer duration of abstinence was found to be associated with greater amygdala RSFC in a frontoparietal network consisting of the superior parietal lobules bilaterally, preSMA and dPCC. Control analyses in a fully independent group of healthy participants confirmed that the same three frontoparietal network regions exhibit robust RSFC at rest, and that the SPL and preSMA are co-activated during inhibitory control. While Camchong et al., 2013b has previously reported a negative relationship between sgACC – Dorsolateral PFC RSFC and abstinence length in ADP, this is the first study to find the effect in relation to amygdala RSFC.

The observed linear relationship between abstinence length and amygdala – frontoparietal RSFC may reflect gradual recovery of brain function. Although the

most striking physiological changes have been reported to occur during the first week of detoxification from alcohol (McKeon et al., 2008), longitudinal studies of cognitive performance indicate that functional recovery extends beyond the first year of abstinence (Stavro et al., 2012). The linear increase in amygdala – frontoparietal RSFC extended from 1 month up to the longest period of abstinence present in the sample (38 months), consistent with persistent long-term recovery network function. However, due to the cross-sectional design of the study, one cannot rule out the possibility that these effects could also be related to individual differences in pre-existing traits rather than recovery. If greater amygdala – frontoparietal RSFC is protective from relapse, then a greater proportion of ADP in longer-term abstinence would be expected to exhibit traits protective from relapse relative to ADP in early abstinence.

ADP as a group did not show differences in amygdala – frontoparietal RSFC compared with HC. This is likely due to the wide range of abstinence lengths present in the ADP sample, since the six ADP who were in the first two months of abstinence did show differences relative to HC, in the form of reduced / more negative RSFC. This point underscores a potential trade-off of studying a clinically heterogeneous sample. Widespread differences in abstinence may have cancelled out potential effects on the group-level, while enabling correlational analyses to detect linear effect across years of abstinence that may go unnoticed in more homogenous samples.

The reduced RSFC in the early-term abstinent subgroup was in the form of inversely correlated or anti-correlated activity between amygdala and frontoparietal regions. He and colleagues (2016) found that negative amygdala – frontoparietal RSFC was associated with greater trait anxiety in a sample of 280 healthy adults. Although this

relationship with anxiety was not replicated in ADP, this finding is an agreement in terms of directionality, suggesting that negative RSFC between amygdala – frontoparietal regions may constitute a maladaptive phenotype.

The literature suggests that these frontoparietal regions are functionally related and can be thought of as a network. The SPL and preSMA are frequently co-activated in experimental paradigms that engage higher-level executive functions e.g. fluid intelligence (Duncan et al., 2010) or stop signal task (Sharp et al., 2010). Although the dPCC tends to show reduced activation during these tasks, it does show functional connectivity with frontoparietal regions at rest (Leech et al., 2011; Yeo et al., 2011; Spreng et al., 2012). Using the SPL as a seed, I confirmed that both the preSMA and dPCC exhibited strong RSFC at rest in a fully independent group of healthy participants (ICCAM Pilot dataset). In addition, the SPL and preSMA also showed co-activation during inhibitory phase of the Go/No-go task in the same independent healthy cohort.

In the pooled samples of HC, Pilot and ADP groups, there was only a trend-level association between SPL/PreSMA activation during the Go/No-go task, and amygdala – SPL/PreSMA RSFC. This effect appeared to be driven by a strongly significant relationship in the Pilot group, while the effect was not significant in the ADP or HC groups alone. Activation in the EIT was also not correlated with amygdala – FPN RSFC at rest across the pooled cohort, nor across each of the three groups. Therefore I summary, Hypothesis VIII, which proposed that individual differences in amygdala RSFC related to abstinence length would be linearly associated with magnitude of task activation, was not supported.

However, it is worth pointing out that tasks other than those available from ICCAM may be more relevant to assessing the functional significance of the amygdala – FPN circuit. The Go-No/Go task showed reliable activation of the SPL/Pre-SMA and had a clear mechanistic relevance to relapse and recovery mechanisms based on the literature (Goldstein & Volkow, 2011), while the EIT task is an effective assay for assessing amygdala activation to aversive stimuli (McGonigle et al., 2017). However, it's possible that neither task was particularly well-suited to probing the interaction of amygdala and FPN regions. A variant of the Go/No-Go task that incorporated an affective component may be more effective in assessing this circuit.

The precise role of amygdala – frontoparietal network interactions in healthy populations is unknown, and the two do not generally exhibit strong connectivity at rest (He et al., 2016). However, since relapse rates tend to decline over the course of abstinence (Dawson et al., 2005), greater amygdala – frontoparietal RSFC is likely to represent an adaptive phenotype in alcohol dependent populations. According to classical models, the amygdala is specialised for extracting motivationally salient features from perceptual input, while frontoparietal association cortices are thought to mediate selection of goal-directed behaviours. One may speculate that their increased interaction may enable more efficient detection of situations that predispose to relapse, and facilitate the formulation of plans that allow inhibition of actions plans or avoidance of situations that predispose to relapse.

Chapter 6: Pharmacological modulation of amygdala RSFC

6.1 Introduction

6.1.1 Pharmacological fMRI

Pharmacological fMRI is an increasingly utilised method for characterising the consequences of manipulating specific neurotransmitter systems on brain function (Borsook et al., 2016), including resting state network interactions (Kelly et al., 2012). For experimental medicine studies, such as ICCAM, it provides a tool for assessing the utility of putative therapeutic compounds in normalising functional deficits or in strengthening function in circuits that mediate clinical vulnerabilities. Comparing response profiles in controls and patient groups to specific pharmacological modulators may also reveal intrinsic differences in receptor system function that can inform models of disease mechanisms.

This ICCAM Platform study was designed with the primary aim of characterising the effects of acute μ-opioid, Dopamine D3 (DRD3) and Neurokinin-1 (NK1) receptor antagonism on neural correlates of core cognitive processes likely to be dysregulated in substance-dependent populations. The rationale for targeting these three particular receptor systems for substance dependence treatment is supported by findings from both animal experiments and clinical studies as outlined below.

6.1.1 μ-Opioid receptor

Ethanol consumption has been found to be associated with β-endorphin release in the ventral striatum in humans (Mitchell et al., 2012), and in the nucleus accumbens (Olive et al., 2001) and amygdala (Lam et al., 2008) in rats. β-endorphin binds with

high affinity to the μ-Opioid receptor, a process that has been thought to mediate positive reinforcement, via disinhibition of dopamine function (Spanagel et al., 1991a, Spanagel et al., 1991b, Spanagel et al., 1992). Several clinical studies have observed upregulated μ-Opioid receptor availability in ADP in limbic regions such as the ventral striatum and amygdala, an effect associated with a greater intensity of craving (Heinz et al. 2005, Williams et al. 2009, Weerts et al., 2011).

In animal models, Naltrexone, a μ-Opioid preferring antagonist, has been shown to reduce alcohol self-administration and to selectively inhibit cue-induced reinstatement, without affecting stress-related reinstatement, e.g. via foot-shock stress (Le et al.,1999; Liu et al., 2002). In a recent study, pre-treatment with Nalmefene, a compound with μ-Opioid antagonistic properties, was found to reduce dorsal striatal activation to anticipation of monetary reward while receipt of 'alcohol clamp' with a target breath level of 0.8%, in non-treatment seeking alcohol dependent men (Lingford-Hughes et al., 2015). In human clinical trials, Naltrexone has shown efficacy in reducing relapse risk (Kranzler & Kirk, 2001) and currently it is one of only two medications approved by the US Food and Drug Administration for relapse prevention in ADP.

6.1.2 Dopamine receptor D3 (DRD3)

Voluntary alcohol consumption for a year in alcohol preferring rats has been associated with upregulation of striatal DRD3 expression (Thanos et al., 2005), while repeated, systemic DRD3 blockade has been shown to dose-dependently reduce cue-induced alcohol seeking and relapse-like drinking behaviours (Vengeliene et al., 2006). *In-vivo* human PET imaging studies have shown high DRD3-related signal in

the SN/VTA, and globus pallidus, and low-levels of signal in the dorsal striatum (Searle et al, 2010, Tziortzi et al., 2011, Erritzoe et al., 2014).

Human post-mortem studies are consistent with these findings, while also observing DRD3 expression in additional regions, including in the central amygdala (Murray et al., 1994, Gurevich & Joyce, 1999). Furthermore, in rats, selective blockade of DRD3 receptors either in the nucleus accumbens or central amygdala, but not in the dorsal striatum, has been found to inhibit expression of cocaine-craving, without affecting sucrose seeking (Xi et al., 2013).

A recent PET study found that abstinent ADP showed similar levels of DRD3-related signal as age-matched healthy participants in most dopaminergic regions, including the SN/VTA and globus pallidus, except in the hypothalamus (Erritzoe et al, 2014). To date only one study has examined any aspect of the DRD3 receptor function and resting state network function. Cole et al., (2011) found that rate of DRD3 availability, as measured by [^{11}C]-(+)-PHNO PET, in healthy participants was associated with the rate of coupling between distinct large-scale resting state networks and subregions of the OFC, as measured by resting state fMRI. However, amygdala network function was not specifically explored, and it is not clear how these findings relate to mechanisms of substance dependence.

6.1.3 Neurokinin-1 receptor (NK1)

Post-mortem autoradiography and in vivo [F-18]SPA-RQ PET experiments indicate that NK1 receptors are localised to dorsal striatal, as well as limbic regions such as hippocampus and amygdala (Hietala et al., 2005). Interest in NK1 receptor antagonism as a potential treatment target for substance dependence disorders has

been mostly motivated by its anti-anxiolytic properties (Ebner & Singlewald, 2006). Rats exposed to even mild levels of psychological stress have shown enhanced substance P release, the preferred ligand of NK1 receptors, in the medial amygdala (Ebner et al., 2004), while pharmacological antagonism of NK1 receptor function has been found to attenuate stress-responses in both rodents (Santarelli et al., 2001) and humans (Furmark et al., 2005). More recently, social anxiety disorder has been found to be associated with greater NK1 receptor availability in the right amygdala (Frick et al., 2015).

In an influential study, George et al., (2008) found that NK1 receptor knockout mice exhibited reduced voluntary alcohol consumption, and additionally that repeated dose of NK1 antagonist reduced endocrine and subjective responses to alcohol-cue challenge in recently detoxified alcohol dependent in-patients. Since then other studies have built on these findings, for example by showing that NK1 knockouts also do not exhibit alcohol consumption in response to repeated cycles of deprivation (Thorsell et al., 2010). In another study, L822429, an NK1 antagonist was shown to suppress stress-induced reinstatement of alcohol-seeking at doses that did not affect cue-induced reinstatement, locomotor motion or sucrose self-administration (Schank et al, 2011).

6.1.4 Hypotheses

In summary, μ-opioid, Dopamine D3 (DRD3) and NK1 receptor pathways are all plausible targets for pharmacological treatment of relapse risk in alcohol dependent populations. However, the consequences of modulating these receptors, on large-scale brain function in human patient populations or even in healthy participants, is largely unknown. As outlined above, all three receptors are expressed in the amygdala,

therefore examining their modulatory effects on amygdala RSFC may provide insights regarding their network-level mechanism.

Chapter 4 showed findings of significantly elevated amygdala RSFC in the SN/VTA in ADP compared with HC. Based on the assumptions that elevated amygdala – SN/VTA RSFC is a feature of the alcohol dependent phenotype, and that the three compounds in ICCAM may be effective therapeutic modulators of circuit-level deficits underlying alcohol dependence, I hypothesised that:

Hypothesis IX: One or more of the three drugs may modulate amygdala RSFC differentially in ADP than in HC, producing a group-by-drug interaction.

A related question of interest was whether any of the three drugs would normalise levels of amygdala – SN/VTA to levels observed in HC, or whether elevated levels of amygdala – SN/VTA RSFC would persist under each drug condition. Therefore, I also tested the hypothesis that:

Hypothesis X: At least one of the three drugs would normalize alterations in amygdala RSFC in ADP to levels observed in HC.

An additional aim of this chapter was to characterise the modulatory effects of the three drugs on amygdala RSFC across all participants. As mentioned before, the target receptors of all three drugs are known to be expressed in the amygdala. Although the three drugs target different receptor systems, all of them are putative pharmaco-therapies for relapse-prevention based on animal studies, and in the case of Naltrexone also based on human studies. Therefore, I hypothesised that:

Hypothesis XI: The three drugs may exhibit both spatially overlapping and spatially non-overlapping effects on amygdala RSFC.

6.2 Methodology

6.2.1 Drug dosage

The first session (Baseline) did not involve administration of a drug. Across sessions 2 to 5, all participants received Placebo (Vitamin C, 100 mg), a μ-Opioid receptor antagonist (Naltrexone, 50 mg), a DRD3 receptor antagonist (GSK598809, 60 mg) and an NK1-antagonist (Vofopitant, 10 mg; or Aprepitant, 80 mg). Around halfway through the study the Vofopitant supply reached its date of expiry, therefore it was replaced with Aprepitant, another NK1-antagonist, for the remainder of the study.

Doses for Naltrexone and Aprepitant were chosen to be equivalent to typical therapeutic doses. In addition, past PET tracer studies of GSK598809 (Searle et al., 2010) and Aprepitant (Bergstrom et al., 2004), indicated that they would both correspond to approximately 80% receptor occupancy. The 80 mg dose for Aprepitant also matched receptor occupancy levels previously achieved for a 10 mg dose of Vofopitant (Paterson et al., 2015).

Previous studies have observed peak plasma concentrations (*tmax*) to occur at 1 hour for Naltrexone (Mason et al., 2002), at 2 hours for GSK598809 (Te Beek et al., 2012), and at 4 hours for Aprepitant (Majumdar et al., 2006), following a single oral dose. In order to maintain blinding of the drug conditions, a fixed period of 2 hours was chosen between dosing and the start of scanning. The resting state scan was always the first task on each scanning session.

Drugs were stored in identical white bottles, and dosing was carried out by nursing staff not involved in the study thereby ensuring that both the participant and the researchers were maximally blinded from the drug conditions.

6.2.2 Pseudo-randomisation of session order

The Baseline session always took place on the first visit, to allow participants to habituate to the protocol, and to provide an opportunity for the researchers to identify any reasons for excluding the participant from the subsequent drug arm of the study, if necessary[2]. The order of the four drug sessions was deployed in a cross-over, pseudo-randomised manner, where Placebo and Naltrexone were always administered on sessions #2 or #3, and GSK598809 and Aprepitant/Vofopitant were always administered on sessions #4 or #5.

The rationale for this design was to minimise loss of data as a result of participants dropping out of the study before their Placebo session. Since all drug effects were contrasted with Placebo, the pseudo-randomisation ensured that the effects of at least one drug: Naltrexone, could be Placebo-controlled, even if participants only attended the first three sessions. This concern over potential dropout rates was motivated by the clinical experience chronic-relapsing nature of substance dependence.

6.2.3 Participants

Originally data was available from 20 ADP and 35 HC participants who completed all five sessions. From this initial pool of 20 ADP, one was removed due to failing abstinence length criteria of at least four weeks. Four additional ADP were removed due to having less than 140 volumes of resting state data intact after scrubbing of volumes with extreme levels of motion (> 0.5 mm FD). This threshold was relaxed from the initial threshold of 150 volumes (five minutes of acquisition) applied to the

[2] For example, claustrophobia, neuroradiological abnormalities or a poor ability to follow instructions in the scanner may become apparent during the Baseline session, allowing the exclusion of the participant from the study prior to the sessions involving drug dosing

Baseline session, since participants had to meet this criterion for all four drug sessions.

From the initial pool of 35 HC, one was removed due to corrupted acquisition during the Placebo session, eight due to having less than 140 volumes intact after scrubbing of motion outliers (> 0.5 mm FD), and four due to being too young (<31 years old) to adequately match the age distribution of the ADP cohort. After these exclusions, 15 ADP and 22 HC remained for analysis of drug effects through sessions 2 to 5.

A subset of these participants, 13 ADP and 16 HC, met inclusion criteria (described in Chapter 4.1.1) on their Baseline scans as well. These two groups were smaller than the 20 ADP and 39 HC that were used in the Baseline analysis in Chapter 4 for two reasons: (i) not all participants with Baseline data went on to complete all five sessions; (ii) not all participants with sufficient data quality on the four drug sessions had sufficient data quality on their Baseline session.

6.2.4 Group effects across different sessions

One question of interest was whether the elevation of amygdala – SN/VTA RSFC, observed at Baseline between ADP and HC, was also present during the other sessions. This question was addressed using two approaches. The first one involved separate voxelwise analyses of the four sessions, comparing amygdala RSFC between ADP and HC (*FLAME1*, FSL). The second approach involved averaging subject-level amygdala RSFC across the four drug sessions (fixed effects), and comparing the voxelwise averages of ADP with HC (random effects), in a single mixed-effects model (*FLAME1*, FSL). Both approaches controlled for scanning site as a confound of no interest in the design matrix.

Significant voxels were determined by a threshold of $Z > 2.3$ and a corrected cluster significance threshold of $P < 0.05$. As a means of increasing statistical power, small volume correction was applied in both analyses using a midbrain region of interest defined as a 40 x 36 x 20 mm box covering the entire midbrain (Figure 6.1).

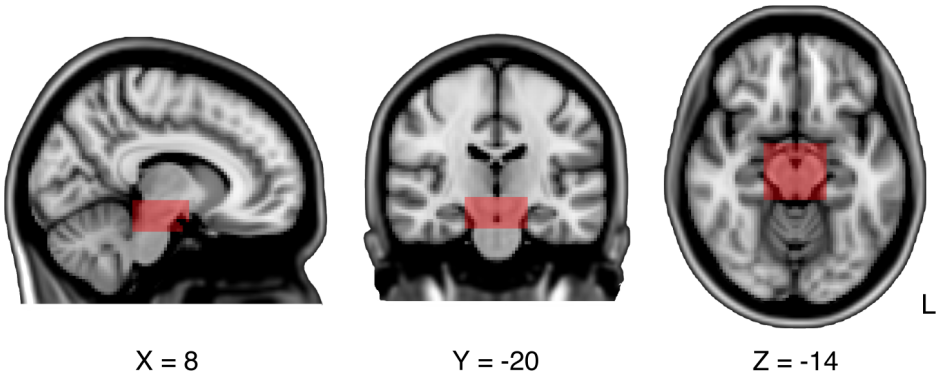


Figure 6.1 A 40 x 36 x 20 mm box positioned around the midbrain for small-volume correction of voxelwise analysis. The box's spatial extent was defined in MNI space as X: -18 to +20, Y: -36 to -2, Z: -24 to -6.

6.2.5 Stability of individual differences across sessions

In order to assess the inter-session stability of individual differences in amygdala – SN/VTA RSFC, subject-level parameter estimates for this measure were correlated between each combination of the five sessions, using a Spearman's Rank correlation. Results were visualised in the form of a 5 x 5 correlation matrix heat map (*Seaborn,* Python). For this analysis, only those participants were included who had usable data on all five sessions (ADP: 13, HC: 16), as described in Chapter 6.2.3.

The same approach was implemented to characterise the inter-session stability of amygdala – fronto-partial RSFC.

6.2.6 Voxelwise analysis of drug effects

Whole-brain voxelwise analysis of drug effects on amygdala RSFC was implemented separately for each of the three drugs (Naltrexone, GSK598809, and Aprepitant/Vofopitant). A mixed effects model was run in FSL (FLAME1) where group (ADP, HC) was treated as a random-effect and session (drug versus Placebo) as a fixed effect. The two main contrasts of interest were the group-by-drug interaction and the main effect of drug. Significant voxels were determined by a threshold of $Z > 2.3$ and a corrected cluster significance threshold of $P < 0.05$.

In order to further interpret the voxelwise effects, mean subject-level parameter estimates of amygdala RSFC in each of the five sessions (Baseline, Placebo, Naltrexone, GSK598809, and Aprepitant/Vofopitant) were extracted from significant clusters of interest. Where these clusters spanned multiple clearly identifiable brain regions (e.g. putamen and insula), anatomical masks were used to constrain them to one region of interest. Parameter estimates extracted from these regions were controlled for effect of scanning site using Ordinary Least Squares regression (Statsmodels, Python) and displayed using column scatter plots, to allow visualisation of differences between groups (HC, ADP) and between the five sessions. Although the significant clusters were always defined based on a single "drug X" versus Placebo contrast, extracting and visualising parameter estimates across all five sessions provided a means of assessing the specificity of apparent drug effects.

Following visualisation of the data, post-hoc paired t-tests were carried out to compare parameter estimates between each drug session and Placebo. Drug sessions, for which significant differences were observed in relation to Placebo, were also compared with Baseline to assess specificity of underlying effects. Drug versus

Baseline comparisons were implemented through independent t-tests, due to fewer of the participants being present in the Baseline group.

6.3 Results

6.3.1 Amygdala – midbrain RSFC

Separate voxelwise comparisons of ADP (n = 15) and HC (n = 22) in each of the four sessions did not reveal significant differences in amygdala RSFC between the groups. However, when the voxelwise average of the four sessions was used for comparison, ADP exhibited significantly greater amygdala - midbrain RSFC relative to HC (Figure 6.1A). The resulting cluster was spatially restricted to an SN/VTA anatomical mask (see Figure 4.2 for method) before extraction of subject-level parameter estimates of amygdala – SN/VTA RSFC for session-level post-hoc comparison.

As shown in Figure 6.2B, parameter estimates of amygdala – SN/VTA RSFC for HC (Placebo: 1.5, Naltrexone: 1.6, GSK598809 1.5, Aprepitant/Vofopitant: 1.7) and to a lesser extent for ADP (Placebo: 3.1, Naltrexone: 2.8, GSK598809 3.2, Aprepitant/Vofopitant: 3.5) exhibited stable group means across the four experimental sessions. Independent-samples *t*-tests confirmed significantly greater amygdala – SN/VTA RSFC in ADP relative to HC under Placebo ($t = 2.1$, $p = 0.04$), GSK598809 ($t = 2.5$, $p = 0.02$) and Aprepitant/Vofopitant ($t = 2.8$, $p = 0.009$). Under Naltrexone there was a trend-level difference between the groups, though in the same direction as on the other sessions ($t = 1.9$, $p = 0.065$).

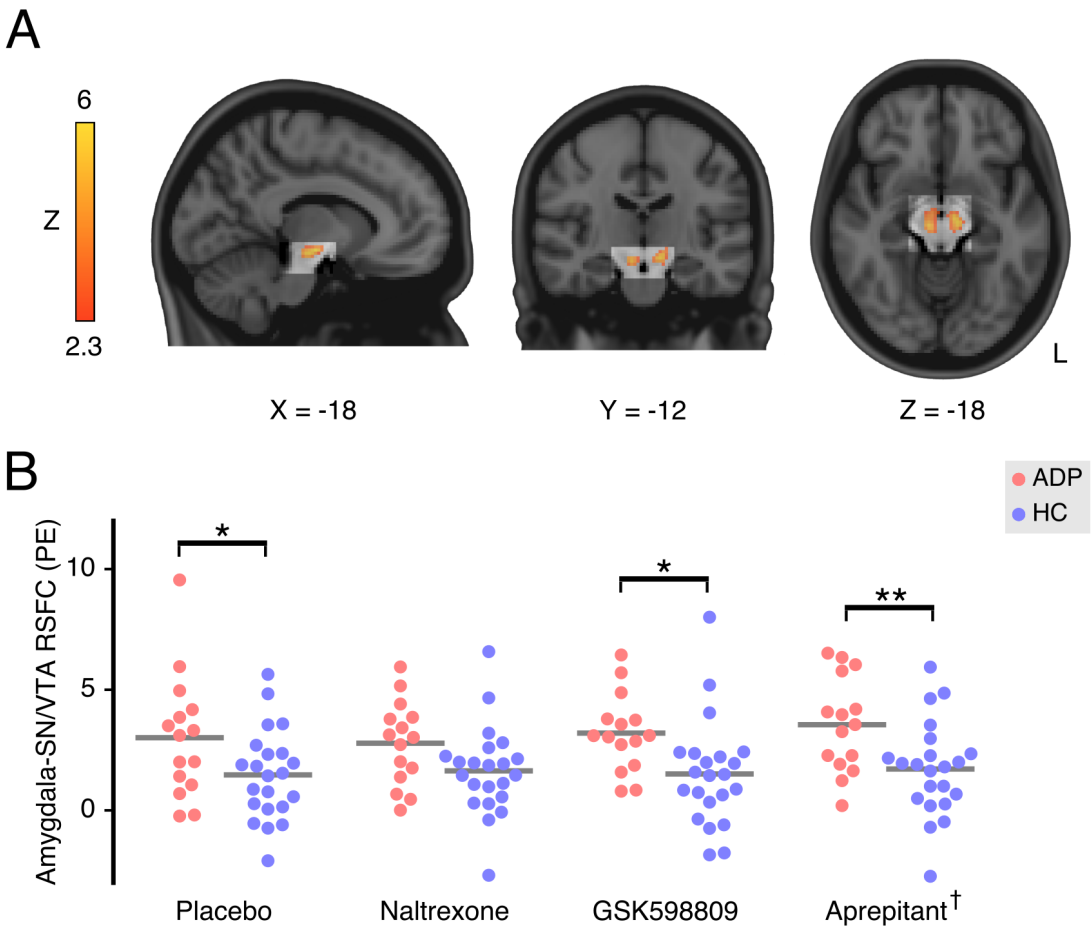


Figure 6.2 Group-level differences in amygdala RSFC across the four drug sessions. (A) Voxelwise effect of group (ADP > HC) on amygdala RSFC across the mean of four experimental sessions, with small volume correction to the midbrain (40 x 16 x 20 mm box; see Figure 6.1 for more details). Significant voxels are shown prior to undergoing anatomical masking with SN/VTA probabilistic atlas region (Murty et al., 2014). (B) Comparison of Amygdala – SN/VTA RSFC between ADP and HC at each of the four experimental sessions. * $p < 0.05$, ** $p < 0.01$. Horizontal lines denote group mean. † denotes Aprepitant/Vofopitant sessions.

The spatial distribution of voxels exhibiting significant group differences (ADP > HC) on the four experimental drug sessions (ADP: 15; HC: 22) revealed a strong overlap with the distribution of voxels showing significant group differences at Baseline in Chapter 4 (ADP: 20; HC: 39). The spatial overlap between the two

effects, both before (Figure 6.3A) and after masking (Figure 6.3B) with an SN/VTA anatomical region of interest, is depicted below.

6.3.2 Subject-level stability of amygdala – SN/VTA RSFC between sessions

Spearman's rank correlations were calculated between each combination of the five sessions to examine the stability of individual differences in amygdala – SN/VTA RSFC over time and under different pharmacological manipulations. For this analysis amygdala – SN/VTA RSFC parameter estimates were extracted from a region of interest based on voxels showing group differences across sessions 2-5 (Figure 6.2A), and not based on group differences at Baseline (Figure 4.1). However, the two versions of the SN/VTA showed substantial overlap with each other (Figure 6.3B).

In a combined group of 29 participants (13 ADP, 16 HC) who had useable data from all five sessions, amygdala – SN/VTA RSFC under Baseline was significantly correlated with amygdala – SN/VTA RSFC under Placebo ($r = 0.68$, $p = 4.4 \times 10^{-5}$; Figure 6.4A), under GSK598809 ($r = 0.74$, $p = 5.4 \times 10^{-6}$), and under Aprepitant/Vofopitant ($r = 0.56$, $p = 0.001$) but not under Naltrexone ($r = 0.19$, $p = 0.3$, Figure 6.4B). In addition, amygdala – SN/VTA RSFC on GSK598809 was also significantly correlated with amygdala – SN/VTA RSFC under both Placebo ($r = 0.48$, $p = 0.009$) and Aprepitant/Vofopitant ($r = 0.59$, $p = 0.0008$).

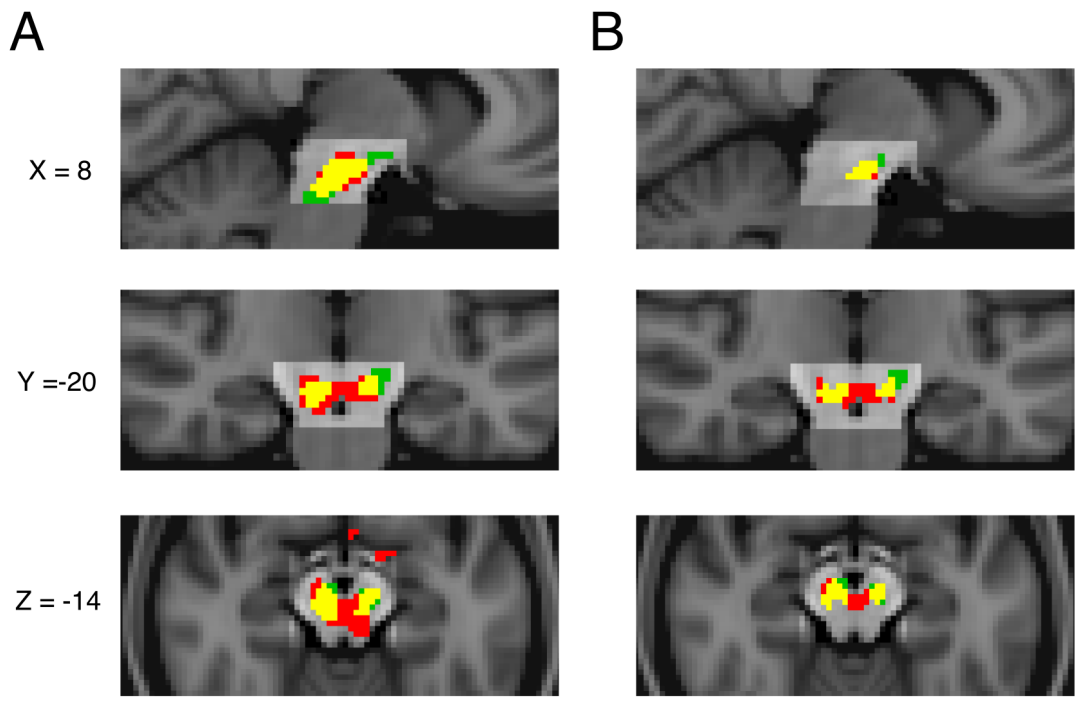


Figure 6.3 Spatial overlap of voxelwise significant group differences at Baseline and across drug sessions. Conjunction of voxels (yellow; Figure 6.2A) showing significantly greater amygdala RSFC in ADP compared with HC at Baseline (red; Figure 4.1) and across the voxelwise average of the four sessions including Placebo, Naltrexone, GSK598809 and Aprepitant/Vofopitant (green, Figure 6.2A). The spatial overlap is presented both before (A) and after (B) the clusters were masked with an SN/VTA anatomical region of interest (see Figure 4.2 for method). Brighter voxels depict the box region that was used for small-volume correction in the analysis of the four drug sessions. Slice coordinates are presented in MNI space.

These same correlations were also tested within ADP (Figure 6.4B) and HC (Figure 6.4C) groups separately. Here, the only correlations that reached significance were in HC, between Baseline and Placebo (r = 0.55, p = 0.03), and between Baseline and GSK598809 (r = 0.55, p = 0.03), showing identical statistics[3].

[3] Since the statistics of the two correlations were identical all the way down to several floating point decimals, the data was further inspected in order to rule out the possibility of a calculation or data handling error. Furthermore, the two correlations

The same framework of analysis was implemented to assess stability of individual differences in amygdala – frontoparietal RSFC. No significant correlations were observed between any of the five sessions in the combined group of ADP and HC, nor in ADP or HC groups taken separately.

6.3.3 Effects of Naltrexone

The effect of Naltrexone on amygdala RSFC in ADP versus HC was not significantly different voxelwise across the brain, therefore the overall effect of the drug was examined across the average of the two groups. Whole-brain analysis across revealed significantly lower amygdala RSFC in the left mPFC, left anterior insula, left dorsal striatum, and bilateral superior temporal gyrus (STG), under Naltrexone relative to Placebo. Amygdala RSFC was significantly greater in left Crus I of the cerebellum and left lateral occipital cortex under Naltrexone relative to Placebo (Figure 6.5).

Anterior insula and dorsal striatum appeared as a single cluster in the Placebo > Naltrexone contrast, therefore they were separated through overlapping them with Harvard-Oxford masks of the insula and caudate/ putamen, respectively.

---

were repeated using Pearson's correlation, instead of Spearman's rank. Here the two statistics were still both significant, but no longer identical.

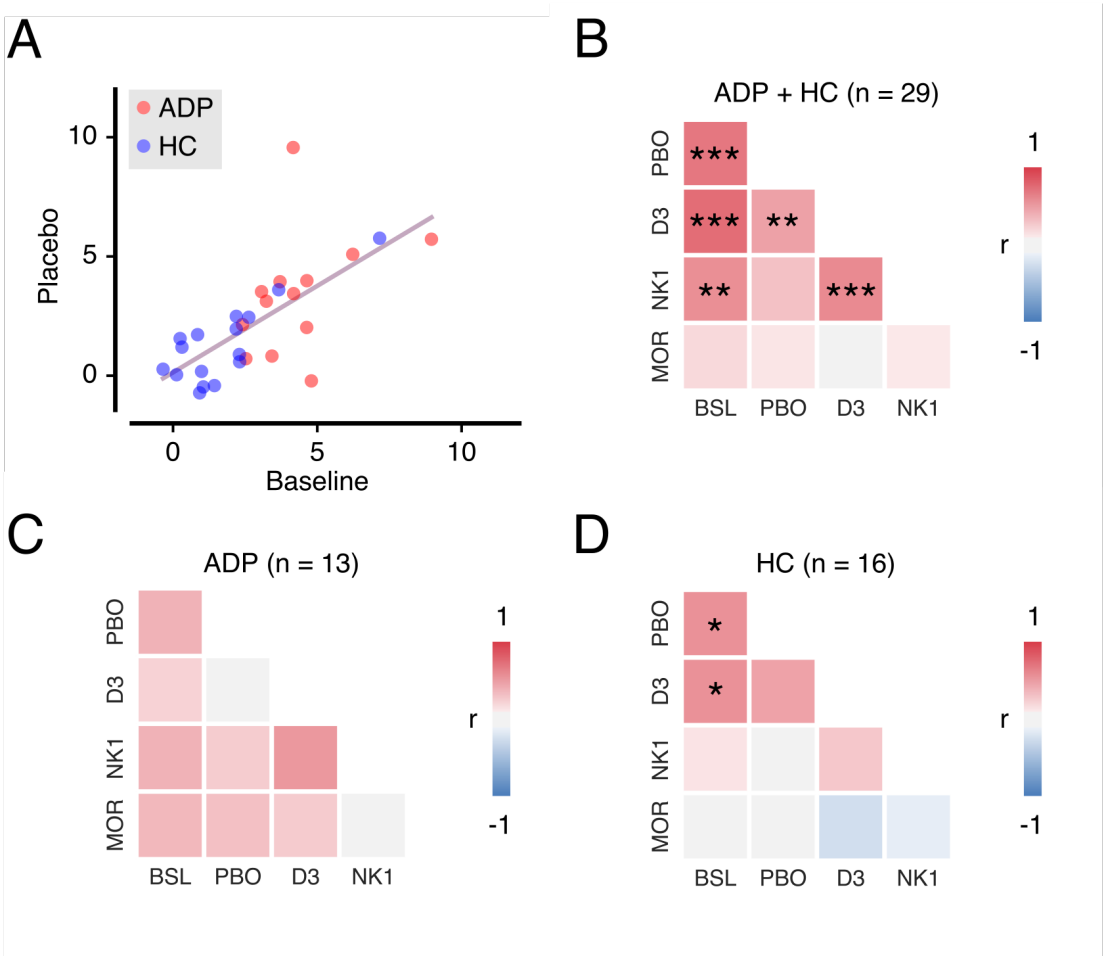


Figure 6.4 Subject-level stability of amygdala – SN/VTA RSFC between sessions. (A) Scatter-plot showing significant correlation between amygdala – SN/VTA RSFC at Baseline (BSL) and Placebo (PBO) within the 29 participants (13 ADP and 16 HC). (B) Correlations between all combinations of the five sessions: Baseline (BSL), Placebo (PBO), Naltrexone (MOR, i.e. μ -Opioid Receptor antagonist) GSK598809 (D3, i.e. DRD3 antagonist) and Aprepitant/Vofopitant (NK1, i.e. NK1 antagonist) within the pooled group participants (n = 29), (C) ADP only (n = 13), and (D) HC only groups (n = 16). Participants were only included if they had usable data from all five sessions. r values to refer to Spearman's r. Significant *p* values are depicted as star symbols. * $p< 0.05$, ** $p < 0.01$, *** $p<0.001$.

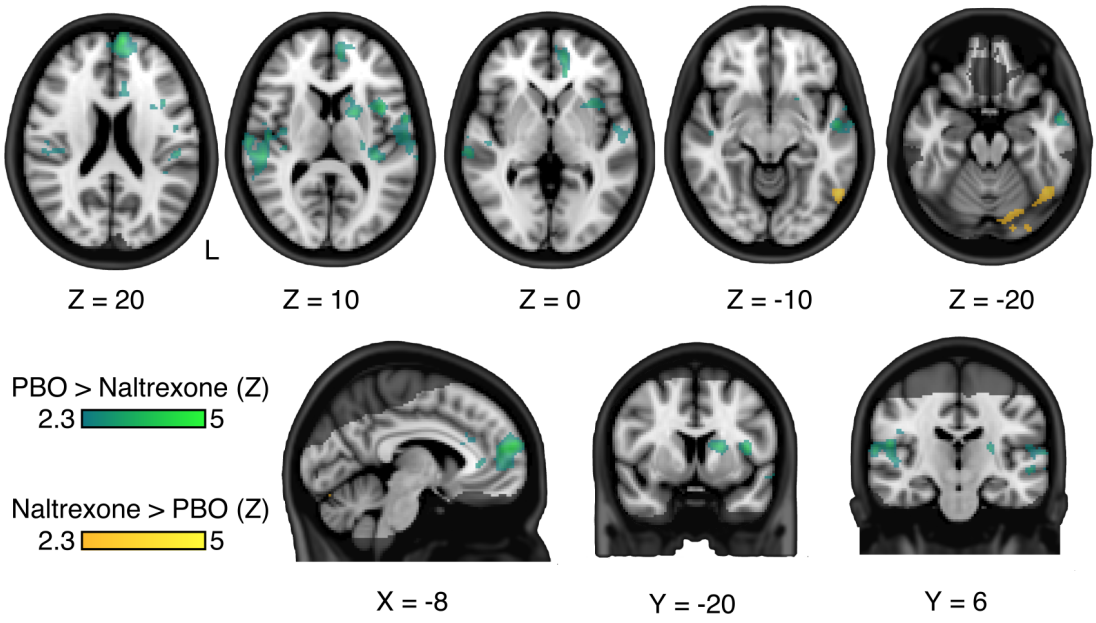


Figure 6.5 Voxelwise effects of Naltrexone on amygdala RSFC. The left medial prefrontal cortex, left anterior insula, left dorsal striatum and bilateral superior temporal gyrus exhibited significantly lower amygdala RSFC under Naltrexone relative to Placebo (PBO). Left Crus I of the cerebellum and lateral occipital cortex exhibited significantly greater amygdala RSFC under Naltrexone relative to Placebo. Contrast were calculated across 37 participants (15 ADP and 22 HC)

Amygdala – dorsal striatal RSFC was significantly reduced under Naltrexone (Figure 6.6) both compared with Placebo (t = -3.9, p = 0.0003) and Baseline (t = -3.4, p = 0.001). Likewise, amygdala – dorsal striatal RSFC was significantly lower under GSK59889 compared with both Placebo (t = -2.2, p = 0.04) and Baseline (t = -2.5, p = 0.02). The effect of Aprepitant/Vofopitant was non-significant for the same contrasts versus Baseline and Placebo.

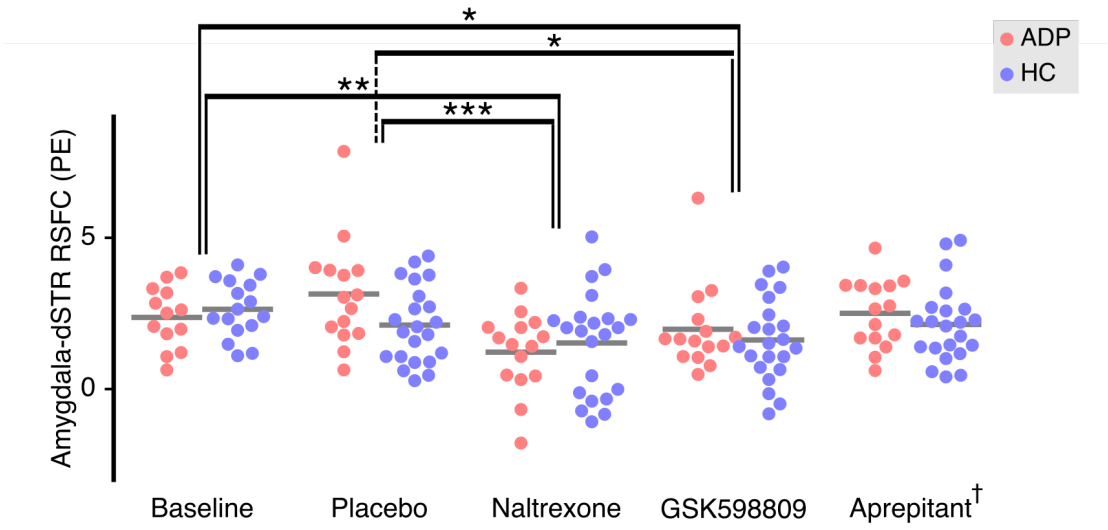


Figure 6.6 Post-hoc comparison of amygdala – dorsal striatal (dSTR) RSFC between the five sessions. Parameter estimates were extracted from a dorsal striatal cluster derived from a Placebo > Naltrexone contrast of amygdala RSFC in 27 participants (15 ADP, 22 HC). Amygdala RSFC was significantly lower under both Naltrexone and GSK598809, compared with Placebo and Baseline sessions. † Aprepitant/Vofopitant * $p < 0.05$; ** $p < 0.01$; *** $p < 0.001$

Anterior insula exhibited a similar overall pattern of modulation to the dorsal striatum, showing significantly reduced amygdala RSFC under both Naltrexone ($t = -3.8$, $p = 0.0005$) and GSK598809 ($t = -2.2$, $p = 0.037$), and no significant effects of Aprepitant/Vofopitant, compared with Placebo (Figure 6.7). However, amygdala - anterior insula RSFC was not significantly different between Baseline and any of the four drug sessions.

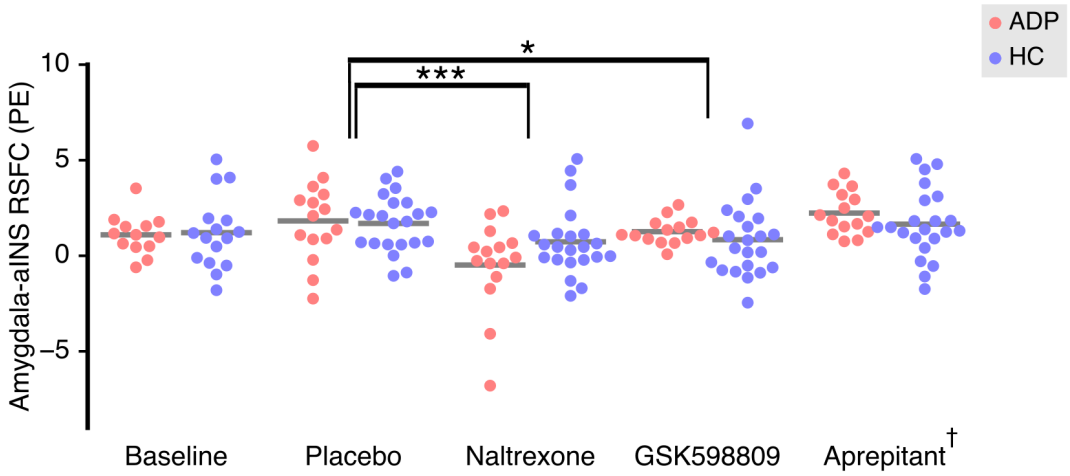


Figure 6.7 Post-hoc comparison of amygdala – anterior insula (aINS) RSFC between the five sessions. Parameter estimates were extracted from an anterior insula cluster derived from a Placebo > Naltrexone contrast of amygdala RSFC in 37 participants (15 ADP, 22 HC). Amygdala RSFC significantly was significantly lower under both Naltrexone and GSK598809, compared with Placebo but not in relation to Baseline. Horizontal lines denote group means. † Aprepitant/Vofopitant * $p < 0.05$; *** $p < 0.001$

6.3.4 Effects of GSK598809 (or Placebo)

Similarly, to Naltrexone, the voxelwise effect of GSK598809 on amygdala RSFC was not significantly different for ADP and HC, therefore effects of GSK598809 modulation were examined across the average of the two groups (15 ADP and 22 HC).

Within this pooled group, whole brain analysis revealed significantly lower amygdala – left mPFC RSFC under both GSK598809 and Naltrexone compared with Placebo. The significant clusters from these two contrasts showed strong overlap (Figure 6.8A), therefore parameter estimates of amygdala RSFC from voxels within this overlapping part of the left mPFC were further explored in post-hoc analyses.

Compared with Placebo, amygdala – left mPFC was significantly lower under all four of the other sessions, including Baseline (t = -3.3, p = 0.001), and Aprepitant/Vofopitant (t = -3.0, p = 0.005), in addition to GSK598809 (t = -3.4, p = 0.002) and Naltrexone (t = -4.6, p = 7.8 x 10^{-5}; Figure 6.8B). Analysis of variance revealed a significant group-by-session interaction ($F(1,27) = 7.1$; $p < 0.01$), between Baseline and Placebo. This effect appeared to be driven by the ADP participants, who showed significantly greater amygdala – left mPFC RSFC compared to their HC counterparts (t = 3.3, p = 0.002).

6.3.5 Effects of Aprepitant/Vofopitant

Again, as with Naltrexone and GSK598809 above, the voxelwise effect of Aprepitant/Vofopitant on amygdala RSFC was not significantly different for ADP and HC, therefore effects of Aprepitant/Vofopitant were examined across the average of the two groups (15 ADP and 22 HC).

Under Aprepitant/Vofopitant amygdala RSFC was elevated compared with Placebo in a number of regions that included the bilateral superior temporal gyrus, bilateral posterior insula, right precuneus and left putamen. There were no significant clusters showing reduced amygdala RSFC under Aprepitant/Vofopitant compared with Placebo.

6.3.6 Opposing effects Naltrexone and Aprepitant/Vofopitant

Naltrexone and Aprepitant/Vofopitant showed opposing effects on amygdala RSFC in the Superior Temporal Gyrus (STG), where Naltrexone significantly increased (t = -4.8, p = 3.0 x 10^{5}), and APR significantly decreased (t = 4.7, p = 4.1 x 10^{5}) RSFC relative to Placebo, across ADP and HC participants (n = 37).

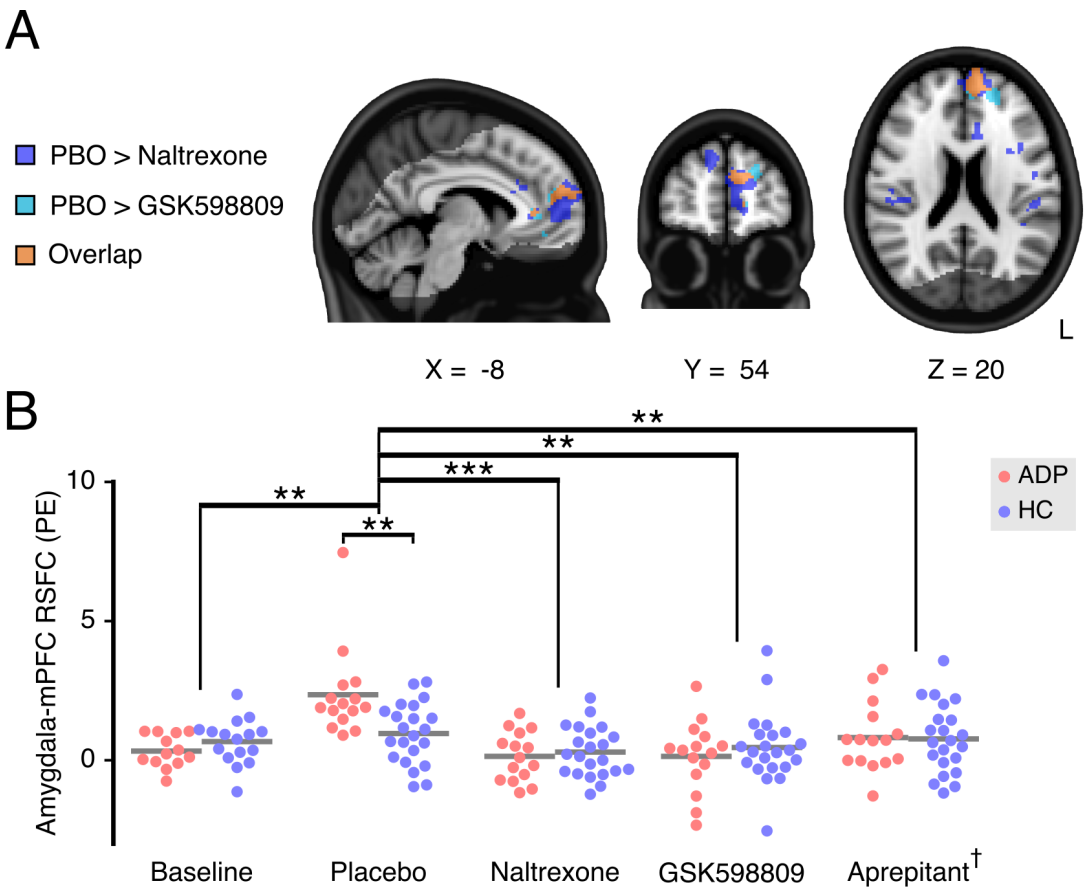


Figure 6.8 Overlapping effects of Placebo on amygdala RSFC in the left mPFC. (A) Overlapping voxels in left mPFC showed significantly differential amygdala RSFC in the Placebo > Naltrexone, and the Placebo > GSK5988009 voxelwise contrasts across a sample of 37 participants (15 ADP and 22 HC). (B) Comparison of amygdala – left mPFC RSFC between baseline and the four drug sessions. Amygdala RSFC was significantly higher under Placebo compared with each of the other four sessions. Under Placebo ADP showed significantly higher amygdala – left mPFC RSFC than HC. Horizontal lines denote group means. * $p < 0.05$; ** $p < 0.01$; *** $p < 0.001$.

Similarly, amygdala – STG RSFC was significantly reduced under Naltrexone (t = -4.7, p = 1.3 x 10^5) and significantly increased under Aprepitant/Vofopitant (t = 2.5, p = 0.01) in relation to Baseline (ADP = 13, HC = 16). Amygdala – STG RSFC was not significantly different between GSK598809 and Placebo, between GSK598809 and Baseline or between Baseline and Placebo.

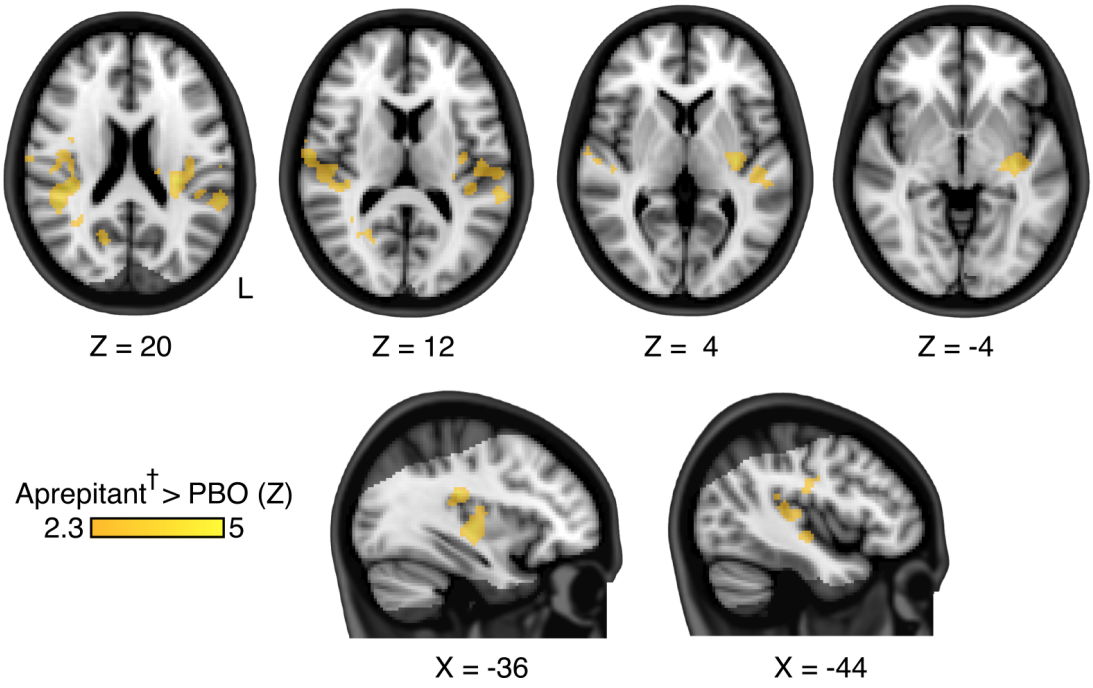


Figure 6.9 Whole-brain voxelwise effects of Aprepitant/Vofopitant on amygdala RSFC. Under Aprepitant, participants showed significantly greater amygdala RSFC in the bilateral superior temporal gyrus, bilateral posterior insula, right precuneus and left putamen than under Placebo. Drug effects were calculated across 37 participants (15 ADP and 22 HC).† Aprepitant/Vofopitant.

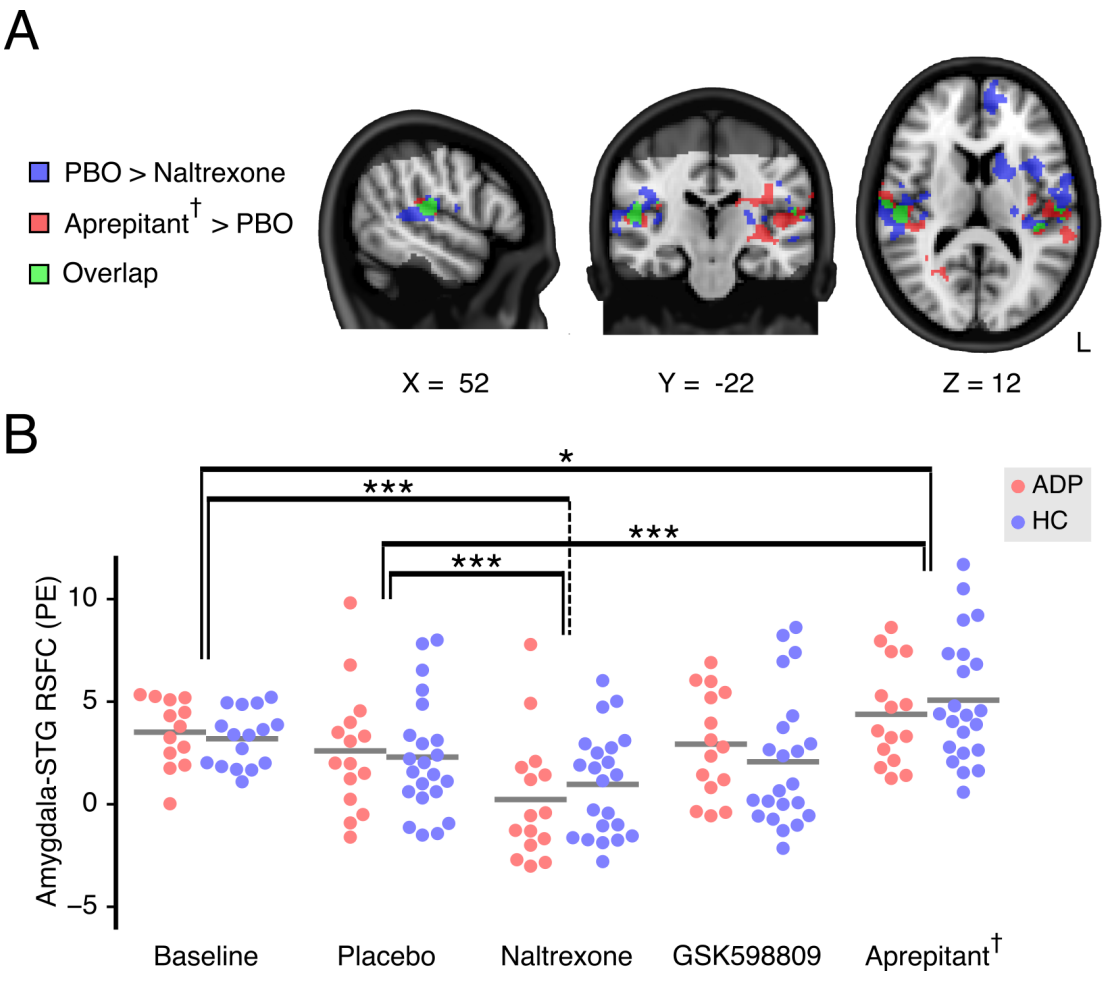


Figure 6.10 Opposing effects of Naltrexone and Aprepitant/Vofopitant on amygdala – superior temporal gyrus (STG) RSFC. (A) Overlap of voxels in the bilateral STG that show negative modulation of amygdala RSFC by Naltrexone with those showing positive modulation by Aprepitant/Vofopitant. These contrasts were calculated across 37 participants (15 ADP and 22 HC). **(B)** Comparison of amygdala – bilateral STG RSFC between baseline and the four drug sessions. Horizontal lines denote group means. .† Aprepitant/Vofopitant.; * $p < 0.05$; ***; $p < 0.001$.

6.4 Discussion

6.4.1 Summary

In contrast to Hypothesis IX, the voxelwise analysis of amygdala RSFC did not reveal a significant group-by-drug interaction for any of the three drugs, i.e. effects of modulation by either Naltrexone, GSK598809 or Aprepitant/Vofopitant did not exert

significantly differential effects on ADP than on HC. Additionally, there was no evidence of normalization of the previously observed elevation of amygdala – SN/VTA RSFC in ADP, therefore hypothesis X was also not supported. Amygdala – SN/VTA RSFC was robustly elevated in ADP compared with HC across the three drug sessions as well as under Placebo.

Furthermore, amygdala – SN/VTA RSFC between Baseline and three of the four drug sessions showed a strong association across ADP, suggesting that this finding may be a relatively robust feature of alcohol dependent populations.

Since group-by-drug interactions were not found, voxelwise effects of drug modulation were explored across all participants. Hypothesis XI was supported as Naltrexone, GSK598809 and Aprepitant/Vofopitant showed both overlapping and differentially distributed effects of modulation, with respect to Placebo. Specifically, under Naltrexone, and to a lesser extent, under GSK598809, amygdala RSFC was significantly reduced in the dorsal striatum and anterior insula, regions that have been associated in the literature with habit formation (Everitt & Robbins, 2005) and salience detection (Menon & Uddin, 2010), respectively.

Aprepitant/Vofopitant and Naltrexone exerted opposite effects on amygdala RSFC, where NK1 antagonism positively and Naltrexone negatively modulated amygdala – STG RSFC in relation to Placebo. This dichotomy may relate to animal models suggesting differential mechanisms, where NK1 antagonism acts through modulation of stress-related behaviours, while μ-opioid receptor antagonism through influencing cue-related relapse behaviours. NK1 was also found to significantly increase amygdala RSFC in the posterior insula bilaterally, a circuit that has been linked to mechanisms of anxiety, as described in Chapter 5.

Perhaps the most intriguing finding was the observation of significantly greater amygdala RSFC in the left mPFC under Placebo, compared with all other sessions, including Baseline. Post-hoc tests revealed that this effect was driven specifically by elevations of amygdala – left mPFC in the ADP group.

6.4.2 Amygdala – SN/VTA RSFC

Whole-brain amygdala RSFC on average across the four sessions, exhibited increased amygdala – SN/VTA in ADP relative to HC, in midbrain voxels that strongly overlapped with the same group effect observed under Baseline in Chapter 4. Pairwise comparison of ADP and HC for amygdala RSFC using an SN/VTA region of interest further confirmed this effect separately within each session. The replication of these findings in an overlapping group of participants, across four sessions, under the modulation of three separate receptor systems or placebo exemplifies the robustness of this effect as a neurophysiological correlate of alcohol dependence.

In addition to the consistency of this effect between ADP and HC over time, its longitudinal stability within ADP is also important for this metric to be a viable pharmacological target. In experimental medicine studies, such as ICCAM, drug and placebo conditions are separated by time, often on the span of days or weeks. It is important for a ~~marker~~ measure of interest to show good test-retest reliability and to not be easily perturbed by daily variation in variables of no interest to the central question of the study e.g. what exactly the participant had for breakfast on each day. Good test-retest reliability increases the chance that the variance related to the experimental manipulation (drug vs placebo) can be separated from variance driven by background variables that are of no interest.

RSFC as measure is intrinsically dynamic, and assumed to be determined by a combination of trait and state effects, whose relative weights may vary depending on the circuit of interest. Subcortical networks generally show greater state-dependence than cortical networks (Mennes et al., 2013), therefore the relative stability of this measure given its subcortical-to-subcortical distribution is intriguing. While amygdala RSFC-based correlates of anxiety-disorders (Etkin et al. 2009) and of smoking dependence severity have previously been replicated across samples (Hong et al., 2009; Hong et al., 2010), to my knowledge this is the first study to show a between-session replication of an alcohol dependence related metric that uses RSFC.

Another important feature of a useful neurophysiological marker in experimental medicine studies is sensitivity to pharmacological manipulation. Since amygdala – SN/VTA RSFC was correlated across sessions characterized by approximately 80% blockade of distinct receptor systems, this may suggest that this measure is not sensitive to pharmacological manipulation. However, it is also possible that while none of the three receptor systems targeted in this study are effective at normalising this marker, others may be. For example, corticotrophin releasing factor (CRF) receptors are expressed at both SN/VTA and amygdala (Grieder et al., 2014), while CRF antagonists have shown success in preventing relapse in animal models (Heilig et al., 2007). Although a recent experimental study of the CRF antagonist, Pexacerfont, was not successful reducing alcohol craving, or anxiety (Kwako et al. 2015), resting state function was not specifically investigated in that study.

6.4.3 Amygdala – insula and amygdala – dorsal striatal RSFC

Acute Naltrexone treatment was associated with a reduction in amygdala RSRC in the dorsal striatum and anterior insula across participants. Neuroadaptations in the dorsal

striatum are thought to underlie the transition from voluntary to compulsive drug use (Everitt & Robbins, 2005). The anterior insula plays diverse roles in brain function, but its main role may be summarised as a salience detector (Menon & Uddin, 2010). Additionally, it has also been proposed to integrate physiological and affective representations that underpin craving (Garavan, 2010). The amygdala, insula and dorsal striatum all show μ-opioid, and κ-opioid receptor associated binding of selective radiotracers (Weerts et al., 2011). Since Naltrexone acts as an antagonist at both receptors (Nutt, 2014), either may have contributed to observed effects of reduced amygdala – anterior insula and amygdala – dorsal striatal RSFC.

Aprepitant/Vofopitant also exerted significant modulation on amygdala – insula RSFC in comparison to Placebo. However, the effects NK1 antagonism on amygdala RSFC were localised to the bilateral posterior, not the anterior insula, and involved an upregulation, of RSFC, instead of the downregulation of RSFC associated with opioid receptor blockade. The literature outlined in the introduction of this Chapter has suggested a role for NK1-antagonism in protecting from stress-related mechanisms of relapse (Schank et al., 2012). However, since high levels of amygdala – posterior insula RSFC are suggestive of greater-levels of anxiety both in the literature (Sripada et al., 2012) and in the findings outlined in Chapter 5, it is difficult to see how the Aprepitant/Vofopitant mediated upregulation of RSFC observed in this circuit would be of therapeutic benefit. However, it is theoretically possible that endogenous upregulation and NK1-antagonist mediated upregulation of amygdala – posterior insula RSFC may be underpinned by different lower-level mechanisms, with opposing consequences for subjective experience of anxiety and clinical outcome.

6.4.4 Amygdala – STG RSFC

Aprepitant/Vofopitant increased amygdala RSFC in the bilateral STG in overlapping voxels where Naltrexone reduced amygdala RSFC relative to placebo. These opposing effects of the two drugs on amygdala – STG RSFC demonstrate that our treatment protocol could exert specific pharmacological effects on amygdala resting state network function. However, their interpretation is made difficult by the dearth of literature on the effects of these two compounds on amygdala – STG circuits and the significance of this circuit to mechanisms of alcohol dependence.

The spatially overlapping effects of Naltrexone and Aprepitant/Vofopitant on amygdala RSFC were localised inferior to the lateral sulcus, therefore indicating involvement of early auditory areas. In previous fMRI studies the STG has been found to be bilaterally engaged by pure tones, voice, music, vocal sounds and noise (Samson et al., 2011, Schirmer et al., 2012), including acoustic scanner noise (Bandettini et al., 1998, Gaab et al., 2007). Although resting state scans are often thought of as stimulus-free (e.g. Preminger et al., 2011), the rapidly alternating currents underlying the acquisition sequence produce repetitive, high-pitched clicking sounds that are loud enough to necessitate the wearing of earplugs.

The amygdala plays an important role in monitoring and signalling the presence of salient and potentially threatening stimuli in the immediate environment, including those in the auditory modality. Tracing and electrophysiology studies in rodents have delineated projections from the auditory cortex and auditory thalamus to the lateral amygdala (Quirk et al., 1997). Glucose utilization as measured by 2-DG autoradiography in the macaque has shown evidence for amygdala engagement during passive listening to acoustic stimuli (Poremba et al., 2003). PET imaging in

humans has also shown correlated activity between amygdala and regions of the primary auditory cortex engaged during discriminative classical conditioning by aversive bursts of white noise (Morris et al., 1998).

Based on these findings one can speculate that the observed differences in amygdala – STG RSFC under Aprepitant/Vofopitant, Naltrexone and Placebo may reflect differential levels of engagement with the scanner sounds that pervade the immediate environment. Although a visual analog scale (Bond and Lader, 1974) was used to assess mental state of participants after each scan (e.g. “Relaxed/Tense”, “Happy/Sad”, “Interested/Bored”), none of the items were relevant to how they coped with acoustic noise in their immediate environment. Differences in amygdala – STG RSFC may reflect differences in overall levels of apprehension, aversion from or attentional focus on scanner noise, but may also involve processes outside conscious awareness.

It is unclear whether these drug effects preferentially modulate auditory processes or whether they affect overall responsivity to lower-level stimuli of other modalities as well, e.g. visual, thermal, tactile. The fact that the scanner noise is arguably the most dominant stimulus in the context of the scanner experience may result in greater sensitivity to detect pharmacological effects in regions subserving auditory processes versus other modalities. Novel, unpublished data (Leor Roseman, personal communication) also indicates that amygdala – left inferior parietal lobule (directly superior to STG above the Sylvian Fissure) RSFC is increased after psilocybin-assisted psychotherapy, compared with scans taken before. It is possible that the modulation of these spatially overlapping auditory regions, may reflect alteration of broad cognitive processes, e.g. increased attention to all environmental stimuli, rather

than a more selective modulation of auditory function. While the role of DRD3 signalling in cognitive function has been a subject of a recent review (Nakajima et al., 2013), this still a relatively unexplored area for research on the NK1 and the Opioid receptor systems.

6.4.5 Amygdala – mPFC RSFC

Individual contrasts between Placebo and GSK598809 and between Placebo and Naltrexone suggested that both drugs reduced amygdala RSFC in overlapping regions of the left mPFC. However, comparison of parameter estimates extracted from Baseline and Aprepitant sessions indicated that the effects were driven by increased amygdala – mPFC RSFC under Placebo, rather than through modulatory effects of Naltrexone and GSK598809. Post-hoc comparison of subject-level parameter estimates of amygdala RSFC from this mPFC region, showed elevated amygdala – mPFC RSFC in Placebo compared with all other four sessions, a finding that was unexpected. It should be reiterated here that the pill labels were packaged in identical containers, the labels were blinded, and were administered by nursing staff there were independent from the research (Paterson et al., 2015).

Novelty effects provide one possible explanation for the observed differences in amygdala – mPFC RSFC between Baseline and Placebo sessions. The Baseline session was for some of the participants, from both the HC and ADP groups, the first experience of entering an MRI scanner. Since RSFC is shaped not only by enduring aspects of brain physiology but also by the participant's current psychological state, the novelty of the first day of the study may have introduced variability into the observed RSFC. Different participants may have responded differently to being in the scanner for the first time, as well as to the novelty of the first day of being in the

study. From this point of view, the first session, i.e. Baseline, may not be ideal for detecting group effects. Since the Baseline condition was always on the first session, and Placebo always on the second or third session, it is impossible to dissociate the specific effects of session order versus effects of the experimental manipulation, i.e. Placebo administration versus the absence of Placebo administration. However, order effects (e.g. novelty on the first session) do not provide a simple account of why no differences were observed in amygdala – mPFC RSFC between Baseline and the three drug sessions: Naltrexone, GSK598809, and Aprepitant/Vofopitant.

6.4.6 Neural mechanisms of Placebo

Another account of these findings is that the increased amygdala – mPFC RSFC under Placebo relative to Baseline may reflect the neural correlates of a placebo effect. The placebo effect is a physiological, cognitive or affective response to treatment driven by individual expectations (Ploghaus et al., 2003) or conditioning (Colloca et al., 2010), rather than through the intended target mechanism of treatment, e.g. in this case pharmacological antagonism of a receptor subtype.

Although participants in ICCAM were not instructed to expect a particular subjective response to the three compounds, they were aware that one of the aims of the study was to understand the effects of these compounds on the brain using MR imaging. This knowledge could have plausible induced an expectation that the compounds may elicit some observable subjective effects on their experience in the scanner. They were also informed that the compounds tested were investigated as potential treatments for abstinence prevention in substance-dependence populations. Therefore, the understanding that the compounds were specifically tailored to affect change in their brains may have resulted in stronger placebo effects in ADP than in HC.

The findings of increased RSFC between amygdala and mPFC under placebo are in tune with previous neuroimaging studies that have investigated the neural correlates of placebo effects. Increased activation of the rostral ACC (rACC) has been observed both under placebo-mediated hypoaglesia (Petrovic et al., 2002), and placebo-mediated reduction of affective responsivity (Petrovic et al., 2005). In the latter study, greater placebo-mediated reductions of subjective ratings of unpleasantness were also associated with lower amygdala activation under placebo across participants. Another study also observed recruitment of rACC, as well as enhanced rACC connectivity with amygdala and PAG during placebo-mediated hypoalgesia (Bingel et al., 2006).

Even if one accepts the interpretation that the placebo effect was responsible for the observed elevation of amygdala – mPFC RSFC under Placebo relative to the Baseline condition, one must still account for the absence of this same effect under Naltrexone, GSK598809 and Aprepitant/Vofopitant administration. A potential explanation is that the three compounds may have each blocked some underlying process associated with the Placebo state, through their own respective pharmacological mechanisms. Providing some support for this interpretation, there is a growing body of literature implicating μ-opioid and dopamine D2/D3 receptor function in the placebo effect (Pecina & Zubieta, 2015).

Opioid mechanisms were first implicated in the placebo effect in a study of post-operative dental pain where naloxone was shown to selectively block placebo-induced hypoalgesia in placebo responders, but not in non-responders (Levine et al., 1978). While no previous study has examined the effects of Naltrexone on mechanisms of the placebo effect, NTX and naloxone have similar affinity profiles for opioid

receptor classes (μ > κ > δ; Nutt et al., 2014), therefore are likely to have similar antagonistic properties on placebo effects.

Since this pioneering study by Levine et al., 1978, modern PET imaging studies using the μ-opioid selective [11C]carfentanil radiotracer have demonstrated robust elevation of opioid neurotransmission in the rACC and amygdala under placebo (Wager et al., 2007, Scott et al., 2008, Peciña et al., 2013), amongst other opioid receptor rich regions such as PAG, OFC and insula. One of these studies measured D2/D3 receptor binding potentials in addition to μ-opioid binding potentials in the same set of participants, showing that μ-opioid and D2/D3 were correlated in the amygdala, subgenual ACC, insula, and putamen (Scott et al., 2008). Activation of both D2/D3 and μ-opioid receptor systems in the striatum was greater for placebo responders, and reduced for nocebo responders.

In another study, using an overlapping cohort, the same team showed that stronger placebo-mediated hypoalgesia was associated both with greater D2/D3 binding potentials in NAc as measured by [11C]raclopride and with greater BOLD activation during monetary reward anticipation as measured by fMRI (Scott et al., 2007). This was not the first study to implicate D2/D3 signalling in the placebo effect. An earlier study has reported that injection of saline as placebo in Parkinson's patients was associated with increased [11C]raclopride binding potential in the dorsal striatum, and greater self-reported clinical improvement (La Fuente-Fernández et al., 2002).

These studies provide evidence for a role of μ-opioid and D2/D3 signalling in placebo mechanisms, and are compatible with the possibility that acute administration of GSK598809 and Naltrexone in the current study may have abolished placebo effects,

resulting in a reduction of amygdala – mPFC RSFC levels that are indistinguishable from measurements at baseline.

The role of NK1 and its ligand Substance P in placebo effects has not been investigated directly. However, Substance P has been shown to regulate both opioid and dopaminergic function, and modulation of NK1 receptors appears to influence pain and reward processing. It is possible that NK1 antagonism may abolish placebo effects through modulation of opioid or dopaminergic pathways.

6.4.7 Possible effects of Vitamin C on amygdala – mPFC RSFC

A competing explanation for the unexpected rise in amygdala – mPFC observed under Placebo versus the other four sessions, is a potential effect of the 50 mg of Vitamin C contained in the placebo pill on brain function. Vitamin C is frequently used as the core ingredient in placebo pills in experimental medicine studies of brain function due to its assumed lack of physiological effects and inability to cross the blood brain barrier (Joules et al., 2015, Carhart-Harris et al., 2015, Kroes et al., 2010, Rubia et al., 2011). However, dehydroascorbic acid, an oxidised form of Vitamin C, can enter the brain via the glucose transporter GLUT1, and remain there in a reduced form as ascorbic acid (Agus and colleagues, 1997).

Ascorbic acid is known to be present in the brain at a manifold higher concentration than in blood, yet its main functions remain elusive. Earlier studies have suggested a role in neuroprotection from free radicals and glutamate toxicity, and potential modulation of neuronal function (reviewed in Grunwald, 1992). Although few studies research neuromodulatory effects of vitamins, a 2011 paper reported allosteric modulation of $GABA_A$ and $GABA_C$ receptors in the retina by ascorbic acid (Calero et

al., 2011). If through future work ascorbic acid turns out to play preferential role in modulating certain neurotransmitters systems in the brain (e.g. GABA), then it may be able to account for preferential modulation of certain large-scale circuits (e.g. amygdala – mPFC) over others (amygdala – SN/VTA). However, until then, this account remains an unlikely explanation for the effects observed in this study under Placebo.

Chapter 7: General discussion

7.1 Thesis summary

7.1.1 Summary of aims

One of the key challenges in the treatment of alcohol dependence is our lack of understanding of the neural mechanisms that underlie disease severity and relapse vulnerability. During the maintenance phase, and in the early stages of abstinence, intensity and frequency of craving, anxiety or dysphoria provide useful clinical measures of alcohol dependence severity, and relapse vulnerability. However, over the course of abstinence these may attenuate or completely subside, and yet individuals may continue to be at a risk for relapse. Since there is no objective measure for assessing disease severity in alcohol dependence, this makes it difficult to assess the potential efficacy of different treatment approaches on abstinence populations. Therefore, the overarching aim of this thesis was to discover novel neurophysiological correlates of disease severity in abstinence ADP populations, which could potentially serve as viable targets for therapeutic modulation.

This aim was pursued in the sequence of steps outlined below:

Chapter 3 – Design and implementation of a preprocessing pipeline for optimal artifact removal in resting state fMRI data, with carefully selected algorithms for each preprocessing step based on recent findings and recommendations from the literature.

Chapter 4 – Experimental identification of brain regions showing altered amygdala RSFC in abstinent ADP relative to HC, and exploring the effects of GM atrophy, age, cumulative alcohol exposure, abstinence and smoking on these alterations.

Chapter 5 - Examination of the effects of self-reported anxiety and abstinence length on amygdala RSFC across the brain, and the relationship between amygdala RSFC and BOLD activation during behavioural tasks relevant to models of addiction.

Chapter 6 - Investigation of the effects of acute pharmacological modulation of amygdala RSFC in abstinent ADP and HC. Three receptor subtypes (μ-opioid, DRD3, NK1) were targeted through antagonists, two that are potential pharmacotherapies (GSK598809, Aprepitant/Vofopitant), and one that is a currently approved therapy for relapse prevention (Naltrexone).

7.1.2 Summary of findings

Chapter 4 presented a comparison of whole brain amygdala seed-based RSFC between ADP and HC in the baseline session of ICCAM. The only significant cluster in this contrast was located to the SN/VTA where ADP showed significantly greater amygdala RSFC than HC, despite the two groups not significantly differing on age, gender, head motion in scanner, resting pulse rate or blood pressure metrics. The ADP sample did contain more smokers, yet HC smokers and HC non-smokers showed similar levels of amygdala-SN/VTA RSFC, indicating that nicotine use by itself was unlikely account for these elevations.

Amygdala-SN/VTA RSFC was significantly correlated with cumulative alcohol exposure and age, but not with abstinence duration in ADP. This pattern of results is compatible with neuroadaptations in amygdala network function from chronic alcohol exposure that fail to recover with abstinence. Although the possibility of pre-existing differences could not be ruled out, family history of alcohol dependence was not associated with elevations of amygdala RSFC in this circuit in either ADP or HC.

Furthermore, animal studies have shown that chronic alcohol exposure can trigger synaptic neuroadaptations that persist into pro-longed abstinence, both in the amygdala (Roberto et al., 2004, Gilpin and Roberto, 2012) and VTA (Diana et al., 1996, Shen et al., 2007).

As anticipated based on previous literature (Makris et al., 2008), ADP showed significantly lower GM volume in subcortical regions, including amygdala and SN/VTA. Amygdala GM volume was inversely correlated with age and cumulative alcohol exposure, but not with abstinence length. Age was not correlated with amygdala GM volume in HC, despite similar distribution of age as ADP, suggesting the possibility of accelerated age-related atrophy in ADP.

These structural findings appeared to mirror the functional effects presented earlier in Chapter 4, thereby suggesting a model whereby chronic alcohol use is associated with both cumulative GM volume atrophy in the amygdala and concurrent elevations in amygdala – SN/VTA RSFC. However, surprisingly the two measures: amygdala – SN/VTA RSFC and amygdala GM volume, were not correlated with each other, across ADP, suggesting partially distinct underlying mechanisms. Since cumulative alcohol exposure and age were strongly correlated with each other in this sample, multiple regression analyses were undertaken to examine their differential effects within a single model. After accounting for their shared variance, only cumulative alcohol exposure was associated with amygdala – SN/VTA, not age, and only age was associated with amygdala GM volume, and not cumulative alcohol exposure. These findings suggest partially separable effects of ageing and cumulative alcohol exposure on amygdala structure and function, respectively, in ADP.

Chapter 5 explored the impact of abstinence length and anxiety, two putative moderators of relapse risk, on amygdala RSFC. Voxelwise whole-brain regression revealed a significant inverse association between abstinence length and amygdala RSFC in a frontoparietal network consisting of the inferior parietal lobules, pre-supplementary motor area (preSMA), and dorsal PCC (dPCC). Post-hoc analyses confirmed that ADP with less than 2 months' abstinence showed significantly reduced amygdala frontoparietal RSFC than HC or ADP with at least 6 months' abstinence. Consistent with previous descriptions of frontoparietal resting state networks (Yeo et al., 2011), the inferior parietal lobule was found to show a high level of RSFC with the preSMA and dPCC, in an independent group of healthy participants collected as part of this study (Pilot cohort, Section 5.2.2). In addition, two of the same frontoparietal regions (inferior parietal lobules, preSMA) were found to engage during successful inhibitions in the Go/No-Go task, with the magnitude of activation showing a trend-level association with amygdala – frontoparietal RSFC across a pooled sample of ADP, HC and Pilot participants.

ADP scored significantly higher on self-report measures of trait and sate anxiety than HC, while also reporting a wider range of anxiety levels. Trait anxiety was found to show a positive association with amygdala RSFC in the posterior insula (after small volume correction to the entire bilateral insula). This finding was consistent with previous studies of amygdala resting state function in patients with PTSD (Rabinak et al., 2011; Sripada et al., 2012), task activation studies of anxiety-prone healthy individuals (Stein et al., 2007) and patients with panic disorder (Etkin & Wager, 2007). However, post-hoc analysis indicated that the significance of this result was driven by a single participant with a high level of anxiety and RSFC in this circuit, questioning the robustness of this effect. In addition, the directionality of this effect

was difficult to reconcile with previous findings from our group that showed reduced amygdala – anterior insula RSFC in ADP relative to HC (Orban et al., 2013).

Chapter 6 investigated the potential capacity of acute μ-opioid, dopamine D3 and NK1 receptor antagonism in modulating amygdala resting state function. One hypothesis (Hypothesis X) tested was whether any of the three antagonists could normalise high levels amygdala – SN/VTA RSFC in ADP, which was shown to be associated with cumulative alcohol exposure in Chapter 4. Despite participants receiving a dose of each drug that was calibrated to produce 80% receptor occupancy, none of the drugs had a significant impact on RSFC in this circuit. ADP continued to show elevated amygdala – SN/VTA RSFC relative to HC under each of the three compounds, as well as Placebo. This observation and the additional finding that individual differences in amygdala – SN/VTA between Baseline, and under Placebo, NK1 and DRD3 blockade were significantly correlated indicated that amygdala – SN/VTA RSFC may be a relatively stable correlate of cumulative alcohol exposure.

In addition to assessing the effects of the three drugs on *a priori* circuits of interest e.g. amygdala – SN/VTA, whole-brain exploratory analysis of their effects on amygdala RSFC was also undertaken. Since none of the three drugs modulated amygdala RSFC differentially between ADP and HC on the voxelwise level, voxelwise drug effects were examined on average across the two groups.

Amygdala – dorsal striatal and amygdala – anterior insula RSFC were significantly reduced under Naltrexone and, to a lesser extent, under GSK598809 relative to Placebo. Amygdala – dorsal striatal RSFC under these two compounds was also significantly reduced in comparison to the Baseline session. Although at first glance

crosschecking these effects with respect to the Baseline session may seem redundant, the following results on amygdala – mPFC RSFC demonstrate its importance.

The same overlapping cluster in the mPFC was found to show significantly lower amygdala RSFC under both Naltrexone and GSK598809 compared with Placebo. Initially these effects were interpreted as a simple down-regulation of amygdala RSFC by both drugs, until the parameter estimates for amygdala – mPFC were plotted and compared across all five sessions. Here it was revealed that amygdala – mPFC was significantly lower not only under Naltrexone and GSK598809, but also under Baseline and Aprepitant/Vofopitant conditions, relative to Placebo.

In light of these findings, the more parsimonious explanation arose that the observed effects of increased amygdala – mPFC may reflect neural correlates of some aspect of the placebo effect. Indeed, previous neuroimaging studies have implicated both the amygdala and mPFC in mechanisms of the placebo effect, albeit in studies of placebo-mediated hypoalgesia (Petrovic et al., 2002) and expectation of relief from aversive perceptual stimuli (Petrovic et al., 2005). In this study, all participants were informed that the experimental drugs they took were investigated for their potential in relapse prevention, and that the fMRI scans were undertaken to understand their potential effects on brain function. Although participants were not told to specifically anticipate any subjective effects, the mere awareness that these drugs were designed for substance-dependent populations may have increased the intensity of placebo effects, associated with subjective expectations, preferentially in the ADP relative to HC. Indeed, a post-hoc assessment of a group-by-drug interaction, indicated that the observed overall increase in amygdala – left mPFC under Placebo versus Baseline, was driven by ADP rather than the HC cohort.

However, this interpretation also had to account for why amygdala – mPFC was not significantly elevated under GSK598809, Naltrexone, Aprepitant/Vofopitant, where placebo effects of expectation would be expected to be similar due to the blinded nature of the study. One viable explanation is that the three drugs may have each inhibited mechanisms of placebo through their respective mechanisms. This interpretation is consistent with previous studies that have linked placebo effects with μ-opioid, and DRD2/DRD3 receptor signalling pathways (Pecina & Zubieta, 2015). The consequence of NK1-receptor blockade on placebo effects has not been studied before, although it is possible that its endogenous ligand, Substance-P may also play a potential role in placebo related effects.

Another key finding to arise from Chapter 6 was that μ-opioid and NK1 antagonism had opposing modulatory effects on amygdala – bilateral superior temporal gyrus (STG) RSFC. Under Naltrexone, the amygdala – STG RSFC was significantly lower, while under Aprepitant/Vofopitant it was significantly higher relative to both Baseline and Placebo sessions. The interpretation of this finding may be informed by the STG's previously described role in auditory processing of environmental sounds, and the amygdala's function as a salience detector. The scanner produces an extremely loud, repetitive stimulus. Acute μ-opioid and NK1 receptor blockade may differentially modulate the processing of aversive stimuli at the perceptual, attentional-level or its cognitive appraisal. Indeed, animal studies suggest that blockade of μ-opioid and NK1 receptor systems may protect from relapse through cue-related (Liu et al., 2002) and stress-related mechanism (Schank et al., 2012), respectively. However, it remains unclear whether the opposite effects of Naltrexone and Aprepitant/Vofopitant on amygdala – STG RSFC observed in current study relate to these differences in their mechanisms.

7.2 Implications, Limitations and Future Research

7.2.1 SN/VTA RSFC: a neurophysiological correlate, but not quite a biomarker

As previously described in Chapter 2, biomarkers provide objective indicators of disease states, which can serve as targets for development of novel therapeutics and as substitutes for clinical endpoints in experimental medicine studies. The desirable features of an ideal biomarker include a high level of sensitivity, specificity, robustness, mechanistic relevance, responsivity to treatment, non-invasiveness, easy of acquisition and low cost. Currently, no neurophysiological measure of any disease derived from fMRI data fulfils all of these criteria, including the current finding of elevated amygdala – SN/VTA RSFC in ADP. However, examining the degree to which such neurophysiological correlates of disease measure up these criteria may be useful in assessing their potential utility.

Amygdala – SN/VTA RSFC exhibited sufficient sensitivity to allow detection of a significant group difference between 39 HC and 20 ADP. However, there was also substantial overlap between the HC and ADP groups in amygdala – SN/VTA RSFC, which would preclude the use of this measure for subject-level diagnostics. The measure's association with cumulative alcohol exposure, but not with other measures that are often comorbid features of alcohol dependence such as smoking status, impulsivity, anxiety or head motion, suggest a certain degree of specificity. At the same time, the measure may not be particularly effective in separating alcohol dependent individuals who have only been alcohol dependent for a few years from healthy controls.

The finding that amygdala – SN/VTA RSFC was greater in ADP than HC across all five sessions, suggests that the measure can be reliably detected in a range of brain states. Drug dosing was calibrated to elicit blockade of three different receptor subtypes, at approximately 80% receptor occupancy, and yet inter-session correlations of amygdala – SN/VTA RSFC between Baseline and three of the other sessions were still significant across the combined groups. The fact that amygdala – SN/VTA RSFC was not significantly modulated by any of the three drugs suggests that it may not be easily amenable to pharmacological modulation, or that it may require modulation of a receptor pathway that was not tested here. In addition, the inter-session reliability, and the out of sample generalizability of amygdala – SN/VTA remains to be established in future studies.

The mechanistic relevance of the measure is supported by a wealth of animal studies implicating the amygdala (Roberto et al., 2004, Gilpin and Roberto, 2012) and the SN/VTA (Diana et al., 1996, Shen et al., 2007) chronic alcohol exposure related neuroadaptations. However, there currently doesn't exist a model that clearly accounts for the role of amygdala – SN/VTA interactions in the long-term effects of alcohol dependence. Importantly, it even remains unclear whether elevated amygdala – SN/VTA RSFC is a pathological feature of alcohol dependence that pharmacotherapies should aim to normalise, or whether it is an endogenous neuroadaptive mechanism for relapse maintenance, which pharmacotherapies should aim to preserve. The transparency of this measure is further limited by our generally limited of understanding of the biological function of resting state functional connectivity.

Future studies employing a longitudinal design could investigate whether the elevation of amygdala – SN/VTA RSFC in ADP develops gradually throughout the course of alcohol exposure or whether it is a neuroadaptation that is triggered at the onset of abstinence in proportion to the participant's history of alcohol exposure. Most importantly, longitudinal follow-up studies of ADP could assess the utility of quantifying amygdala – SN/VTA RSFC as a predictor of relapse. Beck et al. (2012) have shown that greater amygdala – SN/VTA RSFC within an alcohol-cue reactivity paradigm was associated with lower chance of relapse. The same design could be applied to test whether amygdala – SN/VTA circuit function in resting state conditions is similarly protective from relapse.

The remaining pros and cons of amygdala – SN/VTA RSFC from the perspective of a potential biomarker are true to all fMRI-based measures in general. The cost of an hour of fMRI data acquisition is between £300-600 pounds in the United Kingdom. Data acquisition is fairly non-invasive, as it does not involve drawing blood or injecting of a tracer. However, ease of data acquisition is limited by the availability of the MRI scanner infrastructure and the presence of exclusion criteria that preclude the participant from entering the scanner.

7.2.2 The integrative potential of network models

The observed group effect of increased amygdala - SN/VTA RSFC in ADP was not completely surprising since both regions have long been heavily implicated in models of addiction and substance dependence (Everitt & Robbins, 2005; Koob & Volkow, 2010) However, historically work on these two regions has undergone mostly in parallel, spearheaded by different groups of researchers, who have focussed on distinct behavioural components and neurotransmitter subsystems of addiction

pathways (Luthi & Luscher, 2014). The amygdala has been primarily studied in the context of negative reinforcement (McBride, 2002), with studies focussing on alcohol exposure or withdrawal related neuroadaptations to GABA, and neuropeptide (e.g. CRF) signalling (Heilig & Koob, 2007). In contrast, work on the VTA has focussed on its role in positive reinforcement, through regulation of dopamine release in fronto-striatal projection areas (Spanagel & Weiss, 1999), and its modulation by opioid systems (Spanagel & Herz, 1992). This division of focus has persisted despite early studies highlighting the role of amygdala in reinforcement learning and appetitive processing (Everitt & Robbins, 2005; Baxter & Murray, 2000), and the importance of the VTA in aversive conditioning and withdrawal states. The effects relating to amygdala – SN/VTA RSFC presented in this thesis underline the value of further exploring the dynamic interaction between these two hub regions, through a systems-level view of alcohol dependence.

7.2.3 Strengths of exploratory analyses

This thesis adopted an exploratory approach for investigating the effects of alcohol dependence on amygdala network function, (i.e. amygdala RSFC was explored voxelwise across the whole brain), as opposed to focussing on *a priori* amygdala circuits of interest, e.g. amygdala – vmPFC. Choosing regions of interest would have been difficult due to the large number of regions that have been reported to show structural (Wrase et al., 2008) and functional (Sullivan & Pfefferbaum, 2005) alterations in alcohol dependence. Additionally, narrowing down the list of regions to ones with known direct structural connections with the amygdala was not an appropriate strategy, as indirect connections are known to significantly contribute to RSFC across the brain (Sporns et al., 2011). Although the voxelwise exploratory

approach had the disadvantage of a greater likelihood of false negative findings due to having to correct for a higher number of comparisons, it enabled the discovery of unanticipated effects.

The benefit of this voxelwise exploratory approach is nicely demonstrated by the positive association found between abstinence length and amygdala RSFC in dPCC, inferior parietal lobules, preSMA. While latter two of these frontoparietal regions are normally found to co-active in tasks requiring executive processes (e.g. inhibitory control, or task-switching), and to show strong RSFC under resting state conditions, their interaction with the amygdala is not typically observed in studies of healthy individuals nor in substance-dependent populations. Top-down cortical modulation of the amygdala function is typically thought to be driven by inputs from the ACC, vmPFC and dmPFC, while the potential role of frontoparietal network as a unit has not been explored. The findings presented in this thesis suggest that gradual recovery from chronic alcohol abuse may entail greater synchronisation of brain systems that do not under normal conditions operate in close synchrony.

The finding that GSK598809 and Aprepitant/Vofopitant had opposing modulatory effects on amygdala RSFC in a region, i.e. the STG, would've likely not been observed without the exploratory whole-brain approach employed here. Since the function of the STG is not thought to be directly relevant to mechanisms of addiction, it likely would not have been specifically investigated as an *a priori* region of interest. However, the current findings from Chapter 6, as well as from a recent study of the effects of Psilocybin-assisted therapy on amygdala RSFC (Leor Roseman, personal communication), indicate that the STG may be particularly sensitive to differential pharmacological modulation of amygdala network function.

The interpretation of the observed session-related effects on amygdala – left mPFC RSFC was greatly aided by undertaking post-hoc analysis beyond the initial planned voxelwise contrasts. The contrasts of Naltrexone versus Placebo, and GSK598809 vs Placebo had suggested an overlapping down-regulatory effect of both drugs on this circuit. However, post-hoc comparisons with the other two sessions, revealed similar differences at Baseline, and Aprepitant/Vofopitant, with respect to Placebo. These additional comparisons yielded further constraints on the interpretation of data, thereby signifying the importance of exploring datasets beyond the primary contrasts of interest.

7.2.4 Limitations of exploratory analyses

An important limitation of this work is that some of the findings were derived from post-hoc comparisons and therefore incurred the risk of potential false positives and overestimation of effect sizes (Kriegeskorte et al., 2009). For example, the SN/VTA region of interest mask used for computing the correlation between cumulative alcohol exposure and amygdala – SN/VTA RSFC was restricted to voxels that were both within an SN/VTA probability map and to voxels that were significant in the ADP > HC contrast. Ideally, the region of interest should be determined based on measurements independent from the analysis of interest, e.g. to avoid inflation of effect sizes for example by pre-selecting voxels with high signal-to-noise ratio (Kriegeskorte et al., 2009).

However, post-hoc analyses, when considered within their limitations, can provide useful insights for informing the interpretation of the original analyses. For example, had amygdala – SN/VTA RSFC shown an *inverse* correlation with cumulative alcohol exposure in ADP, this finding would have complicated the interpretation of the initial

group effect that showed greater amygdala – SN/VTA RSFC in ADP than HC. Since the directionality of the effects in the initial group comparison and the post-hoc analysis was congruent, the latter increased the interpretability of the former.

An ideal way of determining the robustness of an exploratory finding is through replication of the same effects in an independent group of participants. Earlier, our group has observed significantly reduced amygdala – anterior insula RSFC in a group of abstinent alcohol dependent patients with similar demographic and clinical characteristics as the ADP cohort in this thesis (Orban et al., 2013). However, this same effect was not observed between ADP and HC in ICCAM.

Two possible explanations arise that may account for this discrepancy between the two findings. First, in the other study all participants were scanned early in the morning at around 7-8am, whereas in ICCAM participants underwent their scans generally around noon. Morning scans may be differentially influenced by diurnal variations in cortisol secretion, which may result in differential patterns of amygdala RSFC. Alcohol dependent patients have been previously shown to exhibit dysregulation in hypothalamic-pituitary-axis function (Sinha et al., 2011). Another possibility is that amygdala – insula RSFC may not be a reliable measure in alcohol-dependent populations. For example, Sullivan et al. (2013) has shown that abstinent ADP exhibit markedly reduced perfusion of the bilateral insula, and furthermore they showed that this was associated with disruption of insula network interactions.

7.2.5 Potential follow-up studies in humans

Based on the findings that emerged from Chapter 4, follow-up studies with the specific aim of quantifying amygdala RSFC in the SN/VTA could apply optimised acquisition protocols with substantially greater accuracy over the current implementation in this study. Since the amygdala and the midbrain are located in close proximity to each other, a smaller box with greater spatial and temporal resolution could be used to quantify amygdala – SN/VTA RSFC, than the one employed in the current study. The midbrain is continuously subjected to pulsatile motion due to the close proximity of major arteries, which creates noise and may confound interpretation of BOLD signal. While simple regression of cardiac rate appears to have a limited effect on midbrain signal integrity (Krebs et al., 2011), cardiac-gated fMRI acquisition may provide significantly greater improvement. D'Ardenne and colleauges (2008) have developed a scanning protocol, where the pulse oximeter was used to trigger the EPI acquisition. In addition, the number of slices, repetition time (TR) and maximum length of acquisition window were all calibrated based on each participant's pulse rate.

Causal evidence may also emerge from prospective clinical fMRI studies in the following decades. A large number of adolescents have already undergone resting state fMRI in the context of experimental research on healthy development (Nooner et al., 2012), and a proportion of these will likely succumb to alcohol dependence in their later years, within a large enough sample. In future studies of resting state function, participants will be more likely to have historic resting state data prior to disease onset for comparison. The timespan of data-acquisition for such studies may be facilitated through the increasing adoption of data-sharing initiatives (Milham et al,

2012), or through recruitment adolescents with first-degree relatives of alcohol dependence (Schweinsburg et al., 2004).

7.2.6 Potential follow-up studies in animals

Examination of amygdala – SN/VTA circuits in animal models of alcohol dependence could also help tackle a wider range of questions that are outside the scope of non-invasive methodology. Brain function in ADP likely interacts with a range of genetic and environmental factors that are difficult to account for in experimental medicine studies. In addition to the availability of invasive techniques, animal studies also allow the full randomisation of treatment conditions, as well as the genetic make-up and environmental conditions of the animals.

The causality between long-term alcohol exposure and elevated amygdala – SN/VTA RSFC could be explicitly tested using a within-group design by scanning rodents with resting state fMRI before and after chronic alcohol exposure. A between-group design could also explore the effects of amount, type and patterns of alcohol exposure on long-term changes in amygdala – SN/VTA RSFC, e.g. alcohol vapour exposure versus alcohol containing liquid diet, intermittent versus continuous exposure (Heilig & Koob, 2007).

This reverse-translational approach has already shown some success in elucidating the causal role of amygdala circuits in anxiety disorders. Etkin et al. (2009) observed increased RSFC between the centromedial and basolateral amygdala subregions in patients with generalised anxiety disorder. Although the study reproduced these effects in an independent cohort of generalized anxiety patients, the experimental approach used still precluded the inference of causality between resting state function

and anxiety. For example, based on what we now know the impact of head motion on RSFC (Power et al., 2012), potentially increased head motion amongst patients in this study may have led to a robust overestimation of RSFC between nearby regions, e.g. amygdala subregions. However, Tye and colleagues (2011) built on the findings of Etkin and coworkers (2009) and showed that optogenetical modulation of neural transmission from the basolateral to the central nucleus of the amygdala could bidirectonally influence anxiety-like behaviours in freely moving mice.

A similar approach could be used to observe the effects of optogenetically stimulating SN/VTA - amygdala transmission in mice, specifically on cue- and stress-induced reinstatement. Recent work has shown that phasic stimulation of VTA dopamine neurons using ontogenetic methods elicits upregulation of BOLD signal in the amygdala. (Lohani et al. 2016).

References

Agus, D.B., Gambhir, S.S., Pardridge, W.M., Spielholz, C., Baselga, J., Vera, J.C., Golde, D.W. (1997) Vitamin C crosses the blood-brain barrier in the oxidized form through the glucose transporters. J. Clin. Invest. 100, 2842–2848.

Amunts, K., Kedo, O., Kindler, M., Pieperhoff, P., Mohlberg, H., Shah, N.J., Habel, U., Schneider, F., Zilles, K. (2005) Cytoarchitectonic mapping of the human amygdala, hippocampal region and entorhinal cortex: intersubject variability and probability maps. Anat. Embryol. 210, 343–352.

Attwell, D. & Laughlin, S. B. (2001) An energy budget for signaling in the grey matter of the brain. J. Cereb. Metab. 21(10), 1133–1145.

Avants, B., Epstein, C., Grossman, M., & Gee, J. (2008) Symmetric diffeomorphic image registration with cross-correlation: Evaluating automated labeling of elderly and neurodegenerative brain. Med. Image Anal. 12(1), 26–41.

Aupperle, R.L., Ravindran, L., Tankersley, D., Flagan, T., Stein, N.R., Simmons, A.N., Stein, M.B., Paulus, M.P. (2011) Pregabalin Influences Insula and Amygdala Activation During Anticipation of Emotional Images. Neuropsychopharmacology 1–12.

Bandettini, P. A., Wong, E. C., Hinks, R. S., Tikofsky, R. S., & Hyde, J. S. (1992) Time course EPI of human brain function during task activation. Magn. Reson. Med. 25(2), 390–397.

Bandettini, P.A., Jesmanowicz, A., Van Kylen, J., Birn, R.M., Hyde, J.S. (1998) Functional MRI of brain activation induced by scanner acoustic noise. Magn. Reson. Med. 39, 410–416.

Barnes, L., Harp, D., Jung, W.S. (2002) Reliability generalization of scores on the Spielberger state-trait anxiety inventory. Edu. Psychol. Measurement 62, 603–618.

Baur, V., Hänggi, J., Langer, N., Jäncke, L. (2013) Resting-state functional and structural connectivity within an insula–amygdala route specifically index state and trait anxiety. Biol. Psych. 73, 85–92.

Baxter, M.G. & Murray, E.A. (2002) The amygdala and reward. Nat. Rev. Neurosci. 3, 563–573.

Beck, A., Schlagenhauf, F., Wüstenberg, T., Hein, J., Kienast, T., Kahnt, T., et al., (2009) Ventral striatal activation during reward anticipation correlates with impulsivity in alcoholics. Biol. Psych., 66, 734-742.

Beck, A., Wüstenberg, T., Genauck, A., Wrase, J., Schlagenhauf, F., Smolka, M.N., Mann, K., Heinz, A. (2012) Effect of brain structure, brain function, and brain connectivity on relapse in alcohol-dependent patients. Arch. Gen. Psychiatry 69, 842–852.

Behzadi, Y., Restom, K., Liau, J., & Liu, T. T. (2007) A component based noise correction method (CompCor) for BOLD and perfusion based fMRI. NeuroImage, 37(1), 90–101.

Beier, K.T., Steinberg, E.E., DeLoach, K.E., Xie, S., Miyamichi, K., Schwarz, L.,

Gao, X.J., Kremer, E.J., Malenka, R.C., Luo, L. (2015) Circuit architecture of VTA dopamine neurons revealed by systematic input-output mapping. Cell 162, 622–634.

Benegal, V., Antony, G., Venkatasubramanian, G., Jayakumar, P.N. (2007) Gray matter volume abnormalities and externalizing symptoms in subjects at high risk for alcohol dependence. Addict. Biol. 12, 122–132.

Bergström, M., Hargreaves, R. J., Burns, H. D., Goldberg, M. R., Sciberras, D., Reines, S. A., et al., (2004) Human positron emission tomography studies of brain neurokinin 1 receptor occupancy by aprepitant. Biol. Psych. 55(10), 1007–1012.

Berridge, K. C. (2006) The debate over dopamine's role in reward: the case for incentive salience. Psychopharmacology 191(3), 391–431.

Bianciardi, M., Fukunaga, M., van Gelderen, P., Horovitz, S. G., de Zwart, J. A., & Duyn, J. H. (2009) Modulation of spontaneous fMRI activity in human visual cortex by behavioral state. NeuroImage 45(1), 160–168.

Bingel, U., Lorenz, J., Schoell, E., Weiller, C., Büchel, C. (2006) Mechanisms of placebo analgesia: rACC recruitment of a subcortical antinociceptive network. Pain 120, 8–15.

Birn, R. M. (2012) The role of physiological noise in resting-state functional connectivity. NeuroImage, 62(2), 864–870.

Biswal, B., Yetkin, F. Z., Haughton, V. M., & Hyde, J. S. (1995) Functional connectivity in the motor cortex of resting human brain using echo-planar MRI. Magnet. Reson. Med. 34(4), 537–541.

Biomarkers Definitions Working Group (2001) Biomarkers and surrogate endpoints: preferred definitions and conceptual framework. Clin. Pharmacol Ther. 69. 89–95.

Blum, K., Braverman, E. R., Holder, J. M., Lubar, J. F., Monastra, V. J., Miller, D., et al. (2000) Reward deficiency syndrome: a biogenetic model for the diagnosis and treatment of impulsive, addictive, and compulsive behaviors. J. Psychoactive Drugs, 32 Suppl, 1–112.

Boileau, I., Assaad, J.M., Pihl, R. O., Benkelfat, C., Leyton, M., Diksic, M., et al., (2003) Alcohol promotes dopamine release in the human nucleus accumbens. Synapse 49(4), 226–231.

Bond, A., Lader, M. (1974) The use of analogue scales in rating subjective feelings. Br. J. Med. Psychol. 47, 211-218.

Borsook, D., Becerra, L., Hargreaves, R. (2006) A role for fMRI in optimizing CNS drug development. Nat. Rev. Drug. Discov. 5, 411–425.

Buckner, R. L., & Vincent, J. L. (2007) Unrest at rest: default activity and spontaneous network correlations. NeuroImage 37(4), 1091-1096.

Bullmore, E. T., Brammer, M. J., Rabe-Hesketh, S., Curtis, V. A., Morris, R. G., Williams, S. C., et al. (1999) Methods for diagnosis and treatment of stimulus-correlated motion in generic brain activation studies using fMRI. Human Brain Mapping 7(1), 38–48.

Calero, C.I., Vickers, E., Moraga Cid, G., Aguayo, L.G., Gersdorff, von, H., Calvo,

D.J. (2011) Allosteric modulation of retinal GABA receptors by ascorbic acid. J. Neurosci. 31, 9672–9682.

Camchong, J., Stenger, A., Fein, G. (2013) Resting-state synchrony during early alcohol abstinence can predict subsequent relapse. Cereb. Cortex 23, 2086–2099.

Carhart-Harris, R.L., Murphy, K., Leech, R., Erritzoe, D., Wall, M.B., Ferguson, et al. (2015) Arch. Report. Biol. Psychiatry 78, 554–562.

Carmen, B., Angeles, M., Ana, M., & María, A. J. (2004) Efficacy and safety of naltrexone and acamprosate in the treatment of alcohol dependence: a systematic review. Addiction, 99(7), 811–828.

Carp, J. (2013) Optimizing the order of operations for movement scrubbing: Comment on Power et al. NeuroImage 76(1), 436-438.

Charney, D.A., Zikos, E., Gill, K.J. (2010) Early recovery from alcohol dependence: Factors that promote or impede abstinence. J Subst Abuse Treat 38, 42–50.

Chupin, M., Hammers, A., Liu, R.S.N., Colliot, O., Burdett, J., Bardinet, E., Duncan, J.S., Garnero, L., Lemieux, L. (2009) Automatic segmentation of the hippocampus and the amygdala driven by hybrid constraints: Method and validation. NeuroImage 46, 749–761.

Cole, M.W., Bassett, D.S., Power, J.D., Braver, T.S., & Petersen, S.E. (2014) Intrinsic and task-evoked network architectures of the human brain. Neuron, 83(1), 238–251.

Cole, D. M., Beckmann, C. F., Long, C. J., Matthews, P. M., Durcan, M. J., & Beaver, J. D. (2010) Nicotine replacement in abstinent smokers improves cognitive withdrawal symptoms with modulation of resting brain network dynamics. NeuroImage 52(2), 590–599.

Cole, D.M., Smith, S.M., Beckmann, C.F. (2010) Advances and pitfalls in the analysis and interpretation of resting-state FMRI data. Frontiers in Systems Neurosci. 4, Art 8, 1-15.

Cole, D.M., Beckmann, C.F., Searle, G.E., Plisson, C., Tziortzi, A.C., Nichols, T.E., et al. (2012) Orbitofrontal Connectivity with Resting-State Networks Is Associated with Midbrain Dopamine D3 Receptor Availability. Cereb. Cortex 22, 2784–2793.

Colloca, L., Petrovic, P., Wager, T.D., Ingvar, M., Benedetti, F. (2010) How the number of learning trials affects placebo and nocebo responses. Pain 151, 430–439.

Costafreda, S.G., Brammer, M.J., David, A.S., Fu, C.H.Y. (2008) Predictors of amygdala activation during the processing of emotional stimuli: A meta-analysis of 385 PET and fMRI studies. Brain Res. Rev. 58, 57–70.

Dager, A.D., McKay, D.R., Kent, J.W., Curran, J.E., Knowles, E., Sprooten, E., et al. (2015) Shared genetic factors influence amygdala volumes and risk for alcoholism. Neuropsychopharmacology, 40(2), 412-420.

Dagli, M. S., Ingeholm, J. E., & Haxby, J. V. (1999) Localization of cardiac-induced signal change in fMRI. NeuroImage, 9(4), 407–415.

D'Ardenne, K., McClure, S.M., Nystrom, L.E., Cohen, J.D. (2008) BOLD responses reflecting dopaminergic signals in the human ventral tegmental area. Science 319, 1264–1267.

Dawson, D.A., Grant, B.F., Stinson, F.S., Chou, P.S., Huang, B., Ruan, W.J. (2005) Recovery from DSM-IV alcohol dependence: United States, 2001-2002. Addiction 100, 281–292.

De Simoni, S., Schwarz, A. J., O'Daly, O. G., Marquand, A. F., Brittain, C., Gonzales, C., et al. (2013) Test–retest reliability of the BOLD pharmacological MRI response to ketamine in healthy volunteers. NeuroImage, 64, 75–90.

Diana, M., Pistis, M., Muntoni, A., Gessa, G. (1996) Mesolimbic dopaminergic reduction outlasts ethanol withdrawal syndrome: evidence of protracted abstinence. Neuroscience 71, 411–415.

Duncan, J. (2010) The multiple-demand (MD) system of the primate brain: mental programs for intelligent behaviour. Trends in Cognitive Sciences 14, 172–179.

Ebner, K., Rupniak, N.M. & Saria, A. (2004). Substance P in the medial amygdala: emotional stress-sensitive release and modulation of anxiety-related behavior in rats. Proc. Natl. Acad. Sci. USA 101(12), 4280–4285.

Ebner, K. & Singewald, N. (2006) The role of substance P in stress and anxiety responses. Amino Acids 31, 251–272.

Elholm, B., Larsen, K., Hornnes, N., Zierau, F., & Becker, U. (2011) Alcohol Withdrawal Syndrome: Symptom-Triggered versus Fixed-Schedule Treatment in an Outpatient Setting. Alcohol and Alcoholism 46, 318–323.

Entis, J.J., Doerga, P., Barrett, L.F. & Dickerson, B.C. (2012) A reliable protocol for the manual segmentation of the human amygdala and its subregions using ultra-high resolution MRI. NeuroImage 60, 1226–1235.

Erritzoe, D., Tziortzi, A., Bargiela, D., Colasanti, A., Searle, G.E., Gunn, R.N., et al., (2014) In vivo imaging of Cerebral dopamine D3 receptors in alcoholism. Neuropsychopharmacology 39, 1703–1712.

Ersche, K.D., Jones, P.S., Williams, G.B., Robbins, T.W., & Bullmore, E.T. (2012) Cocaine dependence: a fast-track for brain ageing? Mol Psychiatry 18, 134–135.

Etkin, A., Prater, K.E., & Schatzberg, A.F. (2009) Disrupted amygdalar subregion functional connectivity and evidence of a compensatory network in generalized anxiety disorder. Arch. Gen. Psychiatry 66, 1361–1372.

Etkin, A., & Wager, T.D. (2007) Functional neuroimaging of anxiety: A meta-analysis of emotional processing in PTSD, social anxiety disorder, and specific phobia. Am J Psychiatry 164, 1476–1488.

Everitt, B.J. & Robbins, T.W. (2005) Neural systems of reinforcement for drug addiction: from actions to habits to compulsion. Nat. Neurosci. 8, 1481–1489.

Eysenck, H.J. (1964) Principles and methods of personality description, classification and diagnosis. Br. J. Psychol. 55, 284–294.

Fair, D.A., Cohen, A.L., Power, J.D., Dosenbach, N.U.F., Church, J.A., Miezin, F.M., Schlaggar, B.L., Petersen, S.E. (2009) Functional Brain Networks Develop

from a “Local to Distributed” Organization. PLoS Comput Biol. 5, e1000381.

Fedota, J. R., & Stein, E. A. (2015) Resting-state functional connectivity and nicotine addiction: prospects for biomarker development. Ann. N. Y. Acad. Sci. 1349(1), 64–82.

Fein, G., Torres, J., Price, L.J., Di Sclafani, V. (2006) Cognitive Performance in Long-Term Abstinent Alcoholic Individuals. Alcoholism: Clinical and Experimental Research 30, 1538–1544.

Filbey, F.M., Aslan, S., Calhoun, V.D., Spence, J.S., Damaraju, E., Caprihan, A., Segall, J. (2014) Long-term effects of marijuana use on the brain. Proc Natl Acad Sci USA 111, 16913–16918.

Fjell, A. M., & Walhovd, K.B. (2017) Multimodal Imaging of the Aging Brain in Cognitive Neuroscience of Aging: Linking Cognitive and Cerebral Aging (Edited by Roberto Cabeza, Lars Nyberg, Denise C. Park) Oxford University Press, Oxford, UK

Franz, M., Popp, K., Schaefer, R., Sitte, W., Schneider, C., Hardt, J., Decker, O., Braehler, E. (2007) Alexithymia in the German general population. Soc Psychiat. Epidemiol. 43, 54–62.

Frick, A., Ahs, F., Linnman, C., Jonasson, M., Appel, L., Lubberink, M., Långström, B., et al., (2015) Increased neurokinin-1 receptor availability in the amygdala in social anxiety disorder: a positron emission tomography study with [11C]GR205171. Translat. Psychiatry 5, e597–6.

Friston, K. J., Frith, C. D., Liddle, P. F., & Frackowiak, R. S. (1993) Functional connectivity: the principal-component analysis of large (PET) data sets. J. Cereb. Blood Flow Metab. 13(1), 5–14.

Friston, K. J., Williams, S., Howard, R., Frackowiak, R. S., & Turner, R. (1996) Movement-related effects in fMRI time-series. Magn. Res. Med. 35(3), 346-355.

Fox, M.D., Zhang, D., Snyder, A.Z., & Raichle, M.E (2009) The global signal and observed anticorrelated resting state brain networks. J. Neurophysiol. 101(6), 3270–3283.

Fudge, J.L. & Haber, S.N. (2000) The central nucleus of the amygdala projection to dopamine subpopulations in primates. Neuroscience 97, 479–494.

Funk, C. K., Zorrilla, E. P., Lee, M.J., Rice, K. C., & Koob, G. F. (2007) Corticotropin-releasing factor 1 antagonists selectively reduce ethanol self-administration in ethanol-dependent rats. Biol. Psych. 61(1), 78–86.

Furmark, T., Appel, L., Michelgård, Å., Wahlstedt, K., Åhs, F., Zancan, S., et al. (2005) Cerebral Blood Flow Changes After Treatment of Social Phobia with the Neurokinin-1 Antagonist GR205171, Citalopram, or Placebo. Biological Psychiatry 58, 132–142.

Gaab, N., Gabrieli, J.D.E., Glover, G.H. (2007) Assessing the influence of scanner background noise on auditory processing. II. An fMRI study comparing auditory processing in the absence and presence of recorded scanner noise using a sparse design. Hum. Brain Mapp. 28, 721–732.

Garavan, H. (2010) Insula and drug cravings. Brain Struct Funct 214, 593–601.

Georges, F., & Aston-Jones, G. (2001) Potent regulation of midbrain dopamine neurons by the bed nucleus of the stria terminalis. J. Neurosci., 21(16), RC160.

George, D.T., Gilman, J., Hersh, J., Thorsell, A., Herion, D., Geyer, C., et al., (2008) Neurokinin 1 receptor antagonism as a possible therapy for alcoholism. Science 319, 1536–1539.

Gilman, J.M., & Hommer, D.W. (2008) Modulation of brain response to emotional images by alcohol cues in alcohol-dependent patients. Addiction Biol. 13(3-4), 423–434.

Gilpin, N.W., Herman, M.A., & Roberto, M. (2015) The central amygdala as an integrative hub for anxiety and alcohol use disorders. Biol. Psych. 77, 859–869.

Gilpin, N.W. & Roberto, M. (2012) Neurosci. Biobehav. Rev. 36, 873–888.

Glover, G. H. (1999) Deconvolution of impulse response in event-related BOLD fMRI. NeuroImage, 9(4), 416–429.

Glover, G. H., Li, T. Q., Ress, D. (2000) Image-based method for retrospective correction of physiological motion effects in fMRI: RETROICOR. Magnetic Resonance in Medicine, 44(1), 162–167.

Goldstein, R. Z. & Volkow, N. D. (2002) Drug addiction and its underlying neurobiological basis: Neuroimaging evidence for the involvement of the frontal cortex. Am. J. Psych. 159(10), 1642–1652.

Goldstein, R. Z. & Volkow, N. D. (2011) Dysfunction of the prefrontal cortex in addiction: neuroimaging findings and clinical implications, Nat. Rev. Neurosci. 12, 652-669.

Greicius, M. (2008) Resting-state functional connectivity in neuropsychiatric disorders. Curr. Op. Neurobiol. 21(4), 424-430.

Greitz, D., Wirestam, R., Franck, A., Nordell, B., Thomsen, C., & Ståhlberg, F. (1992) Pulsatile brain movement and associated hydrodynamics studied by magnetic resonance phase imaging. The Monro-Kellie doctrine revisited. Neuroradiology 34(5), 370–380.

Greve, D. N. & Fischl, B. (2009) Accurate and robust brain image alignment using boundary-based registration. NeuroImage, 48(1), 63–72

Grieder, T.E., Herman, M.A., Contet, C., Tan, L.A., Vargas-Perez, H., Cohen, A., et al. (2014) VTA CRF neurons mediate the aversive effects of nicotine withdrawal and promote intake escalation. Nat. Neurosci. 17, 1751–1758.

Gu, H., Salmeron, B.J., Ross, T.J., Geng, X., Zhan, W., Stein, E.A., & Yang, Y. (2010) Mesocorticolimbic circuits are impaired in chronic cocaine users as demonstrated by resting-state functional connectivity. NeuroImage 53, 593–601.

Gurevich, E.V. & Joyce, J.N. (1999) Distribution of dopamine D3 receptor expressing neurons in the human forebrain: comparison with D2 receptor expressing neurons. Neuropsychopharmacology 20, 60–80.

Hahn, J., Hopf, F. W., & Bonci, A. (2009) Chronic cocaine enhances corticotropin-releasing factor-dependent potentiation of excitatory transmission in ventral

tegmental area dopamine neurons. J. Neurosci. 29(20), 6535-6544.

Hahn, A., Stein, P., Windischberger, C., Weissenbacher, A., Spindelegger, C., Moser, E., et al. (2011) Reduced resting-state functional connectivity between amygdala and orbitofrontal cortex in social anxiety disorder. NeuroImage 56, 881–889.

Hajnal, J. V., Myers, R., Oatridge, A., Schwieso, J. E., Young, I. R. & Bydder, G. M. (1994) Artifacts due to stimulus correlated motion in functional imaging of the brain. Magn. Res. Med. 31(3), 283–291.

Hallquist, M. N., Hwang, K. & Luna, B. (2013) The nuisance of nuisance regression: Spectral misspecification in a common approach to resting-state fMRI preprocessing reintroduces noise and obscures functional connectivity. NeuroImage, 82(C), 208–225.

He, Y., Xu, T., Zhang, W. & Zuo, X.-N. (2016) Lifespan anxiety is reflected in human amygdala cortical connectivity. Hum. Brain Mapp. 37, 1178–1193.

Heatherton, T.F., Kozlowski, L.T., Frecker, R.C., Fagerström, K.O. (1991) The Fagerström Test for Nicotine Dependence: a revision of the Fagerström Tolerance Questionnaire. Br. J. Addict. 86, 1119–1127.

Heilig, M., Egli, M., Crabbe, J.C., Becker, H.C. (2010) Acute withdrawal, protracted abstinence and negative affect in alcoholism: are they linked? Addict Biol 15, 169–184.

Heilig, M. & Koob, G.F. (2007) A key role for corticotropin-releasing factor in alcohol dependence. Trends in Neurosci. 30, 399–406.

Heinz, A., Reimold, M., Wrase, J., Hermann, D., Croissant, B., Mundle, G., Dohmen, B.M., et al. (2005) Correlation of stable elevations in striatal mu-opioid receptor availability in detoxified alcoholic patients with alcohol craving: a positron emission tomography study using carbon 11-labeled carfentanil. Arch. Gen. Psychiatry 62, 57–64.

Hernádi, I., Grabenhorst, F. & Schultz, W. (2015) Planning activity for internally generated reward goals in monkey amygdala neurons. Nat. Neurosci. 18(3), 461-469.

Hietala, J., Nyman, M.J., Eskola, O., Laakso, A., Grönroos, T., Oikonen, V., et al. (2005) Visualization and Quantification of Neurokinin-1 (NK1) Receptors in the Human Brain. Mol. Imaging Biol 7, 262–272.

Hill, S.Y., De Bellis, M.D., Keshavan, M.S., Lowers, L., Shen, S., Hall, J., Pitts, T., (2001) Right amygdala volume in adolescent and young adult offspring from families at high risk for developing alcoholism. Biol. Psych. 49, 894–905.

Hong, L.E., Gu, H., Yang, Y., Ross, T.J. (2009) Association of nicotine addiction and nicotine's actions with separate cingulate cortex functional circuits. Arch. Gen. Psychiatry 66, 431–441.

Hong, L.E., Hodgkinson, C.A., Yang, Y., Sampath, H., Ross, T.J., Buchholz, B., Salmeron, B.J., et al. (2010) A genetically modulated, intrinsic cingulate circuit supports human nicotine addiction. Proc. Natl. Acad. Sci. U.S.A. 107, 13509–13514.

Huettel, S. A., Song, A. W., & McCarthy, G. (2008) Functional Magnetic Resonance

Imaging (2nd ed., pp. 1–532). Sunderland, MA, USA: Sinauer Associates, Inc.

Hyman, S. E., 2012. Revolution stalled. Sci. Translat. Med. 4(155), 1-5.

Hyytiä, P., & Koob, G. F. (1995) GABAA receptor antagonism in the extended amygdala decreases ethanol self-administration in rats. European Journal of Pharmacology 283, 151-159.

Ide, K., Eliasziw, M., & Poulin, M. J. (2003) Relationship between middle cerebral artery blood velocity and end-tidal PCO2 in the hypocapnic-hypercapnic range in humans. J. Appl. Physiol., 95(1), 129–137.

Janak, P.H. & Tye, K.M. (2015) From circuits to behaviour in the amygdala. Nature 517, 284–292.

Jennings, J.H., Sparta, D.R., Stamatakis, A.M., Ung, R.L., Pleil, K.E., Kash, T.L., Stuber, G.D. (2013) Distinct extended amygdala circuits for divergent motivational states. Nature 496, 224–228.

Jo, H.J., Saad, Z.S., Simmons, W.K., Milbury, L.A., Cox, R.W., 2010. Mapping sources of correlation in resting state FMRI, with artifact detection and removal. NeuroImage 52, 571–582.

Jo, H. J., Gotts, S. J., Reynolds, R. C., Bandettini, P. A., Martin, A., Cox, R. W., & Saad, Z. S. (2013) Effective Preprocessing procedures virtually eliminate distance-dependent motion artifacts in resting state FMRI. J. Appl. Math. 2013, Art ID. 935194, 1–9.

Joules, R., Doyle, O.M., Schwarz, A.J., O'Daly, O.G., Brammer, M., Williams, S.C., & Mehta, M.A. (2015) Ketamine induces a robust whole-brain connectivity pattern that can be differentially modulated by drugs of different mechanism and clinical profile. Psychopharmacology 232, 4205–4218.

Kamiński, J., Sullivan, S., Chung, J. M., Ross, I. B., Mamelak, A. N., & Rutishauser, U. (2017) Persistently active neurons in human medial frontal and medial temporal lobe support working memory. Nat. Neurosci., in press.

Kelly, C., de Zubicaray, G., Di Martino, A., Copland, D. A., Reiss, P. T., Klein, D. F., et al. (2009) L-Dopa modulates functional connectivity in striatal cognitive and motor networks: A double-blind placebo-controlled study. J. Neurosci. 29(22), 7364–7378.

Kelly, C., Biswal, B.B., Craddock, R.C., Castellanos, F.X., Milham, M.P. (2012) Characterizing variation in the functional connectome: promise and pitfalls. Trends Cogn. Sci. 16, 181–188.

Kim, M.J., Gee, D.G., Loucks, R.A., Davis, F.C. & Whalen, P.J. (2011) Anxiety Dissociates Dorsal and Ventral Medial Prefrontal Cortex Functional Connectivity with the Amygdala at Rest. Cereb. Cortex 21, 1667–1673.

Kim, Y., Park, M.K. & Chung, S. (2009) Regulation of somatodendritic dopamine release by corticotropin-releasing factor via the inhibition of voltage-operated Ca2+ channels. Neurosci. Lett. 465, 31–35.

Klein, A., Andersson, J., Ardekani, B. A., Ashburner, J., Avants, B., Chiang, M.-C., et al. (2009) Evaluation of 14 nonlinear deformation algorithms applied to human brain MRI registration. NeuroImage, 46(3), 786–802.

Koob, G.F. (2008) A Role for brain stress systems in addiction. Neuron 59, 11–34.

Koob, G.F. (2009) Brain stress systems in the amygdala and addiction. Brain Research 1293, 61–75.

Koob, G. F. & Le Moal, M. (2001) Drug addiction, dysregulation of reward, and allostasis. Neuropsychopharmacology, 24(2), 97–129.

Koob, G.F. & Le Moal, M. (2008) Addiction and the brain antireward system. Annu. Rev. Psychol. 59, 29–53.

Koob, G.F., Volkow, N.D. (2010) Neurocircuitry of addiction. Neuropsychopharmacology 35, 217–238.

Kosten, T.R., O'Connor, P.G. (2003) Management of drug and alcohol withdrawal. N. Engl. J. Med. 348, 1786–1795.

Kranzler, H.R. & Van Kirk, J. (2001) Efficacy of naltrexone and acamprosate for alcoholism treatment: A meta-analysis. Alcoholism: Clinical and Experimental Research 25, 1335–1341.

Krebs, R.M., Heipertz, D., Schuetze, H., & Duzel, E. (2011) Novelty increases the mesolimbic functional connectivity of the substantia nigra/ventral tegmental area (SN/VTA) during reward anticipation: Evidence from high-resolution fMRI. NeuroImage 58, 647–655.

Kriegeskorte, N., Simmons, W.K., Bellgowan, P.S.F., Baker, C.I. (2009) Circular analysis in systems neuroscience: the dangers of double dipping. Nat. Neurosci. 12, 535–540.

Kroes, M.C.W., Strange, B.A., Dolan, R.J. (2010) Beta-adrenergic blockade during memory retrieval in humans evokes a sustained reduction of declarative emotional memory enhancement. J. Neurosci. 30, 3959–3963.

Kwako, L.E., Spagnolo, P.A., Schwandt, M.L., Thorsell, A., George, D.T., Momenan, R., et al. (2015) The Corticotropin Releasing Hormone-1 (CRH1) receptor antagonist Pexacerfont in alcohol dependence: A Randomized controlled experimental medicine study. Neuropsychopharmacology 40, 1053–1063.

Kwong, K. K., Belliveau, J. W., Chesler, D. A., Goldberg, I. E., Weisskoff, R. M., Poncelet, B. P., et al., (1992) Dynamic magnetic resonance imaging of human brain activity during primary sensory stimulation. Proc. Natl. Acad. Sci. USA , 89(12), 5675–5679.

La Fuente-Fernández, de, R., Phillips, A.G., Zamburlini, M., Sossi, V., Calne, D.B., Ruth, T.J., Stoessl, A.J. (2002) Dopamine release in human ventral striatum and expectation of reward. Behav. Brain Res. 136, 359–363.

Lam, M.P., Marinelli, P.W., Bai, L., & Gianoulakis, C. (2008) Effects of acute ethanol on opioid peptide release in the central amygdala: an in vivo microdialysis study. Psychopharmacology 201, 261–271.

LeDoux, J. (2007) The amygdala. Curr. Biol. 17(20), R868–74.

LeDoux, J. E. (2014) Coming to terms with fear. Proc. Natl. Acad. Sci. USA 111(8), 2871–2878.

Lee, H.J., Gallagher, M., & Holland, P. (2010) The central amygdala projection to the substantia nigra reflects prediction error information in appetitive conditioning. Learning & Memory 17, 531–538.

Leech, R., Kamourieh, S., Beckmann, C.F., & Sharp, D.J. (2011) Fractionating the Default Mode Network: Distinct Contributions of the Ventral and Dorsal Posterior Cingulate Cortex to Cognitive Control. Journal of Neuroscience 31, 3217–3224.

Lê, A. D., Poulos, C. X., Harding, S., Watchus, J., Juzytsch, W., & Shaham, Y. (1999) Effects of naltrexone and fluoxetine on alcohol self-administration and reinstatement of alcohol seeking induced by priming injections of alcohol and exposure to stress. Neuropsychopharmacology, 21(3), 435–444.

Lê, A.D., Harding, S., Juzytsch, W., Watchus, J., Shalev, U., & Shaham, Y. (2000) The role of corticotrophin-releasing factor in stress-induced relapse to alcohol-seeking behavior in rats. Psychopharmacology 150, 317–324.

Li, C.-S. R., Luo, X., Yan, P., Bergquist, K., & Sinha, R. (2009) Altered Impulse Control in Alcohol Dependence: Neural Measures of Stop Signal Performance. Alcoholism: Clin. Exp. Res. 33(4), 740–750.

Liappas, J., Paparrigopoulos, T., Tzavellas, E., & Christodoulou, G. (2002) Impact of alcohol detoxification on anxiety and depressive symptoms. Drug Alcohol Depend. 68, 215–220.

Lingford-Hughes, A., McGonigle, J., & Mick, I. (2015) An fMRI study of nalmefene on alcohol effects in reward anticipation in alcohol dependence. ECNP Congress.

Liu, X. & Weiss, F. (2002) Additive effect of stress and drug cues on reinstatement of ethanol seeking: Exacerbation by history of dependence and role of concurrent activation of corticotropin-releasing factor and opioid mechanisms. J. Neurosci. 22, 7856–7861.

Loas, G., Fremaux, D., Otmani, O., Lecercle, C., & Delahousse, J. (1997) Is alexithymia a negative factor for maintaining abstinence? A follow-up study. Compr. Psychiatry 38, 296–299.

Lohani, S., Poplawsky, A.J., Kim, S.G., & Moghaddam, B. (2016) Unexpected global impact of VTA dopamine neuron activation as measured by opto-fMRI. Mol Psychiatry, in press.

Loughlin, S. E., & Fallon, J. H. (1983) Dopaminergic and non-dopaminergic projections to amygdala from substantia nigra and ventral tegmental area. Brain Res. 262(2), 334-338.

Lu, H., Zou, Q., Gu, H., Raichle, M. E., Stein, E. A., & Yang, Y. (2012) Rat brains also have a default mode network. Proc. Natl. Acad. Sci. USA 109(10), 3979–3984.

Lüthi, A. & Lüscher, C. (2014) Pathological circuit function underlying addiction and anxiety disorders. Nat. NeuroSci. 17, 1635–1643.

Majumdar, A. K., Howard, L., Goldberg, M. R., Hickey, L., Constanzer, M., Rothenberg, P. L., et al., (2013) Pharmacokinetics of aprepitant after single and multiple oral doses in healthy volunteers. J. Clin. Pharmacol. 46(3), 291–300.

Makris, N., Oscar-Berman, M., Jaffin, S.K., Hodge, S.M., Kennedy, D.N., Caviness, V.S., et al., (2008) Decreased volume of the brain reward system in

alcoholism. Biol. Psychiatry 64, 192–202.

Mann, K., Gunther, A., Stetter, F., Ackermann, K. (1999) Rapid recovery from cognitive deficits in abstinent alcoholics: A controlled test-retest study. Alcohol and Alcoholism 34, 567–574.

Mason, B. J., Goodman, A. M., & Dixon, R. M. (2002) A pharmacokinetic and pharmacodynamic drug interaction study of acamprosate and naltrexone. Neuropsychopharmacology 27(4), 596-606.

McBride, W.J. (2002) Central nucleus of the amygdala and the effects of alcohol and alcohol-drinking behavior in rodents. Pharm. Biochem. and Behavior 71, 509–515.

McGonigle, J., Murphy, A., Paterson, L. M., Reed, L. J., Nestor, L., Nash, J., et al. (2017) The ICCAM platform study: An experimental medicine platform for evaluating new drugs for relapse prevention in addiction. Part B: fMRI description. J. Psychopharmacol. 31(1), 3–16.

McKeon, A., Frye, M.A., Delanty, N. (2008) The alcohol withdrawal syndrome. J. Neurol. Neurosurg. Psych.79, 854–862.

Mennes, M., Kelly, C., Colcombe, S., Castellanos, F.X., Milham, M.P. (2013) The extrinsic and intrinsic functional architectures of the human brain are not equivalent. Cereb. Cortex 23, 223–229.

Mennes, M., Kelly, C., Zuo, X.-N., Di Martino, A., Biswal, B. B., Castellanos, F. X., & Milham, M. P. (2010) Inter-individual differences in resting-state functional connectivity predict task-induced BOLD activity. NeuroImage, 50(4), 1690–1701.

Menon, V. & Uddin, L.Q. (2010) Saliency, switching, attention and control: a network model of insula function. Brain Struct. Funct. 214, 655–667.

Milham, M.P. (2012) The NKI-Rockland sample: a model for accelerating the pace of discovery science in psychiatry. Frontiers in Neuroscience 6, Art 152.

Milham, M.P., Fair, D., Mennes, M. (2012) The ADHD-200 consortium: a model to advance the translational potential of neuroimaging in clinical neuroscience. Frontiers in systems neuroscience 6, Art 62.

Mitchell, J.M., O'Neil, J.P., Janabi, M. (2012) Alcohol consumption induces endogenous opioid release in the human orbitofrontal cortex and nucleus accumbens. Sci. Translat. Med. 4, 116ara6.

Morris, J.S., Friston, K.J., Dolan, R.J. (1998) Experience-dependent modulation of tonotopic neural responses in human auditory cortex. Proc. Biol. Sci. 265, 649–657.

Murphy, K., Birn, R. M., Handwerker, D.A., Jones, T.B., & Bandettini, P.A. (2009). The impact of global signal regression on resting state correlations: are anti-correlated networks introduced? NeuroImage, 44(3), 893-905.

Murphy, K., Birn, R. M., & Bandettini, P. A. (2013) Resting-state fMRI confounds and cleanup. NeuroImage, 80, 349–359.

Murphy, K., & Fox, M. D., 2017. Towards a consensus regarding global signal regression for resting state functional connectivity MRI. NeuroImage, in press.

Murphy, K., Harris, A. D., & Wise, R. G. (2011) Robustly measuring vascular reactivity differences with breath-hold: Normalising stimulus-evoked and resting state BOLD fMRI data. NeuroImage, 54(1), 369–379.

Murray, A.M., Ryoo, H.L., Gurevich, E., & Joyce, J.N. (1994) Localization of dopamine D3 receptors to mesolimbic and D2 receptors to mesostriatal regions of human forebrain. Proc. Natl. Acad. Sci. U.S.A. 91, 11271–11275.

Murty, V.P., Shermohammed, M., Smith, D.V., Carter, R.M., Huettel, S.A., Adcock, R.A. (2014) Resting state networks distinguish human ventral tegmental area from substantia nigra. NeuroImage 100, 580–589.

Muschelli, J., Nebel, M. B., Caffo, B. S., Barber, A. D., Pekar, J. J., Mostofsky, S. H., (2014) Reduction of motion-related artifacts in resting state fMRI using aCompCor. NeuroImage, 96(C), 22–35.

Nakajima, S., Gerretsen, P., Takeuchi, H., Caravaggio, F., Chow, T., Le Foll, B., Mulsant, B., Pollock, B., Graff-Guerrero, A., 2013. The potential role of dopamine D. Eur. Neuropsychopharmacol. 23, 799–813.

Nie, Z., Schweitzer, P., Roberts, A. J., Madamba, S. G., Moore, S. D., & Siggins, G. R. (2004) Ethanol augments GABAergic transmission in the central amygdala via CRF1 receptors. Science, 303(5663), 1512–1514.

Nooner, K. B., Colcombe, S., Tobe, R., Mennes, M., Benedict, M., Moreno, A., ... & Sikka, S. (2012) The NKI-Rockland sample: a model for accelerating the pace of discovery science in psychiatry. Frontiers Neurosci. 6, Art152.

Nutt, D.J. (2014) The role of the opioid system in alcohol dependence. Journal of Psychopharmacology 28, 8–22.

Nutt, D.J., King, L.A., Phillips, L.D., Independent Scientific Committee on Drugs, (2010) Drug harms in the UK: A multicriteria decision analysis. Lancet, 376, 1558–1565.

Nutt, D. J., Lingford-Hughes, A., & Erritzoe, D. (2015) The dopamine theory of addiction: 40 years of highs and lows. Nat. Rev. Neurosci., 16, 305-312

Nutt, D. J., & Rehm, J. (2014) Doing it by numbers: a simple approach to reducing the harms of alcohol. Journal of Psychopharmacology, 28(1), 3–7.

Ogawa, S., Tank, D. W., Menon, R., Ellermann, J. M., Kim, S.-G., Merkle, H., & Ugurbil, K. (1992) Intrinsic signal changes accompanying sensory stimulation: functional brain mapping with magnetic resonance imaging. Proc. Natl. Acad. Sci. USA , 89(13), 5951–5955.

Oldfield, R.C. (1971) The assessment and analysis of handedness: the Edinburgh inventory. Neuropsychologia 9, 97–113.

Olive, M.F., Koenig, H.N., Nannini, M.A., Hodge, C.W. (2001) Stimulation of endorphin neurotransmission in the nucleus accumbens by ethanol, cocaine, and amphetamine. J. Neurosci. 21, RC184.

Orban, C., McGonigle, J., Kalk, N.J., Erritzoe, D., Waldman, A.D., Nutt, D.J., Rabiner, E.A., Lingford-Hughes, A.R. (2013) Resting state synchrony in anxiety-related circuits of abstinent alcohol-dependent patients. Am J Drug Alcohol Abuse 39, 433–440.

Patel, A. X., Kundu, P., Rubinov, M., Jones, P. S., Vértes, P. E., Ersche, K. D., et al., (2014) A wavelet method for modeling and despiking motion artifacts from resting-state fMRI time series. NeuroImage, 95(C), 287–304.

Paterson, L.M., Flechais, R.S., Murphy, A., Reed, L.J., Abbott, S., Boyapati, V., et al. (2015) The Imperial College Cambridge Manchester (ICCAM) platform study: An experimental medicine platform for evaluating new drugs for relapse prevention in addiction. Part A: Study description. Journal of Psychopharmacology 29, 943–960.

Paulus, M.P., Feinstein, J.S., Castillo, G. (2005) Dose-dependent decrease of activation in bilateral amygdala and insula by lorazepam during emotion processing. Arch. Gen. Psychiatry 62(3):282-288.

Peciña, M., Azhar, H., Love, T.M., Lu, T., Fredrickson, B.L., Stohler, C.S., Zubieta, J.-K. (2012) Personality Trait Predictors of Placebo Analgesia and Neurobiological Correlates. Neuropsychopharmacology 38, 639–646.

Peciña, M. & Zubieta, J.-K. (2015) Molecular mechanisms of placebo responses in humans. Mol. Psychiatry 20, 416–423.

Petrovic, P. (2002) Placebo and opioid analgesia - Imaging a shared neuronal network. Science 295, 1737–1740.

Petrovic, P., Dietrich, T., Fransson, P., Andersson, J., Carlsson, K., Ingvar, M. (2005) Placebo in Emotional Processing— Induced Expectations of Anxiety Relief Activate a Generalized Modulatory Network. Neuron 46, 957–969.

Pfefferbaum, A., Lim, K.O., Zipursky, R.B., Mathalon, D.H., Rosenbloom, M.J., Lane, B., Ha, C.N., Sullivan, E.V. (1992) Brain gray and white matter volume loss accelerates with aging in chronic alcoholics: a quantitative MRI study. Alcoholism: Clinical and Experimental Research 16, 1078–1089.

Phan, K.L., 2011. Altered amygdala resting-state functional connectivity in post-traumatic stress disorder. Front. Psychology 2, Art62.

Ploghaus, A., Becerra, L., Borras, C., Borsook, D. (2003) Neural circuitry underlying pain modulation: expectation, hypnosis, placebo. Trends in Cognitive Sciences 7, 197–200.

Poremba, A., Saunders, R.C., Crane, A.M., Cook, M., Sokoloff, L., Mishkin, M. (2003) Functional mapping of the primate auditory system. Science 299, 568–572.

Posse, S., Kemna, L. J., Elghahwagi, B., Wiese, S., & Kiselev, V. G. (2001) Effect of graded hypo- and hypercapnia on fMRI contrast in visual cortex: quantification of T*2 changes by multiecho EPI. Magnetic Resonance in Medicine, 46(2), 264–271.

Poulin, M. J., Liang, P. J., & Robbins, P. A. (1996) Dynamics of the cerebral blood flow response to step changes in end-tidal PCO2 and PO2 in humans. J. Appl. Physiol. 81(3), 1084-1095.

Poulin, J. F., Zou, J., Drouin-Ouellet, J., Kim, K. Y. A., Cicchetti, F., & Awatramani, R. B. (2014) Defining midbrain dopaminergic neuron diversity by single-cell gene expression profiling. Cell Rep. 9(3), 930-943.

Power, J. D., Barnes, K. A., Snyder, A. Z., Schlaggar, B. L., & Petersen, S. E. (2012) Spurious but systematic correlations in functional connectivity MRI networks arise from subject motion. NeuroImage, 59(3), 2142–2154.

Power, J.D., Barnes, K.A., Snyder, A.Z., Schlaggar, B.L., Petersen, S.E. (2013) Steps toward optimizing motion artifact removal in functional connectivity MRI; a reply to Carp. NeuroImage 76, 439–441. 7

Power, J. D., Mitra, A., Laumann, T. O., Snyder, A. Z., Schlaggar, B. L., & Petersen, S. E. (2014a) Methods to detect, characterize, and remove motion artifact in resting state fMRI. NeuroImage, 84(C), 320–341

Power, J. D., Schlaggar, B.L., & Petersen, S.E. (2014b). Studying brain organization via spontaneous fMRI signal. *Neuron*, *84*(4), 681-696.

Power, J. D., Plitt, M., Laumann, T. O., & Martin, A. (2016) A simple but powerful way to assess fMRI scan qualities. NeuroImage, in press.

Preminger, S., Harmelech, T., Malach, R. (2011) Stimulus-free thoughts induce differential activation in the human default network. NeuroImage 54, 1692–1702.

Quirk, G.J., Armony, J.L., LeDoux, J.E. (1997) Fear conditioning enhances different temporal components of tone-evoked spike trains in auditory cortex and lateral amygdala. Neuron 19, 613–624.

Rabinak, C. A., Angstadt, M., Welsh, R. C., Kenndy, A. E., Lyubkin, M., Martis, B., & Phan, K. L. (2011) Altered amygdala resting-state functional connectivity in post-traumatic stress disorder. Front. Neurosci. 2, Art62

Rabiner, E.A., Beaver, J., Makwana, A., Searle, G., Long, C., Nathan, P.J., Newbould, R.D., et al. (2011) Pharmacological differentiation of opioid receptor antagonists by molecular and functional imaging of target occupancy and food reward-related brain activation in humans. Mol. Psychiatry 16, 826–835.

Raichle, M. E., & Mintun, M. A. (2006) Brain work and brain imaging. Annual Review of Neuroscience, 29, 449–476.

Rassnick, S., Heinrichs, S. C., Britton, K. T., & Koob, G. F. (1993) Microinjection of a corticotropin-releasing factor antagonist into the central nucleus of the amygdala reverses anxiogenic-like effects of ethanol withdrawal. Brain Res. 605(1), 25-32.

Rehm, J., Mathers, C., Popova, S., Thavorncharoensap, M., Teerawattananon, Y., Patra, J. (2009) Global burden of disease and injury and economic cost attributable to alcohol use and alcohol-use disorders. Lancet 373, 2223–2233.

Rezayof, A., Zarrindast, M. R., Sahraei, H., & Haeri-Rohani, A. (2002) Involvement of dopamine D2 receptors of the central amygdala on the acquisition and

expression of morphine-induced place preference in rat. Pharm. Biochem. Behav. 74(1), 187-197.

Roberto, M. (2004) Increased GABA release in the central amygdala of ethanol-dependent rats. J. Neurosci. 24, 10159–10166.

Roberto, M., Madamba, S. G., Moore, S. D., Tallent, M. K., & Siggins, G. R. (2003) Ethanol increases GABAergic transmission at both pre- and postsynaptic sites in rat central amygdala neurons. Proc. Natl. Acad. Sci. USA 100(4), 2053–2058.

Roberto, M., Schweitzer, P., Madamba, S. G., Stouffer, D. G., Parsons, L. H., & Siggins, G. R. (2004) Acute and chronic ethanol alter glutamatergic transmission in rat central amygdala: an in vitro and in vivo analysis. Journal of Neuroscience, 24(7), 1594–1603.

Robinson, T. E., & Berridge, K. C. (1993) The neural basis of drug craving: an incentive-sensitization theory of addiction. Brain Research Reviews, 18(3): 247-291.

Robledo, P., Maldonado-Lopez, R., & Koob, G. F. (1992) Role of dopamine receptors in the nucleus accumbens in the rewarding properties of cocaine. Ann. N. Y. Acad. Sci., 654, 509–512.

Rodaros, D., Caruana, D. A., Amir, S., & Stewart, J. (2007) Corticotropin-releasing factor projections from limbic forebrain and paraventricular nucleus of the hypothalamus to the region of the ventral tegmental area. Neuroscience 150(1), 8-13.

Roelofs, S.M., Dikkenberg, G.M. (1987) Hyperventilation and Anxiety - Alcohol-Withdrawal Symptoms Decreasing with Prolonged Abstinence. Alcohol 4, 215–220.

Rostrup, E., Law, I., Blinkenberg, M., Larsson, H. B., Born, A. P., Holm, S., & Paulson, O.B. (2000) Regional differences in the CBF and BOLD responses to hypercapnia: a combined PET and fMRI study. NeuroImage, 11(2), 87–97.

Roy, A.K., Shehzad, Z., Margulies, D.S., Kelly, A.M.C., Uddin, L.Q., Gotimer, K., Biswal, B.B., Castellanos, F.X., Milham, M.P. (2009) Functional connectivity of the human amygdala using resting state fMRI. NeuroImage 45, 614–626.

Rubia, K., Halari, R., Cubillo, A., Smith, A.B., Mohammad, A.-M., Brammer, M., Taylor, E. (2011) Methylphenidate normalizes fronto-striatal underactivation during interference inhibition in medication-näıve boys with Attention-Deficit Hyperactivity Disorder. Neuropsychopharmacology 36, 1575–1586.

Rubia, K., Russell, T., Overmeyer, S., Brammer, M.J. (2001) Mapping motor inhibition: conjunctive brain activations across different versions of go/no-go and stop tasks. NeuroImage 13, 250–261.

Salminen, J. K., Saarijärvi, S., Äärelä, E., Toikka, T., & Kauhanen, J. (1999) Prevalence of alexithymia and its association with sociodemographic variables in the general population of Finland. J. Psychosomat. Res. 46(1), 75-82.

Samson, F., Zeffiro, T.A., Toussaint, A., Belin, P. (2011) Stimulus Complexity and Categorical Effects in Human Auditory Cortex: An Activation Likelihood Estimation Meta-Analysis. Front. Psychology 1, Art241.

Santarelli, L., Gobbi, G., Debs, P.C. (2001) Genetic and pharmacological disruption of neurokinin 1 receptor function decreases anxiety-related behaviors and increases serotonergic function. Proc. Natl. Acad. Sci. USA 98(4), pp. 1912–1917.

Satterthwaite, T. D., Elliott, M. A., Gerraty, R. T., Ruparel, K., Loughead, J., Calkins, M. E., et al. (2013) An improved framework for confound regression and filtering for control of motion artifact in the preprocessing of resting-state functional connectivity data. NeuroImage, 64, 240–256.

Satterthwaite, T. D., Wolf, D. H., Loughead, J., Ruparel, K., Elliott, M. A., Hakonarson, H., et al. (2012) Impact of in-scanner head motion on multiple measures of functional connectivity: Relevance for studies of neurodevelopment in youth. NeuroImage 60(1), 623–632.

Schank, J.R., Pickens, C.L., Rowe, K.E., Cheng, K., Thorsell, A., Rice, K.C., Shaham, Y., Heilig, M. (2011) Stress-induced reinstatement of alcohol-seeking in rats is selectively suppressed by the neurokinin 1 (NK1) antagonist L822429. Psychopharmacology 218, 111–119.

Schank, J.R., Ryabinin, A.E., Giardino, W.J., Ciccocioppo, R., Heilig, M. (2012) Stress-Related Neuropeptidesand Addictive Behaviors: Beyond the Usual Suspects. Neuron 76, 192–208.

Schirmer, A., Fox, P.M., Grandjean, D. (2012) On the spatial organization of sound processing in the human temporal lobe: A meta-analysis. NeuroImage 63, 137–147.

Schweinsburg, A.D., Paulus, M.P., Barlett, V.C., Killeen, L.A., Caldwell, L.C., Pulido, C., Brown, S.A., Tapert, S.F. (2004) An fMRI study of response inhibition in youths with a family history of alcoholism. Ann. N. Y. Acad. Sci. 1021, 391–394.

Scott, D.J., Stohler, C.S., Egnatuk, C.M. (2008) Placebo and nocebo effects are defined by opposite opioid and dopaminergic responses. Arch. Gen. Psychiatry 65, 220–231.

Scott, D.J., Stohler, C.S., Egnatuk, C.M., Wang, H., Koeppe, R.A., Zubieta, J.K. (2007) Individual Differences in Reward Responding Explain Placebo-Induced Expectations and Effects. Neuron 55, 325–336.

Searle, G., Beaver, J.D., Comley, R.A., Bani, M., Tziortzi, A., Slifstein, M., Mugnaini, M., Griffante, C., Wilson, A.A., Merlo-Pich, E., Houle, S., Gunn, R., Rabiner, E.A., Laruelle, M. (2010) Imaging Dopamine D. Biol. Psych. 68, 392–399.

See, R. E., Kruzich, P. J., & Grimm, J. W. (2001) Dopamine, but not glutamate, receptor blockade in the basolateral amygdala attenuates conditioned reward in a rat model of relapse to cocaine-seeking behavior. Psychopharmacology, 154(3), 301–310.

Seifert, J., Seeland, I., Borsutzky, M., Passie, T., Rollnik, J., Wiese, B., Emrich, H., Schneider, U. (2003) Effects of acute alcohol withdrawal on memory performance in alcohol-dependent patients: a pilot study. Addict. Biol. 8, 75–80.

Setlow, B., Holland, P. C., & Gallagher, M. (2002) Disconnection of the basolateral

amygdala complex and nucleus accumbens impairs appetitive Pavlovian second-order conditioned responses. Behav. Neurosci. 116(2), 267–275.

Shah, S.G., Klumpp, H., Angstadt, M., Nathan, P.J., Phan, K.L. (2009) Amygdala and insula response to emotional images in patients with generalized social anxiety disorder. J. Psychiatry. Neurosci. 34, 296–302.

Sharp, D.J., Bonnelle, V., De Boissezon, X., Beckmann, C.F., James, S.G., Patel, M.C., Mehta, M.A. (2010) Distinct frontal systems for response inhibition, attentional capture, and error processing. Proc. Natl. Acad. Sci. USA. 107, 6106–6111.

Sheehan, D.V., Lecrubier, Y., Sheehan, K.H., Amorim, P., Janavs, J., Weiller, E., Hergueta, T., Baker, R., Dunbar, G.C. (1998) The Mini-International Neuropsychiatric Interview (M.I.N.I.): the development and validation of a structured diagnostic psychiatric interview for DSM-IV and ICD-10. J Clin Psychiatry 59 Suppl 20, 22–57.

Shen, R.-Y., Choong, K.-C., Thompson, A.C. (2007) Long-Term Reduction in Ventral Tegmental Area Dopamine Neuron Population Activity Following Repeated Stimulant or Ethanol Treatment. Biological Psychiatry 61, 93–100.

Sinha, R. (2011) Effects of Adrenal Sensitivity, Stress- and Cue-Induced Craving, and Anxiety on Subsequent Alcohol Relapse and Treatment Outcomes. Arch. Gen. Psychiatry 68, 942.

Smith, S. M., Fox, P. T., Miller, K. L., Glahn, D. C., Fox, P. M., Mackay, C. E., et al. (2009) Correspondence of the brain's functional architecture during activation and rest. Proc. Natl. Acad. Sci. USA 106(31), 13040-13045.

Smith, S.M. & Nichols, T.E. (2009) Threshold-free cluster enhancement: Addressing problems of smoothing, threshold dependence and localisation in cluster inference. NeuroImage 44, 83–98.

Solano-Castiella, E., Schäfer, A., Reimer, E., Türke, E., Pröger, T., Lohmann, G., Trampel, R., Turner, R. (2011) Parcellation of human amygdala in vivo using ultra high field structural MRI. NeuroImage 58, 741–748.

Sommer, W. H., & Saavedra, J. M. (2008) Targeting brain angiotensin and corticotrophin-releasing hormone systems interaction for the treatment of mood and alcohol use disorders. Journal of Molecular Medicine (Berlin, Germany), 86(6), 723–728.

Spanagel, R. & Herz, A. (1992) Opposing tonically active endogenous opioid systems modulate the mesolimbic dopaminergic pathway. Proc. Natl. Acad. Sci. USA 89, 2046–2050.

Spanagel, R., Herz, A., Bals-Kubik, R., Shippenberg, T.S. (1991a) β-Endorphin-induced locomotor stimulation and reinforcement are associated with an increase in dopamine release in the nucleus accumbens. Psychopharmacology 104, 51–56.

Spanagel, R., Herz, A., Shippenberg, T.S. (1991b) Modulation of the mesolimbic dopaminergic system by β-endorphin-(1-27) as assessed by microdialysis. Eur. J. Pharmacol. 200, 319–324.

Spanagel, R. & Weiss, F. (1999) The dopamine hypothesis of reward: past and

current status. Trends in Neurosciences 22, 521–527.

Spielberger, C.D., Gorsuch, R.L., Lushene, P.R., Vagg, P.R. Jacobs, A.G. (1983) Manual for the State-Trait anxiety inventory (form Y). Palo Alto, CA, USA; Consulting Psychologists Press.

Sporns, O. (2011) The Non-Random Brain: Efficiency, Economy, and Complex Dynamics. Front. Comput. Neurosci. 5, Art5.

Spreng, R.N. (2012) The fallacy of a "task-negative" network. Front. Psychol. 3, Art145.

Sripada, R., King, A., Garfinkel, S., Wang, X., Sripada, C., Welsh, R., Liberzon, I. (2012) Altered resting-state amygdala functional connectivity in men with posttraumatic stress disorder. J. Psychiatry. Neurosci. 37, 241–249.

Stavro, K., Pelletier, J., Potvin, S. (2012) Widespread and sustained cognitive deficits in alcoholism: a meta-analysis. Addict. Biol. 18, 203–213.

Stein, M.B., Simmons, A.N., Feinstein, J.S. (2007) Increased amygdala and insula activation during emotion processing in anxiety-prone subjects. Am. J. Psychiatry. 164, 318–327.

Sterling, P., & Eyer, J. (1988) Allostasis: a new paradigm to explain arousal pathology. In: Fisher, S., Reason K., eds. Handbook of life stress, cognition and health. New York: John Wiley, 629-49.

Sullivan, E.V., Müller-Oehring, E., Pitel, A.-L., Chanraud, S., Shankaranarayanan, A., Alsop, D.C., Rohlfing, T., Pfefferbaum, A. (2013) A selective insular perfusion deficit contributes to compromised salience network connectivity in recovering alcoholic men. Biol. Psych. 74, 547–555.

Sullivan, E.V., Pfefferbaum, A. (2005) Neurocircuitry in alcoholism: a substrate of disruption and repair. Psychopharmacology 180, 583–594.

Sutherland, M.T., Carroll, A.J., Salmeron, B.J., Ross, T.J., Hong, L.E., Stein, E.A. (2013) Down-regulation of amygdala and insula functional circuits by Varenicline and nicotine in abstinent cigarette smokers. Biol. Psych. 74, 538–546.

Tan, K.R., Yvon, C., Turiault, M., Mirzabekov, J.J., Doehner, J., Labouèbe, G., Deisseroth, K., Tye, K.M., Lüscher, C. (2012) GABA Neurons of the VTA Drive Conditioned Place Aversion. Neuron 73, 1173–1183.

Tavor, I., Jones, O. P., Mars, R. B., Smith, S. M., Behrens, T. E., & Jbabdi, S. (2016) Task-free MRI predicts individual differences in brain activity during task performance. Science, 352(6282), 216-220.

Taylor, G. J., & Bagby, R. M. (2004) New trends in alexithymia research. Psychotherapy Psychosomat. 73(2), 68–77.

Te Beek, E. T., Zoethout, R., Bani, M., Andorn, A., Iavarone, L., Klaassen, E. S., et al. (2012) Pharmacokinetics and central nervous system effects of the novel dopamine D 3receptor antagonist GSK598809 and intravenous alcohol infusion at pseudo-steady state. J. Psychopharmacol. 26(2), 303–314.

Thanos, P.K., Katana, J.M., Ashby, C.R. (2005) The selective dopamine D3 receptor antagonist SB-277011-A attenuates ethanol consumption in ethanol preferring (P) and non-preferring (NP) rats. Pharmacology, Biochemistry and Behavior

81, 190–197.

Thorsell, A., Schank, J.R., Singley, E., Hunt, S.P., Heilig, M. (2010) Neurokinin-1 receptors (NK1R:s), alcohol consumption, and alcohol reward in mice. Psychopharmacology 209, 103–111.

Tye, K. M., Prakash, R., Kim, S.-Y., Fenno, L. E., Grosenick, L., Zarabi, H., et al. (2013) Amygdala circuitry mediating reversible and bidirectional control of anxiety. Nature 471(7338), 358–362.

Tziortzi, A.C., Searle, G.E., Tzimopoulou, S., Salinas, C., Beaver, J.D., Jenkinson, M., Laruelle, M., Rabiner, E.A., Gunn, R.N., (2011) Imaging dopamine receptors in humans with [11C]-(+)-PHNO: Dissection of D3 signal and anatomy. NeuroImage 54, 264–277.

Upadhyay, J., Maleki, N., Potter, J., Elman, I., Rudrauf, D., Knudsen, J., Wallin, D., Pendse, G., McDonald, L., Griffin, M., Anderson, J., Nutile, L., Renshaw, P., Weiss, R., Becerra, L., Borsook, D. (2010) Alterations in brain structure and functional connectivity in prescription opioid-dependent patients. Brain 133, 2098–2114.

Urban, N. B. L., Kegeles, L. S., Slifstein, M., Xu, X., Martinez, D., Sakr, E., et al., (2010) Sex Differences in Striatal Dopamine Release in Young Adults After Oral Alcohol Challenge: A Positron Emission Tomography Imaging Study With [^{11}C]raclopride. Biol. Psych. 68(8), 689–696.

Van de Moortele, P.F., Akgun, C., Adriany, G., Moeller, S., Ritter, J., Collins, C.M., Smith, M.B., Vaughan, J.T., Uğurbil, K. (2005) B1 destructive interferences and spatial phase patterns at 7 T with a head transceiver array coil. Magn. Reson. Med. 54, 1503–1518.

Van Dijk, K. R. A., Hedden, T., Venkataraman, A., Evans, K. C., Lazar, S. W., & Buckner, R. L. (2010) Intrinsic Functional Connectivity As a Tool For Human Connectomics: Theory, Properties, and Optimization. J. Neurophysiol. 103(1), 297–321.

Van Dijk, K. R. A., Sabuncu, M. R., & Buckner, R. L. (2012) The influence of head motion on intrinsic functional connectivity MRI. NeuroImage, 59(1), 431–438.

Van Marle, H.J.F., Hermans, E.J., Qin, S., Fernández, G. (2010) Enhanced resting-state connectivity of amygdala in the immediate aftermath of acute psychological stress. NeuroImage 53, 348–354.

Van Zessen, R., Phillips, J.L., Budygin, E.A., Stuber, G.D. (2012) Activation of VTA GABA Neurons Disrupts Reward Consumption. Neuron 73, 1184–1194.

Vengeliene, V., Leonardi-Essmann, F., Perreau-Lenz, S., Gebicke-Haerter, P., Drescher, K., Gross, G., Spanagel, R. (2006) The dopamine D3 receptor plays an essential role in alcohol-seeking and relapse. FASEB J. 20, 2223–2233.

Vincent, J. L., Patel, G. H., Fox, M. D., Snyder, A. Z., & Baker, J. T., 2007. Intrinsic functional architecture in the anaesthetized monkey brain. Nature, 447, 83-86.

Wager, T.D., Scott, D.J., Zubieta, J.-K. (2007) Placebo effects on human mu-opioid activity during pain. Proc. Natl. Acad. Sci. U.S.A. 104, 11056–11061.

Weerts, E.M., Wand, G.S., Kuwabara, H., Munro, C.A., Dannals, R.F., Hilton, J.,

Frost, J.J., McCaul, M.E., (2011) Positron Emission Tomography Imaging of Mu- and Delta-Opioid Receptor Binding in Alcohol-Dependent and Healthy Control Subjects. Alcoholism: Clin. Exp. Res. 35, 2162–2173.

Williams, T.M., Davies, S.J.C., Taylor, L.G., Daglish, M.R.C., Hammers, A., Brooks, D.J., Nutt, D.J., Lingford-Hughes, A. (2009) Brain opioid receptor binding in early abstinence from alcohol dependence and relationship to craving: An [11C]diprenorphine PET study. Eur. Neuropsychopharmacol. 19, 740–748.

Willinger, U., Lenzinger, E., Hornik, K., Fischer, G., Schönbeck, G., Aschauer, H. N., et al. (2002) Anxiety as a predictor of relapse in detoxified alcohol-dependent patients. Alcohol and Alcoholism 37(6), 609–612.

Wise, R. G., Ide, K., Poulin, M. J., & Tracey, I. (2004) Resting fluctuations in arterial carbon dioxide induce significant low frequency variations in BOLD signal. NeuroImage, 21(4), 1652-1664

Woo, C.-W., & Wager, T. D. (2015) Neuroimaging-based biomarker discovery and validation. Pain 156(8), 1379–1381.

Wrase, J., Schlagenhauf, F., Kienast, T., Wüstenberg, T., Bermpohl, F., Kahnt, T., et al. (2007) Dysfunction of reward processing correlates with alcohol craving in detoxified alcoholics. NeuroImage, 35(2), 787–794.

Wrase, J., Makris, N., Braus, D.F., Mann, K., Smolka, M.N., Kennedy, D.N., et al. (2008) Amygdala volume associated with alcohol abuse relapse and craving. Am. J. Psychiatry 165, 1179–1184.

Xi, Z.-X., Li, X., Li, J., Peng, X.Q., Song, R., Gaál, J., Gardner, E.L. (2012) Blockade of dopamine D3 receptors in the nucleus accumbens and central amygdala inhibits incubation of cocaine craving in rats. Addict. Biol. 18, 665–677.

Yeo, B.T., Krienen, F.M., Sepulcre, J., Sabuncu, M.R., Lashkari, D., Hollinshead, M., et al. (2011) The organization of the human cerebral cortex estimated by intrinsic functional connectivity. J. Neurophysiol. 106, 1125–1165.

Appendix A: Figures

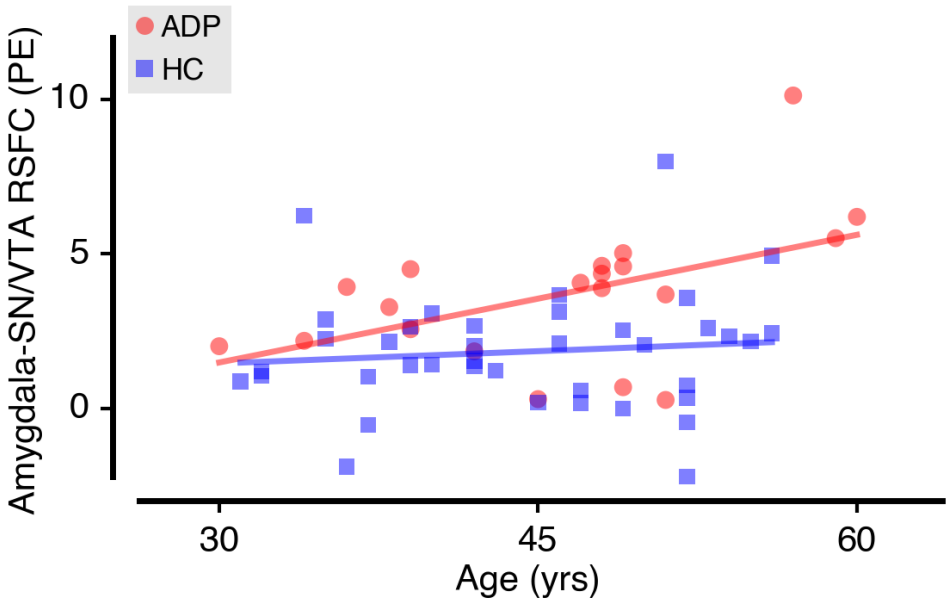


Figure A1.1 The relationship between age and amygdala – SN/VTA RSFC in ADP and HC. Amygdala-SN/VTA RSFC was positively correlated with age in ADP ($r = 0.5$, $p = 0.03$), but not in HC ($r = 0.1$, $p = 0.5$). PE: parameter estimate.

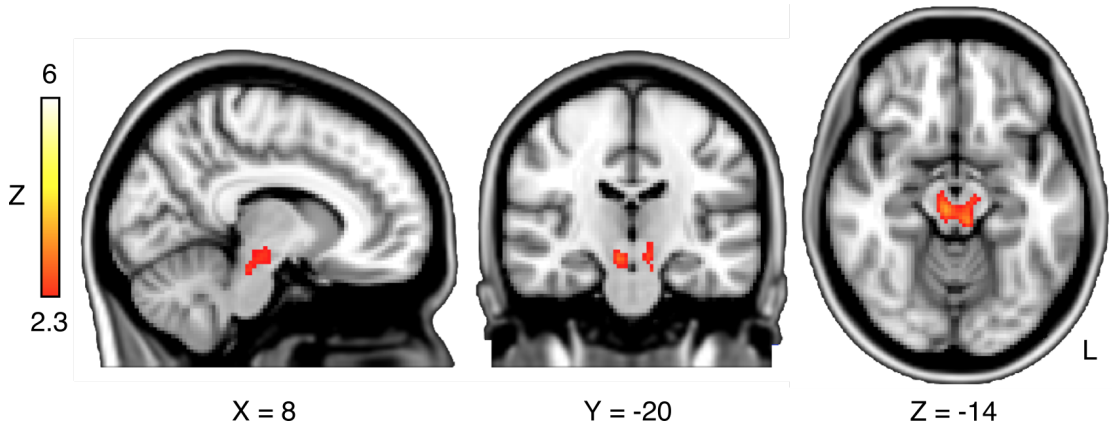


Figure A1.2 Group-level comparison of whole-brain amygdala RSFC with an extended list of covariates. ADP showed significantly greater amygdala RSFC in the midbrain than HC, while controlling for site, amygdala GM volume, ICV and voxelwise GM volume. Significant voxels were determined by a threshold of $Z > 2.3$ and a corrected cluster significance threshold of $p < 0.05$. Slice coordinates are presented in MNI space.

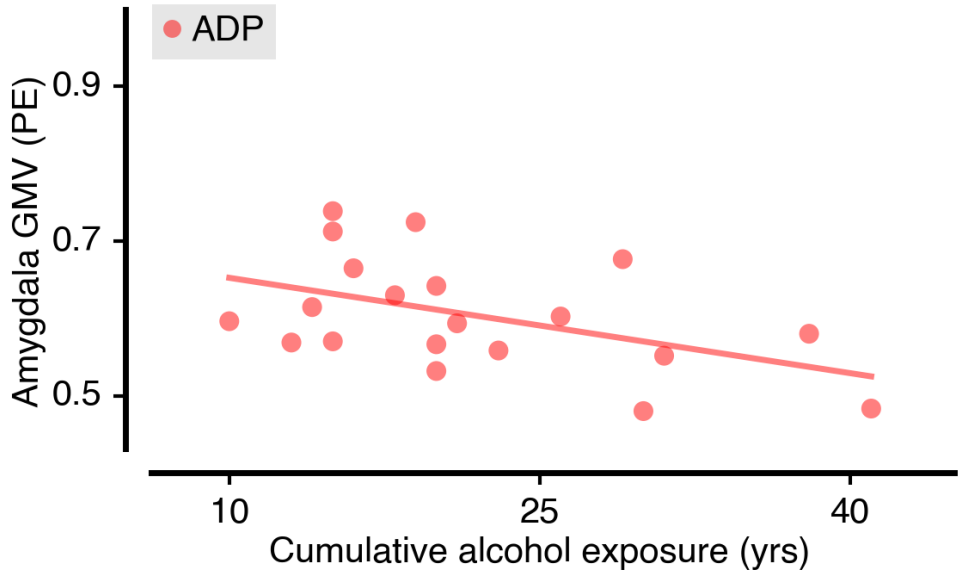


Figure A1.3 The relationship between cumulative alcohol exposure and amygdala GM volume in ADP. Amygdala GM volume was inversely correlated with cumulative alcohol exposure in ADP ($r = -0.48$, $p = 0.03$). PE: parameter estimate.

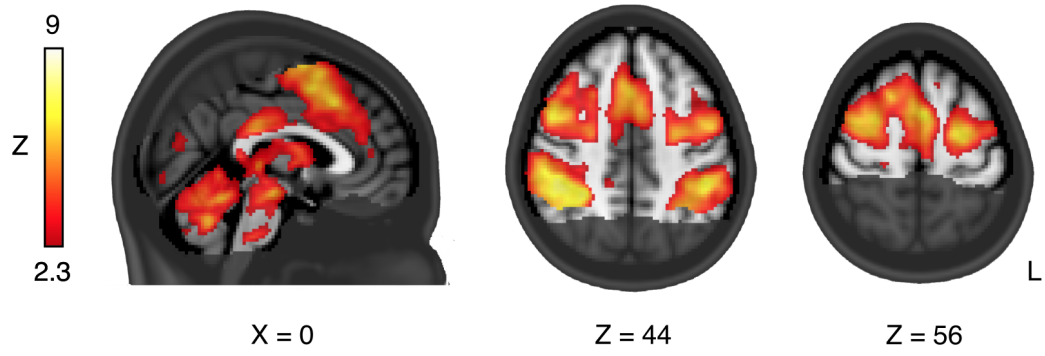


Figure A1.4 Clusters associated with correct inhibition trials in the Go/No-Go task in 70 participants pooled from Pilot, HC and ADP groups. Significant voxels were determined by a threshold of $Z > 2.3$ and a corrected cluster significance threshold of $p < 0.05$. Slice coordinates are presented in MNI space.